Alma Mater Studiorum – Università di Bologna

DOTTORATO DI RICERCA IN

CHIMICA

Ciclo XXVI

Settore Concorsuale di afferenza: 03/C2 – CHIMICA INDUSTRIALE

Settore Scientifico disciplinare: CHIM/04 – CHIMICA INDUSTRIALE

Structure-property relations
in polymers from renewable resources

Presentata da: **Lucrezia Martino**

Coordinatore Dottorato   **Relatore**

Chiar.mo Prof.   **Chiar.mo Prof.**
Aldo Roda   **Mariastella Scandola**

Esame finale anno 2014

A mio padre

Abstract

The present research project focuses its attention on the study of structure-property relations in polymers from renewable sources (bio-based polymers) such as polymers microbially produced, i.e. polyhydrohyalkanoates (PHAs) or chemically synthesized using bio-based monomers, i.e. polyammide 11 (PA11).

As concerns the study on polyhydrohyalkanoates, since the high price of the bacterial polyesters is the major limiting factor to their large use, especially the cost of the substrates (e.g. glucose, sucrose) used in the fermentation process, PHAs produced using widely available and low cost feedstocks, like agricultural by-products, have been investigated in this work. As concerns the PHA accumulating bacteria, both pure cultures of *Cupriavidus necator* as well as mixed microbial cultures (MMCs) were used. Vegetable fried oils (i.e used cooking oil, UCO) or olive oil mill wastewater (OMW) were used as carbon sources respectively. The study carried out in this Thesis focused on the characterization of PHAs recovered from the two mentioned productions and on the dependence of the PHA solid-state properties on both fermentation process conditions (e.g. bacterial strain, carbon substrate used) and method adopted for polymer recovery from the biomass. The latter was either a chemical extraction (with NaClO or NaOH) in the case of the mixed cultures or a chemically assisted enzymatic recovery when the pure culture was used. The scope of the mild enzymatic extraction was to recover the polymer in its native form, i.e. granules in the amorphous state, a goal that was successfully achieved. These investigations lead to the assessment of the influence on PHA properties of (i) carbon source, (ii) operation time of the fermentation process in MMCs, (iii) recovery method applied.

Further investigations concerning PHAs, using a commercially available poly(hydroxybutyrate-co-valerate), PHBV, involved the search of a safe and efficient plasticizer for the biopolymer and the development of a composite for food packaging applications, using wheat straw fibers as filler. This part of the Thesis work was performed within the EU-Project EcoBioCap 'Ecoefficient Biodegradable Composite Advanced Packaging' (FP7/2011-2015). Acetyl-tributyl citrate was shown to efficiently plasticized

PHBV, decreasing its intrinsic brittleness and providing a good matrix material for the composite with the low cost and widely available lignocellulosic fibers.

Novel copolymers synthesized from poly-3-hydroxybutyrate (PHB) and polybutyleneadipate (PBA) by microwave assisted transesterification were also studied and the dependence of their solid-state properties on chemical structure was assessed. Such copolymers represent a new family of biodegradable copolyesters that are potential suitable in biomedical applications (e.g. matrices for drug delivery systems) or as compatibilizers in PHB/PBA immiscibile blends.

As concerns the study of polyamide 11 (PA11), structure-property relations in bio-based PA11 polymers with either linear or star architectures (linear chains linked to a central core) were investigated. Both the rheological and the solid-state characterization of PA11 star samples with different arm number and length were performed in order to assess the impact of such architectural modifications on PA11 properties. Introduction of arms in polymer allows to modulate melt viscosity behavior which is advantageous for industrial applications. Also, several important solid-state properties, in particular mechanical properties, are found to be affected by the presence of branching.

Lastly, given the importance of the use of 'green' synthetic strategies in polymer chemistry, novel poly(β-amino esters), synthesized via enzymatic-catalyzed polymerization, have been investigated in this work.

1. INTRODUCTION

1.1. Context and definitions

Evergrowing concerns about the intensive exploitation of fossil resources which are not renewable within a useful time scale, the continue fluctuation in oil price with an overall tendency to rise and the unstable politics of the fossil sources suppliers have been increasing steadily in the last decade. Equally alarming problems are related to the environmental impact of fuels and other petrochemical products (organic chemicals, plastics) which are responsible for atmospheric pollution and for the increasing level of greenhouse gases that perturb the Earth's climate. The concept of the biorefinery in which **renewable resources** (**biomass**) are used arises from the need to overcome environmental challenges and simultaneously finding an alternative to limited fossil resources [1,2]. **Biorefinery** is defined as "the sustainable processing of biomass into a spectrum of marketable products (food, feed, materials, chemicals) and energy (fuels, power, heat)" by the International Energy Agency (IEA) [3]. **Sustainability** is defined as 'the development which meets the needs of the present time without compromising the ability of future generations to meet their own needs'. An equitable access to the constrained resource by the society and reorientation of technological efforts is required to reach such an objective [4].

Within a biorefinery scheme, chemical commodities can be produced from widely available and renewable resources by chemical or biotechnological processes as they are traditionally produced in the petroleum refinery, linking renewability to the concept of sustainability.

Biomass production by nature is estimated at 170 trillion tones per year, only 3.5% of which are used by humans. Most of these compounds are used for food, 33% for energy, paper, furniture and construction, and only 5% (300 million tones) are used for other non-food applications such as chemicals and clothing [5].

The main goals sought when adopting the biorefinery strategy are:

- minimization of society dependence on fossil resources by using biomasses which are renewable, widely available and equally distributed in the planet allowing a "democratic" use of the resources;

1

- reduction of fossil CO_2 emissions;
- production of chemicals via 'green' process strategies with low environmental impact;
- waste minimization;
- rural development;
- creation of a market for main commodities that can be economically more attractive by introduction of novel elements (in the products, properties and technologies used), thus allowing new competitiveness.

Other important aspects to take into consideration are: the contribution to rural development through revitalization of marginal rural areas; valorization of biomass residues and process by-products avoiding competition with food production; the adaptation of existing industrial plant technologies to produce and to process the new bio-sourced materials to the greatest feasible extent.

Among chemical commodities, polymers, the unique or main component of the plastics, are one of the most used fossil-based products in several sectors of everyday life (packaging, building & construction, automotive, transportation, electrical & electronics, agriculture, health care). Considering also the growing demand of polymers from developing countries, the profitable business around such materials, their relatively low costs and unique properties, it is clear that replacing non-renewable resources with renewables in polymer production within the biorefinery concept is undoubtedly a necessary objective towards a sustainable development.

Polymers from renewable sources, also named **bio-based polymers,** can be produced [6,7]:
- by direct extraction and separation from biomass (e.g starch, cellulose, alginates);
- by classical chemical synthesis from bio-based building blocks produced via biotechnological routes (e.g. polylactic acid, polyamide 11);
- by fermentation processes using microorganisms (e.g. polyhydroxyalkanoates).

The concept of obtaining polymers from renewable resources is not new considering that bio-based polymers have been used for food, furniture and clothing for thousands of years. The emergence of polymer chemistry hails during the second half of the 19th century: the

discovery of the vulcanization process of natural rubber by Charles Goodyear's in 1839 determined the development in the next years of the rubber industry; the first plastic material obtained from cellulose by chemical modification named celluloid (cellulose nitrate blended with camphor), was successfully commercialized thanks to the discovery of Alexander Parkes. The petrochemical revolution after the Second World War determined a shift towards the use of fossil resources and within a few decades huge quantities of plastics were produced. Nowadays polymers continue to be one of the most used materials in the global economy and an essential part of our modern lifestyle [8].

The return to the exploitation of renewable sources in recent years, promoted by the economic and the environmental reasons discussed above, has produced a tremendous increase in the number of publications on bio-based polymers. At the same time in the industrial world, a number of biorefineries have been developed to convert biomass into starch and cellulose-based products or into building blocks (monomers) like lactic acid and amino acids [9].

However, the relatively high production cost and the often poor performance of some bio-based plastics are limiting factors to their market growth and to widening of their applicability.

In order to extend the large-scale applicability of bio-based polymers it is necessary (i) to decrease the chemical/biotechnological processes costs by increasing scientific and technologic understanding of biomass conversion into plastics, (ii) to improve properties of some biobased polymers in order to fit requirements of industrial applications through a deeper knowledge of structure-properties relations, (iii) to create innovative bio-based plastics allowing new competitiveness. Indeed, in addition to economic and environmental advantages, the production of bio-based polymers also represents an occasion for the scientific and industrial innovation in the polymer area.

Examples of approaches explored to overcame the limitations regarding the use of bio-based polymers are the use of available and low cost feedstocks, like agricultural by-products, chemical modifications (cross-linking, copolymerization) or blending of bio-based polymers.

The present research project focuses its attention on the study of structure-property relations in polymers from renewable sources such as polymers microbially produced, Polyhydrohyalkanoates (PHAs), and chemically synthesized using monomers from renewable sources, Polylactic acid and Polyammide 11. Structural modifications, addition of reinforcing agents and plasticizers are among the strategies explored to obtain an improvement of the properties of such bio-based polymers. The use of waste as low cost substrates in PHA production and their impact on polymers properties is also investigated with the aim to contribute to an efficient use of the renewable resources.

In the following section, in order to understand how bio-based polymers can contribute to the sustainable development, the concepts of carbon footprint, of bio-based content, of biodegradability and compostability will be described together with the current certifications relative to **bioplastics**. The latter term refers to plastics that are either bio-based or biodegradable plastics or both and this definition was proposed by the European Bioplastics Association [10].

1.1.1. Carbon footprint and greenhouse effect

Bio-based polymers can potentially contribute to reduce carbon dioxide emissions whose uncontrolled increase is the major responsible of the greenhouse effect and of the consequential climate changes. Plants fix carbon dioxide to organic carbon by photosynthesis and it returns in part to the atmosphere by breathing of living organisms. Over geological time ($>10^6$ years), after death the living organic matter is fossilized. When such fossil carbon is transformed into petrochemical products it is released back into the atmosphere in a much shorter time scale (1-10 years). Due the disparity between the rate of conversion to fossil and the rate of CO_2 release to the environment at end of life of the product, the CO_2 emitted is more than that is fixed as fossil sources resulting in a total carbon imbalance. By using renewable sources to produce polymers and other products, the rate at which CO_2 is fixed equals the rate at which it is released at the end of life of the product. Considering the material carbon footprint, defined as the carbon emissions and removals resulting from carbon stored in materials, fully bio-based polymers that are in

harmony with the rates and time scale of the biological carbon cycle, represent materials with zero carbon footprint [11-13].

Thus, opposed to plastics from petroleum feedstocks, the use of bio-based plastics can contribute to manage carbon in a sustainable manner.

CO$_2$ → Biomass (renewable sources)

1-10 years

'Green' Chemical Industry

>10^6 years

Polymers Chemicals Fuels ← Chemical Industry ← Fossil sources
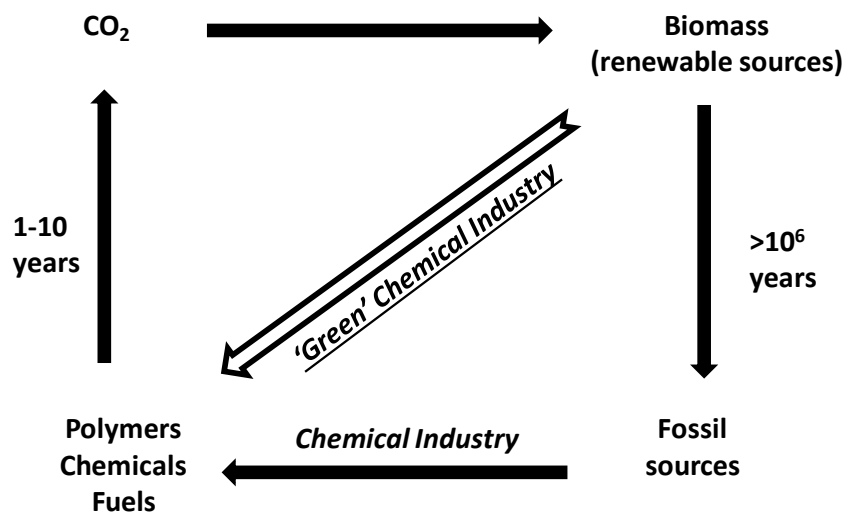
Figure 1. Carbon cycle - time scales of CO$_2$ utilization using renewable sources (balanced cycle) opposed to using fossil feedstocks (unbalanced cycle).

In order to evaluate the environmental impact of a product, the overall directly and indirectly emitted CO$_2$ (and other green house gases) through its whole life cycle - from the process of converting the carbon feedstock to ultimate disposal ("from cradle to grave") - must be taken into account.

Life cycle assessment (LCA) methodology and standards [14-16] are used to evaluate the carbon footprint together with all potential environmental and economic impacts associated with a product/process/activity throughout its entire life cycle. [11,13] This kind of analysis must be applied to bio-based polymers in order to evaluate their sustainability.

1.1.2. Bio-based content

To evaluate the material carbon footprint it is necessary to accurately determine the amount of carbon within a bio-based product that is derived from renewable sources: the bio-based

carbon or bio-based content. According to the ASTM D6866 standard [17], the **bio-based content** of solid, liquid, and gaseous samples can be determined by quantifying the ^{14}C isotope (or radiocarbon) content. The isotope ^{14}C decays slowly and it is naturally present in all living organisms in which its concentration is stable due to the continue exchange with the environment where it is close to constant. After organism death, ^{14}C absorption from the environment stops and the isotope begins its natural decay. Since the half-life of ^{14}C is around 5730 years, materials from fossil sources containing carbon produced millions of years earlier ("old carbon") no longer have appreciable amounts of this radioactive isotope, while ^{14}C is still present in materials made of "new carbon". By measuring the ^{14}C isotope amount in products from renewable resources, the bio-based content can be calculated as the percentage (by weight) of the total organic carbon in the product [17].

The two most important certification organizations in Europe, DIN CERTCO (Germany) and VINCOTTE (Belgium), developed certification logos (Figure 2) on the basis of the bio-based carbon content in a manufactured product, evaluated according to ASTM D6866 standard methods, providing proof of material conformity to standard requirements.

The Vincotte organization adopted certification symbol "OK-biobased" (Figure 2a) to certify the origin from renewable resource of a material in which a number of stars applied on the label correspond to a certain range of bio-based percentage determined in that product [18].

In Din Certco certification symbols (Figure 2b), percentage of bio-based carbon content measured in a product is displayed in the relative label and three quality levels of bio-based carbon content (20 - 50%, 50 - 85%, over 85%) are available.
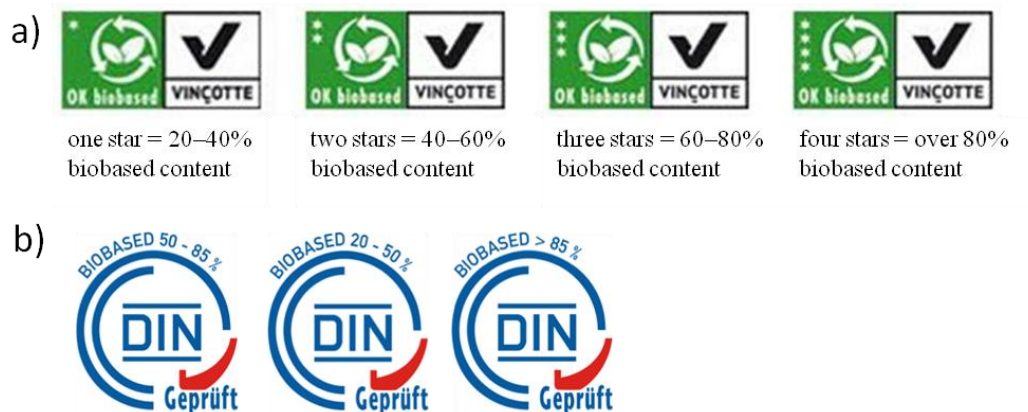
Figure 2. Certification logos for product from renewable resources by (a) Vincotte [19] and (b) Din Certco [20] organizations.

1.1.3. Biodegradability and Compostability

The term '**biodegradability**' refers to the degradation processes that results from the action of naturally-occurring micro-organisms such as bacteria, fungi and algae [21]. The biodegradation of polymers (macromolecules) consists of two steps: (1) fragmentation of the polymer chain into lower molar mass species and it occurs outside of the cell via chemicals or enzymes secreted by the microorganism; (2) bioassimilation inside the cell of the polymer chain fragments and their transformation into biomass, water and carbon dioxide and/or methane [22,23]. Biodegradability is not related to the origin of the material (fossil or renewable) but it depends on both polymer chemical structure (functional group stability, reactivity, crystallinity, molecular weight), and the environmental degrading conditions [24]. It can occur under aerobic conditions producing CO_2, water and biomass or under anaerobic conditions releasing CH_4, water and biomass.

Biodegradability is an end-of-life option useful in single or short-term use applications (disposable packaging, mulch-films). The use of biodegradable plastics as well as plastic recycling can contribute to decreasing the amount of plastic waste addressed to landfill.

However, biodegradability can be not useful by itself: a material can biodegrade over a longer time period or under unfavorable conditions. More accurate term is **compostability** that means biodegradation under controlled conditions in compliance with standard

specifications developed by the CEN-European Committee for Standardization such as EN 13432 [25] and EN 14995 [26] (this standard broadens applicability of EN 13432 to compostable plastic with different use than packaging).

Other standard specifications for compostability are: ASTM D6400 [21,27] and ISO 18606 [28], as well as the standard specification by Australia Standard AS 4736 [29].

According to the broadly used specification for compostability EN 13432, in order to be classified as compostable a material must satisfy all the following specific requirements:

- Biodegradation: 90 percent of the organic material has to be converted into CO_2 within 6 months in controlled composting conditions to demonstrate complete biodegradability. The carbon dioxide released is measured through the standard EN 14046 [30], also published as ISO 14855 [31].

- Disintegrability: physical fragmentation and loss of visibility in the final compost measured in a pilot-scale composting test [32];

- Absence of negative effects on the composting process;

- Concentrations of regulated metals must not exceed specific values (chemical tests)

- Absence of negative effect on the final compost (examination of the effect of resultant compost on plant growth - ecotoxicity test).

If a product satisfies compostable criteria, the certificate is awarded and it can receive the certification logo 'compostable'.

The certification organizations, DIN Certco and Vincotte in Europe, are authorized to release compostable logo owned by European Bioplastics Association and, in addition, they release their own specific composting symbols to indicate the organization emanating the certification. Certificates for biodegradable products are also released by the Italian Composting Association (CIC) [33], and by the Biodegradable Products Institute - BPI (United States) [34].

Figure 3 collects labels for compostable plastics released by the main certification organizations.

| European Bioplastics Association | Vincotte | Din Certco | Italian Composting Association (CIC) | Biodegradable Products Institute (BPI) |

Figure 3. Main certification organizations attesting industrial compostability and their respective labels.

In addition to industrial compostability certifications, other certifications exist for home composting by both DIN Certco and Vincotte, that guarantees complete biodegradability in garden compost pile (home composting). The temperature in home composting process is lower and less constant than in an industrial composting environment and smaller volumes of waste are involved. For those reasons composting in the garden is a more difficult, slower process with respect to industrial composting process. Furthermore, Vincotte developed specific certification marks to guarantee complete biodegradation in soil or in water [19].

1.2. Bio-based building blocks for polymer synthesis

Bio-based polymers can be produced by conventional chemical routes from building blocks synthesized using renewable sources. Such polymers are 100% bio-based if their monomer/s totally derive from renewable sources; whereas they are partially bio-based if both bio- and fossil-derived monomers are used in the polymerization to produce the polymer.

Polylactid acid (**PLA**) a thermoplastic aliphatic polyester, and highly versatile polymer, is an example of 100% bio-based polymer since it result from polymerization of **lactic acid** (2-hydroxypropionic acid) which is produced via bacterial fermentation of carbohydrates from different renewable sources like corn starch, sugarcane, molasses.

PLA is produced either by polycondensation of lactic acid or by ring-opening polymerization (ROP) of lactide, the cyclic dimer of lactic acid. Because of some

limitations of the polycondensation process (necessity to remove the water generated, long reaction time, high temperature used), especially the fact that only PLA with low molecular weight can be produced, the ROP is the process industrially used to produce this aliphatic polyester with high molecular weight. The starting lactide monomer is the result of the depolymerization of oligomers which are in turn produced by polycondensation of lactid acid [35].

PLA being a thermoplastic material, it can be processed by different routes (injection moulding, blow moulding, fiber spinning, etc) to be converted in various forms. Currently PLA sectors of application include packaging (cups, bottles, films, trays), textiles (shirts, furniture), electronics (mobile phone housing), agriculture and cutlery [9,36,37]. Biodegradability and biocompatibility make PLA useful also for biomedical applications [38].

Today PLA is one of the most important bio-based plastics although improvements on downstream processing of lactic acid, material processing and property are still in progress [9].

Vegetable oils are important building blocks for bio-based polymers production. They are extracted from the seeds or fruits of various plant species.

Castor oil is extracted from *Ricinus communis* and it consists mainly of esters of 12-hydroxy-9-octadecenoic acid (ricinoleic acid) [39]. The susceptibility to chemical reactions due to the presence of hydroxyl groups and double bonds make it a versatile raw material for the production of building blocks like 1,10 decanediamine, sebacic acid and 11-amino undecanoic acid that are typical monomers of **polyamides** (**PA**).

Polyamides (also known under the name nylons) are synthesized by polycondensation of diamines and diacids, or ring-opening polymerization of lactams. They are widely used as engineering thermoplastics in automotive, packaging, electronics and electrical applications. Some of them are commercially available products from renewable source like polyamide 11 (PA11) and partial bio-based polyamide 6,10 (PA6,10) [40].

Polyamide 11 (**PA11**) is produced by polycondensation of 11-aminoundecanoic acid (C11) which is obtained by castor oil methanolysis to yield methyl ester of ricinoleic acid followed by various chemical reactions [39]. PA11 has a low amide to methylene group

ratio (1:10) that confers to the polymer an excellent dimensional stability and toughness at low-temperature. Like the other polyamides, PA11 possess good resistance to oils and solvents, fatigue and abrasion resistance and good mechanical properties.

Currently, PA11 is produced by the Company Arkema (France) under the name Rilsan 11 and it is used for a wide range of applications like hydraulic hoses for vehicles, electrical cable and optical fiber sheathing, food packaging film, ultra tough sports socks, travel bags etc. PA11 is also used in pipes for natural gas transportation due to its exceptional resistance at high pressures and good barrier properties allowing to minimize the methane emissions [41].

In this work, structure-property relations in PA11 polymers with both linear and star architectures (linear chains linked to a central core) will be described. Both the rheological and the solid-state characterization of PA11 star samples with different arm number and length have been performed in order to investigate the impact of such architectural modifications on PA11 properties.

Other building blocks produced from castor oil are s**ebacic acid** (C10) and **1,10-Decanediamine** (C10).

Sebacic acid is obtained from ricinoleic acid which is in turn produced by castor oil heating with alkali at high temperatures. Polymerization of sebacic acid and hexamethylene diamine (HMDA) give **polyamide 6,10** (**PA610**), while 1,10-Decanediamine and sebacic acid polymerize into **PA10,10** [39].

The building block **hexamethylene diamine** (**HMDA**) can be also produced from renewable source as product of glucose fermentation or from bio-based propylene [42]. Indeed, adipic acid can be produced from glucose fermentation and converted by chemical process (amidation and dehydration) into adipodinitrile which is the starting material for the production of HMDA and **ε-caprolactam** (C6). Adipic acid and HMDA are polymerized into **polyamide 6,6** (**PA6,6**), while from ε-caprolactam (C6) polymerization **polyamide 6** (**PA6**) is obtained. The latter monomer, ε-caprolactam, can be also produced starting from the amino acid lysine, another product of glucose fermentation [42].

Succinic acid (1,4-butanedioic acid) is an important building blocks for polymers and other intermediates like 1,4-butanediol (BDO) and tetrahydrofuran (THF) produced by succinic

acid hydrogenation. Such dicarboxilic acid traditionally produced from n-butane via chemical synthesis, can be produced via anaerobic fermentation by using various microorganisms and sources like starch and different C5 and C6 sugars. [42]. Succinic acid and its derivatives diamines and diols can be used as monomers for production of polyesters, polyamides, and polyester amides [43]. Among such polymers, **polybutylenesuccinate (PBS)** and its copolymers, represent a family of biodegradable polyesters useful in a wide range of applications [43,44]. They are currently started being commercialized from bio-succinic acid by companies like Showa Denko (Japan) and Mitsubishi Chemical (Japan) [7,44].

1,4-Butanediol (BDO) produced from succinic acid is a raw material for the production of **polybutylene terephthalate (PBT)**, an engineering polymer used in automotive, electrical and electronics industries [45].

Ethanol, produced by fermentation of sugars, in addition to its bio-fuel utilization, can be used to obtain ethylene by dehydration. Ethylene is the building block for production of polyolefins like **polyethilene** (**PE**), and an important intermediate to produce polypropylene (PP), polyvinylchloride (PVC), polyethylene terephthalate (PET), polystyrene (PS) and polyols for polyurethanes (PUR) [9,46].

Polyolefins, PE and PP, cover the largest share of plastic market in Europe, followed by PVC mainly used in building and construction [47].

Polyurethanes (**PUR**) are high performance and versatile polymers which are produced from isocyanates and **polyols**. Although the potential production of isocianates from renewable sources is not excluded [48], many efforts have been made in the recent years in replacing petroleum-derived polyols with those bio-sourced due to the many possibilities for production of such building blocks from renewable source. Those include the use of vegetable oils (castor oil, rapeseed oil), bio-based 1,3-propanediol and sugars like sorbitol and sucrose [5].

1,3-propanediol (**PDO**) is currently produced from renewable sources by the joint venture DuPont Tate&Lyle BioProducts [49]. They developed a process in which PDO is produced from corn sugar and engineered bacteria in a single fermentation stage with the further advantage to obtain higher product purity with respect to that produced by conventional

chemistry [50]. Bio-PDO and dimethyl terephthalate (DMT) or terephthalic acid (TPA) are used to produce by polycondensation **polytrimethylene terephthalate (PTT)**, a thermoplastic non biodegradable polyester which can be used either alone or in conjunction with other polymers to obtain materials with similar properties to those of conventional plastics like Polyamide 6 (PA6), polypropylene, (PP) polybutylene terephthalate (PBT) [50].

Polyethylene terephthalate (PET), one of the widely used polyesters especially in beverage packaging, is obtained by polyesterification of terephthalic acid (TPA) with ethylene glycol. The latter monomer can be produced from bio-based ethylene by oxidization to ethylene oxide, followed by its hydrolysis [51]. Possibilities to produce **terephthalic acid (TPA)** from renewable sources include the use of bio-iso-butanol from glucose to produce through several processing steps para-xylene monomers [42]. Alternatively, TPA could be replaced by bio-derived compounds as 2,5-furandicarboxylic acid (FDCA) [52] to produce furanic polyesters as substitute of PET applications [53].

Large amounts of **glycerol** are generated as by-product of biodiesel production and they can be exploited to produce a wide range of chemicals as diols, diacids, hydroxyacids for polymers production like polyesters [54,55]. Glycerol can also be used as the starting material for the production of **epichlorohydrin** (**ECH**), the basic compounds of **epoxy resins**, largely used materials especially in electrical and structural applications [9].

The commercial application of the new bio-based polymers depend on the feasibility of the production process, cost of the raw materials, purity of the product obtained. With the increasing interest in renewable sources and knowledge about biomass conversion to useful products it is expected that the number of bio-sourced building-blocks will constantly extend [40].

1.3. Polymers directly extracted from renewable sources

Among polymers from renewable sources directly extracted and separated from biomass are polymers like starch, cellulose, alginates, chitin and chitosan.

Cellulose is one of the first natural polymers used by humanity and it still continues to represent a resource. It is a linear polysaccharide in which glucose units are linked by β-

13

1,4-glycosidic bonds. The establishment of a regular network of intra- and inter-molecular hydrogen bonds between chains leads to a hierarchical structure: cellulose chains are self-assembled in crystalline microfibrills and amorphous regions that are in turn organized in cellulose macrofibrills. Cellulose is the predominant constituent of cell walls of the plants, green algae and of some flagellates, in membranes of most fungi and tunic of sea animals (Tunicatae) [56]. In the native state cellulose is often found assembled to other minor components with complex interactions such as lignin, hemicellulose, pectin. Several types of microorganisms are able to extracellularly synthesize highly pure cellulose which finds applications mainly in food and biomedical fields [9,57-60]. However, large-scale applicability of bacterial cellulose is difficult because of the high prices and low yields achieved through current fermentation processes [7,9,59].

Molecular structure of cellulose determines the characteristic properties of cellulosic materials such as relative surface reactivity usable for chemical modifications, hydrophilicity, chirality, biodegradability [9,61-63]. High tensile strength, high modulus and low density of cellulose fibers (1.5 g/ml) compared to glass fibers for example (density = 2.5 g/ml), make them good candidates as reinforcing agents in composites [61,64]. Also, nanocomposites based on cellulose nanocrystals (also named as microcrystals, whiskers, nanowiskers) isolated through specific method (mechanical, chemical) from different cellulose sources (e.g wood [65], bacterial cellulose) have been widely investigated. Such materials having high tensile strength can improve mechanical and barrier properties at low filler content and they exhibit some potentially useful changes also in electrical, optical, dielectric, conductive properties with respect to their micro counterparts [66,67].

Today, cellulose esters (cellulose nitrate, cellulose acetate), cellulose ethers (carboxymethyl cellulose, hydroxyethyl cellulose) and regenerated cellulose (precipitated from solution, e.g. rayon fibers) are the derivates mainly used for a wide range of applications like food, personal care, pharmaceuticals, paint, film and fiber applications [68-70].

Other highly abundant polysaccharides present in nature are starch, chitin and chitosan.

Starch is produced by green plants and differently from cellulose it is stored in granules as energy reserve. Starch consists of two macromolecular components: the almost linear amylose with α-(1–4)-linked D-glucose units and branched amylopectin with α-(1–4)-

linked D-glucose backbone and side chains linked via a glicosidic bond to the C-6 of the backbone sugar rings [71].

Native starch granules are mainly used in plastic applications as rigid fillers [72], as additives in polymers to enhance their biodegradability due to voids formation and consequentially increasing of matrix porosity when starch degradation takes place [73,74]. Alternatively, in order to use starch as the main polymer component and to process it as a thermoplastic material, a destructuring treatment i.e. gelatinization is adopted in which the starch semi-crystalline granule structure is destroyed. The resulting materials are referred to with the name of thermoplastic starches (TPS) since they can be processed following conventional plastic processing techniques (injection moulding, extrusion).

TPS materials as well as native starches can be chemically modified (through esterification, etherification, cross-linking) [75], blended with other polymers [76-78], used in composites [79-81] with applications mainly in food packaging sector. Examples of starch based products commercially available today [7] are Materbi from Novamont-Italy [82], Biopar from Biop-Germany [83] used in packaging, food packaging, health care.

Chitin is a structural polysaccharide like cellulose that is highly abundant in nature and it is the organic constituent of the exoskeleton of insects and of crustacean shells. The chemical structure of chitin resembles that of cellulose (glucose units linked by β-1,4-glycosidic bonds) except for the presence of an acetamido group at position C-2 instead of an hydroxyl. **Chitosan** is produced from chitin by fully or partially removing the acetate moieties at C-2 through alkaline or enzymatic hydrolysis [84]. Such aminopolysaccharide can be used as functional material though chemical and structural modifications to impart desired properties and functions (formation of cross-linked networks or complexation with small anionic molecules to form hydrogels) with a wide range of potential applications especially in biomedical sector due to its biocompatibility, biodegradability and non-toxic properties: drug [85] and gene delivery systems [86], antibacterial agents [87] scaffold for tissue engineering [88], biosensors and nanoparticles [89] and other applications (water treatment, cosmetics) [90].

Alginates are a family of polysaccharides present in algae and also produced by bacteria [91]. They are copolymers constituted by 1–4-linked α-L-guluronic acid and β-D-

mannuronic acid blocks with sequence distributions varying with species of origin and with harvesting season in the case of algal sourced alginates [92]. The ability to form thermostable gels in presence of counterions (e.g. Ca^{2+}), to stabilize aqueous dispersions and emulsions and the positive effects on human health of alginates, make them and alginate derivates useful in food, pharmaceutical and medical applications [93,94] like food additives [95,96], wound dressings [97], formulations for preventing gastric reflux [98], etc.

Examples of naturally-occurring polymers diverse from polysaccharides are proteins like collagen and wheat gluten. **Collagen** is found in the extracellular matrix and in connective tissue and it is used as a biomaterial especially in tissue engineering applications [99,100]. **Wheat gluten** is a mixture of protein by-products of the starch fabrication. It has been used as functional material in different applications like natural superabsorbent materials [101,102], and film coatings for packaging [103-105].

1.4. Polyesters synthesized by bacteria: Polyhydroxyalkanoates (PHAs)

Polyhydroxyalkanoates (PHAs) are aliphatic polyesters synthesized as intracellular carbon and energy reserve by various microorganisms comprising Gram-negative and Gram-positive bacteria, aerobic (cyanobacteria) and anaerobic photosynthetic bacteria and some archaebacteria [106]. Within the cytoplasm of the cells, PHAs are stored in form of insoluble, amorphous and osmotically inert inclusions i.e. **granules** which are complex structures consisting of a coating layer of proteins (mainly phasins) and possibly phospholipids that surround the polyesters [107]. Bacteria use carbon sources to produce PHA granules in condition of nutrient limitation (nitrogen, phosphorous or oxygen) to prevent starvation ensuring the cells growth.

PHAs are fully bio-based polymers that are also biodegradable in almost all environments including soil and sea water [106].

The best known PHA is the homopolymer poly-3-hydroxybutyrate, PHB was firstly described in 1920s by the French bacteriologist Lemoigne who isolated and characterized this polymer from *B. megaterium* bacteria [108,109].

In most bacteria, PHB is synthesized from acetyl-CoA by a sequence of three enzymatic reactions: 3-ketothiolase catalyze the condensation of two molecules of acetyl-CoA to form acetoacetyl-CoA; acetoacetyl-CoA is reduced to 3-hydroxybutyryl-CoA by NADH-linked acetoacetyl-CoA reductase; finally, PHB synthase polymerizes 3-hydroxybutyryl-CoA into PHB [110]. When bacteria is in condition of nutrient limitation, the polymer degradation is activated by PHB depolimerase and it is reconverted to acetoacetyl-coA by enzymatic reactions to close the cyclic PHB metabolic process [110].

Since PHB discovery, a great number of bacteria strains capable of PHA synthesis (around 300) and more than 150 type of monomers were discovered [111] thank to the biotechnological processes development.

PHAs have the general **structure** shown in Figure 4 where x is 1 for the most PHAs and R can be either hydrogen or hydrocarbon chain of variable length.

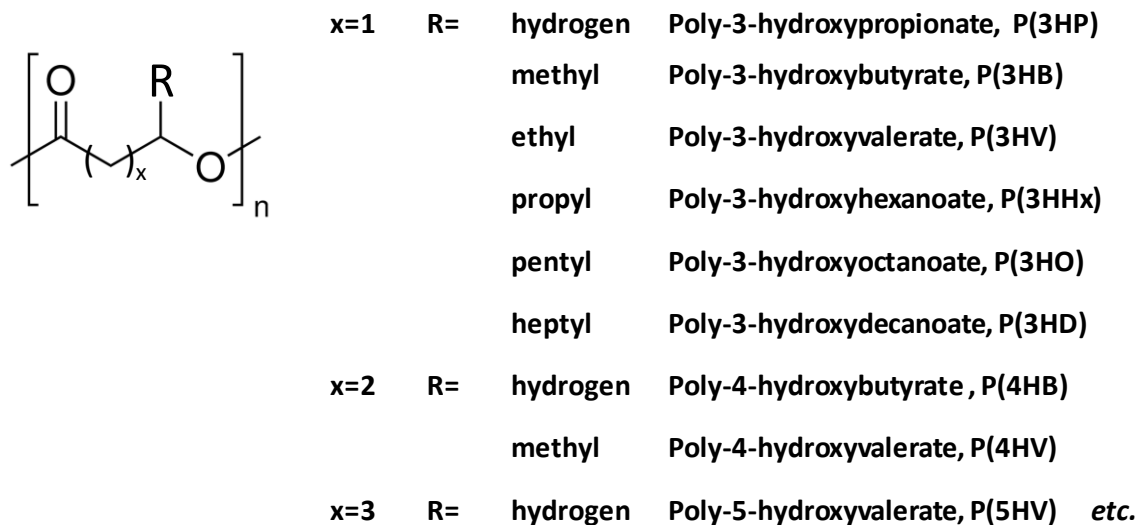|			
x=1	**R=**	**hydrogen**	**Poly-3-hydroxypropionate, P(3HP)**
		methyl	**Poly-3-hydroxybutyrate, P(3HB)**
		ethyl	**Poly-3-hydroxyvalerate, P(3HV)**
		propyl	**Poly-3-hydroxyhexanoate, P(3HHx)**
		pentyl	**Poly-3-hydroxyoctanoate, P(3HO)**
		heptyl	**Poly-3-hydroxydecanoate, P(3HD)**
x=2	**R=**	**hydrogen**	**Poly-4-hydroxybutyrate, P(4HB)**
		methyl	**Poly-4-hydroxyvalerate, P(4HV)**
x=3	**R=**	**hydrogen**	**Poly-5-hydroxyvalerate, P(5HV)** *etc.*

Figure 4. General structure of polyhydroxyalkanoates (PHAs).

According to the number of carbon atoms in the monomer units, two main classes of PHAs are usually distinguished [111]:

-   short-chain-length (scl) PHAs: R= 3–5 carbon atoms;
-   medium-chain-length (mcl) PHAs: R= 6–18 carbon atoms;

The fist class includes monomers like 3-hydroxybutyrate and 3-hydroxyvalerate, while mcl-PHAs comprise 3-hydroxyhexanoate, 3-octanoate, etc.

The type of PHA produced strongly depends on the bacterial strain and on the carbon substrate used. *Cupriavidus necator* (also named *Alcaligenes eutrophus* or *Ralstonia eutropha*), one of the most extensively studied microorganisms, is able to produce scl-PHAs [112], while *Pseudomonas oleovorans* and *Pseudomonas putida* [113] synthesize mcl-PHAs.

Most of the PHA monomers are optically active due to the presence of a chiral carbon and they exist in R-configuration, although linear monomers like 4-hydroxybutyrate, 4-hydroxyvalerate can also be produced. P(3HB-co-4HB) copolymers were produced in *Alcaligenes eutrophus* using as carbon sources 4-hydroxybutiric acid or γ-butyrolactone [114,115].

PHA random copolymers with different monomer type and composition are produced through the addition of the suitable precursors (co-substrates) to the carbon sources in the growth media during fermentation processes. For instance, propionic acid or valeric acid are used to produce the most known copolymer of this family, poly(3-hydroxybutyrate-co-3-hydroxyvalerate), P(3HB-co-3HV) also abbreviated as PHBV, constituted of the monomers with R= methyl and R= ethyl (Figure 4) [116,117]. Block PHA copolymers can also be produced by using periodic co-substrate addition to the growth media [118,119].

1.4.1. PHAs production: fermentation process and recovery from the cells

Currently, PHAs are produced industrially using feedstocks like sucrose and fatty acids fermented by **pure cultures** of either natural or genetically engineered microorganisms such as recombinant strains of *Escherichia coli* [120,121].

Fermentation processes are most often operated in two-stages in a batch reactor where the cells at first grow in a medium enriched of nutrients and carbon source ('growth phase'). Then, limitation of an essential nutrient (oxygen, phosphorous or ammonium) activates the production of PHAs which are accumulated during the second stage ('accumulation phase'). To produce PHA copolymers, the suitable precursor is added to the carbon substrates during the second fermentation stage. Due to the cyclic PHA metabolism in

18

which synthesis and degradation of the polymer occur simultaneously in condition of nutrient limitation, PHA homopolymer produced in the first stage is replaced by PHA copolymers [122].

Bacterial cells may accumulate up to 90% of their cell dry weight (CDW) by means of this process [111].

Many efforts are being made to improve fermentation process efficiency and to lower PHA production costs in order to widen PHA uses, those including the use of inexpensive carbon substrate and of mixed microbial cultures (MMCs).

Different renewable vegetable oils and various waste products can be successfully used as carbon substrate like olive oil, corn oil, palm oil [123], soybean oil [124], mixture of palm oils [125], waste frying oils [126], molasses [127], olive oil mill effluents [128], etc.

The use of mixed microbial cultures (e.g. activated sludge) is an active research field. Mixed cultures offer important advantages as simpler process control, no requirement of strict sterilization conditions as needed for pure cultures and a better adaptability to complex waste feedstocks. It was observed that in such MMCs the absence of an external substrate for a certain period of time ('famine') causes a decrease in the amount of intracellular components needed for cell growth. When a period of excess of carbon ('feast') follows, storage becomes the favorite mechanism of substrate removal due to the fewer enzymes required for PHA storage opposed to cell growth [129,130]. Under unsteady conditions in which the cells are subjected to intermittent substrate availability (feast/famine cycles), the microorganisms continuously adapt to the new conditions. Microorganisms which are able to quickly use substrate to grow are favorite and this results in natural selection of a robust population having an enhanced ability to produce PHAs [130]. In the last decade, reactors simulating feast and famine conditions called sequencing batch reactors (SBR) were operated by many authors representing a very promising solution for industrial PHA production [131-135].

Although, the physicochemical properties of PHAs obtained by pure cultures have been largely studied [110,111], those of PHAs produced by MMCs have been scarcely investigated [130,136]. Due to the numerous and different organisms present and thus the

various PHA production pathways possible, much effort should be dedicated to investigations on composition and properties of PHAs produced by MMCs.

PHA production in transgenic plants has also been investigated over recent years [137]. Although this approach is interesting from a scientific point of view, it appears rather infeasible.

Fermentation process is followed by **PHA recovery from the biomass** (downstream process) i.e. polymer extraction from the cells and purification which plays a fundamental role in determining the overall PHA production costs and final material quality.

The oldest method of PHA recovery is the application of organic solvents such as chloroform [138] in which the polymer is soluble. After solubilization, in order to separate PHA from the solvent, usually the polymer is precipitated in a PHA non-solvent (solvent in which PHA is insoluble) and then the polymer is recovered by common techniques like centrifugation or filtration. Although solvent extraction allows both high yield of recovery and high degree of purity, this method is not environmentally friendly and, since it consumes a large quantity of solvents, it is not economically feasible for large-scale productions.

Many alternative downstream processes [139] have been proposed. Opposed to solvent extraction, they consist in solubilization of the non-PHA cell mass − NPCM (digestion treatment). Those include the use of alkali alone [140,141] or in combination with acids [142], surfactants [143,144], surfactants combined with chelates [145,146] or alkaly [147], enzymes and chemicals [148-151].

In addition to chemical disruption, recovery methods can employ heat or mechanical treatment (e.g. bead mill, high pressure homogenization) to cause lysis of the cells although their use has to be avoided when it is expensive and not easily industrially scalable [152,153]. Particularly interesting are the methods in which autolysis of the microbial cells is stimulated by specific cultivation conditions to facilitate the subsequent PHA recovery procedure [154].

After digestion treatment, PHA granules are separated from the NPCM by centrifugation or filtration techniques.

Efficiency of the recovery method employed is measured by the yield and purity of PHA recovered from the cells, with the latter (level of purity) depending on the specific requirement for polymer application.

Applicability of the recovery procedure has to be evaluated taking into account, among various factors, the impact of the isolation method on PHA final properties. Indeed, the recovery procedure applied should selectively act on NPCM avoiding PHA molecular weight decrease and a consequential detrimental effect on material properties [155].

It is known that within the cells PHAs exist in a 'rubbery' amorphous state to be readily utilizable (depolimerized and metabolized i.e. mobilization) mobilized as necessary [156,157]. Crystallization doesn't occur in such isolated granules because of the low nucleation rate of PHAs and they require an external nucleating agent to start the process. If the coating layer surrounding the PHA amorphous granules is damaged, heterogeneous nucleation is promoted and thus rapid crystallization of the polymer occurs [158].

Generally, recovery methods cause removal of such coating layer leading to PHA crystallization [159]. However, by means of specific extraction procedures that allow to keep granule coating intact, it is possible to recover PHA granules in their amorphous state i.e. native form [159]. Native PHA granules are recovered in latex form i.e. aqueous PHA granules suspension suitable for specific applications like paints, lacquers and surface treatments of paper such as sizing and coating [160,161].

In this work, a recovery method that allow to recover native PHAs granules will be described. The recovered polymer is deeply characterized in order to investigate on the impact of the extraction procedure applied on PHA properties.

1.4.2. PHAs properties and applications

Due to the different structures whose PHAs can be made of, such polymers exhibit different properties ranging from those of hard materials (e.g. PHB, PHBV) to elastomeric ones (e.g. poly-3-hydroxybutyrate-co-3-hydroxyhexanoate, PHBHHx).

The most studied PHA of this family, **PHB** has molecular weight typically in the range around $1 \cdot 10^4$ - $3 \cdot 10^6$ Da and polydispersity which depend on cultivation conditions like temperature and pH, type and concentration of substrate, microorganism strain used

[106,110]. PHB produced by an engineered Escherichia coli strain with higher molecular weight ($2 \cdot 10^7$ Da) has also been reported [162].

PHB is a highly crystalline (60-80%), thermoplastic polymer characterized by glass transition temperature (T_g) and melting point (T_m) around 4°C and 180°C, respectively [110]. The high crystallinity amount is responsible of the excellent PHB resistance to solvents; whereas it shows low resistance to acids and bases.

PHB has Young's modulus and tensile strength around 3.5 GPa and 40 MPa respectively, similar to those of polypropylene (PP); however, the elongation at break of PHB is very poor (1-2%) and therefore it behaves as a brittle and stiff material [106,110].

Another drawback is the narrow processing window of PHB because it undergoes thermal degradation slightly above its melting point. Thermal degradation occurs following a mechanism of random chain scission at the ester groups according to a β-hydrogen elimination, with a consequent decrease of molecular weight [163]. Therefore, the polymer can be processed by conventional techniques like injection molding but carefully controlling conditions like temperatures and residence times.

A common way to reduce melt temperatures of PHB is through incorporation of valerate units leading to random PH(3HB-co-3HV), PHBV, copolymers.

PHBV copolymers show the rare phenomenon of isodimorphism, firstly observed by Bluhm et.al in 1986 [164]. Whereas most of random copolymers with monomers capable to crystallize become amorphous at intermediate compositions due to the incompatibility of the crystal lattices, PHBV compolymers show high crystallinity (>50%) over the whole composition range exhibiting the crystal phase of either homopolymer depending on the composition range. In such isodimorphic systems, each homopolymer crystallizes in its own crystal lattice accommodating foreign comonomer units up to a given extent. At a given composition (around 40 HVmol% in PHBV) the crystalline phase changes from the one lattice to other and the melting point reaches a minimum showing an eutectic-like behavior [165,166].

This phenomenon is peculiar to PHBV copolymers and it is not observed in other PHA copolymers [111,166,167].

Incorporation of hydroxyvalerate units to obtain random PHBV copolymers also leads to a less brittle material showing a reduction of Young's modulus from 3.5 GPa for 100mol% 3HB to 0.7 GPa for copolymer with 25mol% valerate content [168]. The increase in impact strength with increase of valerate content observed is relatively small due to the high value of crystallinity present over the whole composition range [165,166].

In order to improve PHA properties, substances such as nucleating agents, plasticizers, antioxidants, photostabilizers, or other polymers are usually blended with commercial PHAs. Nucleating agents are used to increase crystallization rate limiting secondary crystallizations of the polymer [169].

Plasticizers are usually low molecular weight substances that added to the polymer enhance molecular mobility of the amorphous phase by increasing the free volume (the volume fraction not occupied by the macromolecules) and thus lowering the glass transition temperature. They are generally used to improve polymer processing and impact properties [170].

The use of different substances as suitable plasticizers for PHB and PHBV have been studied, like vegetable oils (e.g. soybean oil), triethyl citrate (TEC) [171], acetyl tributyl citrate (ATBC) [172], polyethylen glycol (PEG) [173-175] glycerol triacetate (GTA) [176,177]. In addition to lower values of Tg with respect to the neat polymer, in most cases the plasticizer leads to decreasing stiffness and increasing elongation at break of PHAs [171,173-177].

Blending PHAs with other polymers and the use of fiber as reinforcement are useful approach to improve polymer properties.

Blends of PHAs with other polymers has been widely investigated. It was found total or partial miscibility of PHAs in the molten state (the blend exhibits single values of T_g dependent on composition) with some polymers like polyethylene oxide (PEO) [178-180], cellulose derivates [165,181], polyvinyl phenol (PVPh) [182], polyvinyl acetate (PVAc) [183], whereas immiscibility was observed with many other polymers like polybutylene adipate (PBA) [183], poly-L-lactic acid (PLLA) > 20 kDa [184], Polycaprolactone (PCL) [185], etc.

PHA **composites** have been prepared by incorporation of reinforcing fillers like organo-modified montmorillonite clay [172], different cellulosic fibers as flax fibers [160,186], wheat straw [187,188], maple wood [189], kenaf fibers [190].

PHAs are polyesters that can be processed to be converted into various products like injection-molded articles, film and sheet, fibers, paints, foams, coated articles. PHAs are suitable materials for various application fields like cosmetic, health care, packaging and food packaging. Indeed, PHBV from Telles and from Tianan being toxicologically safe have received certification by FDA (Food and Drug Administration) for use in food contact applications [191,192].

PHAs are widely used in biomedical sector due to their biocompatibility and biodegradability in applications like sutures, meniscus repair devices, bone plates, surgical mesh, drug delivery, tissue repair/regeneration devices, etc. [193-198].

Today, PHAs are in an early stage of large commercialization with still small capacity production compared to petrochemical plants.

The PHAs products available in the market are principally PHB and PHBV copolymers [5]. Tianan Biological Material Co. Ltd. (China) is the first large-scale PHBV producer in the world with an annual capacity of 2,000 tonnes with the plan to further expand their production.

Other company like PHB Industrial (Brazil) announce to increase their production from pilot to large scale [5].

The high price of PHAs still prevents their large use. However, the material cost could be reduced by improving fermentation process by using inexpensive feedstock as an example, by adding cheaper product to the final polymer. Furthermore, PHAs modifications (e.g. blending with low cost substances) to improve material properties could extend polymer performances and simultaneously applicability of such polymers.

In the present work, the impact of fermentation process (e.g. carbon substrate used), recovery methods and PHAs modifications on polymer properties have been investigated.

2. MATERIALS AND METHODS

2.1. Materials

Table 1 lists all polymers used in this work with their composition and suppliers.

Table 1. Polymers used in this work.

Polymer	Composition	Supplier
Poly3-hydroxybutyrate, PHB	-	Department of Chemistry, Universidade Nova de Lisboa (Portugal)
		BIOMER (Germany)
Poly(3-hydroxybutyrate-co-3-hydroxyvalerate), PHBV	HV fraction (mol%): from 8 to 11 [a]	Department of Chemistry, Sapienza University of Rome, (Italy)
	HV=3 mol% [b]	Tianan Biologic Material Co. Ltd (China)
Poly(1,4-butyleneadipate), PBA	-	Sigma Aldrich (Italy)
Poly(3-hydroxybutyrate-co-butyleneadipate), P(HB-co-BA)	HB fraction (mol%): from 61 up to 66 [c]	Department of Chemistry, University of Catania (Italy)
Linear Polyamide 11, PA11	-	Dept. Chemistry, University of Milano (Italy)
Star Polyamide 11, PA11	Multifunctional agent content (mol%): from 0.125 up to 1.45 [d]	
Poly[3-(4-(methylene)piperidin-1-yl)propanoate], PMPP	-	Biomedical Engineering Department of Yale University (USA)
Polypentadecalactone, PPDL	-	
Poly[pentadecalactone-co-3-(4-(methylene)piperidin-1-yl)propanoate], Poly(PDL-co-MPP)	PDL fraction (mol%): from 21 to 82 [e]	

[a] determined by Gas Cromatography (GC), as described in [133].

[b] as reported by the supplier.

c) determined by proton nuclear magnetic resonance, ^{1}H-NMR, as described in [199].

d) amounts used in the feed.

e) determined by proton nuclear magnetic resonance, ^{1}H-NMR, as described in [200].

Polyhydroxyalkanoates (PHAs) produced via different fermentation processes have been studied:

(1) Poly(3-hydroxybutyrate-co-3-hydroxyvalerate) PHBV samples produced from mixed microbial cultures (MMCs) by Prof. Mauro Majone's research group (Department of Chemistry, Sapienza University of Rome, Italy) as previously described [133]. Either a synthetic mixture of acetic and propionic acid or olive oil mill wastewaters (OMW) were used as carbon substrate.

(2) Poly(3-hydroxybutyrate), PHB samples from pure culture (*Cupriavidus necator* DSM 428), provided by Prof. Maria Reis's research group of University of Lisbon (REQUIMTE/CQFB, Chemistry Department of FCT/Universidade Nova de Lisboa, Portugal). Different vegetable frying oils, also named used cooked oil (UCO), were used as the sole carbon source: a) soybean, b) a mixture of peanut and sunflower, c) a mixture of rapeseed, d) sunflower and grape seed, d) unknown fried oil from a canteen. After fermentation, PHAs were recovered by chloroform extraction.

A biomass enriched of PHAs was also provided by the University of Lisbon. It was produced by *Cupriavidus necator* bacterium grown on UCO (20 g L^{-1}) provided by the university canteen as carbon source. This biomass was used to perform PHA recovery experiments.
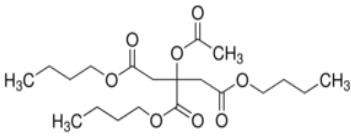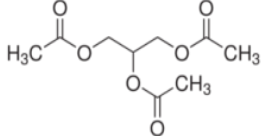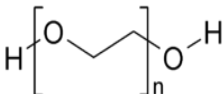
PHA recovery was carried out using the following substances: Na_2HPO_4, Alcalase 2.4L (protease from *Bacillus licheniformis*), sodium dodecyl sulfate (SDS) and ethylenediaminetetraacetic acid (EDTA). All chemicals were purchased from Sigma Aldrich (Italy) and used without further purification.

Commercial PHBV (HV 3 %mol) in the form of pellets (ENMAT Injection Molding Grade Y1000P) was provided by Tianan Biologic Material Co. Ltd (China). As reported by the manufacturer, PHBV contains less than 0.5% of unspecified nucleating agents and

antioxidants. Such copolymer was used as polymeric matrix for plasticized and composite materials preparation.

The following chemicals were purchased from Sigma Aldrich (France) and used as plasticizers for PHBV: Acetyl-tri-butyl citrate (ATBC), Glycerol triacetate (GTA) and Polyethylen glycol (PEG) with molecular weight 400 (PEG-400), 1000 (PEG-1000) and 4000 Da (PEG-4000). Table 2 reports the chemical structure, molecular weight and thermal properties of the chemicals indicated above, as reported by the manufacturer.

Table 2. Chemicals used for PHBV plasticization.

Family's substance	Substance Name	Chemical Structure	Molecular weight	Thermal properties	
				Tm (°C)	Tb (°C)
Citrates	acetyltributyl citrate, ATBC		402	-59	343
Acylglycerols	glycerol triacetate, GTA		218	-78	258
Polyethers	poly(ethylene glycol), PEG		400	4-8	-
			1000	35-40	-
			4000	58-61	-

Wheat straw fibers (WSF) used for the preparation of PHBV composites were provided by Nathalie Gontard's research group (Joint Research Unit, Agropolymers Engineering and Emerging Technologies, UMR-IATE, University of Montpellier 2 (UM2), CIRAD, INRA, SupAgro; Montpellier, France). Wheat straw fibers were obtained from wheat straw (*T. aestivum* 'Apache') by grinding processes (cut and impact milling) as described in [201]. The obtained particle size was determined in the range 100-150μm by light microscopy measurements [201]. The particle size is expressed as equivalent diameter which is the diameter of a circumference with the same area.

Poly(3-hydroxybutyrate-co-butyleneadipate), P(HB-co-BA) copolymers with different composition, were synthesized by Prof. Alberto Ballistreri's research group from Chemistry Department of University of Catania (Italy) by microwave-assisted transesterification as previously described [199]. After synthesis, each sample was purified by dissolution in chloroform and precipitation of the solution in ethanol. The product was re-precipitated three times and then dried in vacuum at 50°C for 24 h. Poly(1,4-butyleneadipate), PBA, and PHB were supplied by Sigma Aldrich (Italy) and BIOMER (Germany), respectively, and they were used without further purification.

Polyamide 11 (PA11) samples with linear and star architectures were provided by Prof. Giuseppe Di Silvestro's research group, Chemistry Department of University of Milano (Italy). Star-shaped samples were synthesized by using 11-aminoundecanoic acid (99% purity) as monomer and bis hexamethylendiamine (T3) or 2,2,6,6-tetra[β-carboxyethylcyclohexanone] (T4), as tri- and tetra-functional branching agents respectively. The synthesis was carried out in one-pot by adding the multifunctional comonomer during the polymerization step. A linear polyamide 11 was also synthesized using only 11-aminoundecanoic acid as monomer in the feed. All PA11 samples were synthesized in bulk at 240°C for 4 hours under nitrogen flow.

Novel Poly[3-(4-(methylene)piperidin-1-yl)propanoate], PMPP, homopolymer and Poly[pentadecalactone-co-3-(4-(methylene)piperidin-1-yl)propanoate], Poly(PDL-co-MPP), copolymers were synthesized via enzymatic catalysis by Prof. Zhaozhong Jiang of Biomedical Engineering Department, Yale University (USA), as reported in [200]. Immobilized CALB (*Candida antarctica* lipase B supported on acrylic resin) from Sigma Aldrich was used as enzymatic catalyst. The poly(PDL) (PPDL) reference homopolymer prepared via ring-opening polymerization [200] by Prof. Zhaozhong Jiang's research group was also provided. After synthesis, all of the samples were purified by precipitation from solution (see [200] for details).

2.2. Sample preparation

2.2.1. PHBV plasticization and reinforcement with fibers

PHBV was processed in a co-rotating twin-screw extruder Prism Eurolab 16XL (Termo Scientific, Germany) with a screw length to diameter ratio L/D= 40:1 (D= 15.6 mm). The extruder was assembled with an one-hole filament die of 3 mm in diameter.

Before processing, PHBV copolymer was dried over night at 60°C, whereas both powdery additives (PEG-1000 and PEG-4000, see Table 1) and wheat straw fibers were dried over night at 35°C.

The desired plasticizer content (5, 10 or 20%) was added during extrusion process using a syringe pump (KDS100, Kd Scientific) for liquid plasticizers (GTA, ATBC, PEG-400) and a gravimetric feeder (MiniTwin Feeder MT, Brabender) for those in the form of powder (PEG-1000, PEG-1500, PEG-4000). After extrusion, plasticized samples were cooled in a water bath and air-dried at room temperature (RT) before being cut using a Prism Eurolab pelletizer (Termo Scientific, Germany). The pellets obtained were stored at 60°C for at least 12h. Composites were prepared by extrusion of the plasticized PHBV pellets together with the wheat straw fibers (20%, w/w) that were fed to the extruder through the gravimetric feeder. The same procedure described above for plasticized PHBV (cooling, drying, cutting) was applied to the extruded composites.

Samples characterization was performed on sheets (average thickness=0.25 mm) prepared by hot-pressing the pellets between two Teflon coated plates with an appropriate spacer to control thickness, at 170 °C in a hydraulic press (PLM 10 T, Techmo). The samples were allowed to melt for 3 min, then a pressure of 150 bar was applied for 2 min. Finally, the samples were cooled at room temperature.

2.2.2. Polyamide films and injection-molded bars

PA11 samples were compression-molded between two Teflon coated plates Carver laboratory press at 210°C for 2 min. Then, a pressure of 27 bar was applied for 1 min. Sheets 0.2 mm thick were obtained using an appropriate spacer.

Sample bars were prepared by using a miniature mixing/injection molding machine, supplied with a rectangular mould. The samples were mixed for 1 min at 215 °C, they were

injection-molded into small bars ($30\times7.5\times2$ mm^3) and then the mold was quench-cooled in water.

2.3. Instrumental methods

2.3.1. Thermogravimetric analysis (TGA)

Thermogravimetric (TGA) measurements were carried out using a TGA 2950 (TA instruments). Only PHBV plasticized samples and composites were analyzed using a TGA-Q50 (TA Instruments) thermogravimetric analyzer. The analyses were performed at 10°C/min from room temperature to 600°C (700°C for PA11 samples) under air flow.

2.3.2. Differential Scanning Calorimetry (DSC)

Differential Scanning Calorimetry (DSC) measurements were carried out using a DSC-Q100 (TA Instruments) apparatus, equipped with a Liquid Nitrogen Cooling System (LNCS) accessory. The samples were initially heated up to above the melting temperature to cancel the previous thermal history. Then, temperature was lowered and DSC heating scans were run at 20 °C min^{-1} in helium atmosphere. The DSC temperature range explored is specified in Result and Discussion section. Controlled cooling at 10° C/min or quench cooling was applied between scans. Glass transition temperature (Tg) was taken at half-height of heat capacity increment. Crystallization (Tc) and melting (Tm) temperatures were taken at the peak maximum of the corresponding exotherm and endotherm. When multiple endotherms were present, the melting temperature was taken as specified in Result and Discussion section.   Temperature modulated DSC measurements (TMDSC) were performed from 10°C to 210°C. The heating rate of the TMDSC scan was 3 °C/min, the oscillation amplitude 0.32 °C and oscillation period 40 s.

2.3.3. Tensile test

Stress-strain measurements on polyamide and on PHBV samples (plasticized PHBV copolymers and composites) were carried out using an INSTRON 4465 and a Zwick tensile testing machine, respectively. At least five specimens of each sample were tested. Strain

rate and specimen shape are specified in Results and Discussion section. The results are reported as average values with standard deviation.

2.3.4. Dynamic mechanical analysis (DMA)

Dynamic-mechanical measurements were performed with a DMTA MkII (Polymer Laboratories Ltd) operated in the dual cantilever bending mode, at a frequency of 3 Hz and a heating rate 3°C/min, on samples in the form of injection molded bars ($30 \times 7.5 \times 2$ mm^3). The temperature range investigated was -150 to 160°C.

2.3.5. Wide angle x-ray diffraction (WAXS)

Wide-angle X-ray diffraction measurements (WAXS) were recorded at room temperature (RT) with a PANalytical X'Pert PRO diffractometer equipped with an X'Celerator detector (for ultrafast data collection). A Cu anode was used as X-ray source (K$_\alpha$ radiation: $\lambda =$ 0.15418 nm) and 1 degree divergence slit was employed to collect the data in the 2θ range from 3° to 60°. The degree of crystallinity (X_c) was evaluated as the ratio between the crystalline diffraction area (obtained from the total area of the diffraction profile by subtracting the amorphous halo) and the total area of the diffraction profile.

WAXS measurements above and below RT were performed by assembling an Anton Paar TTK-450 heating device with the diffractometer. Cooling and heating runs were performed at 3°C/min, with 50 s isothermal steps every 10°C to allow data collection.

2.3.6. Scanning electron microscopy (SEM)

Scanning electron microscopy (SEM) observations were performed using a Philips 515 Scanning Electron Microscope. Prior to examination, samples were deposited on a stub, they were dried and then sputter-coated with gold.

2.3.7. Transmission Fourier transform infrared spectroscopy (FT-IR)

Infrared spectra were recorded using a Nicolet 380 FT-IR spectrometer (64 scans from 4000 to 400 cm$^-$1; resolution: 2 cm$^-$1) on samples cast on KBr discs from chloroform solution.

3. RESULTS AND DISCUSSION

3.1. Production, recovery and characterization of bacterial Polyhydroxyalkanoates

3.1.1. Characterization of PHAs produced from waste feedstock

The high price of PHAs is the major limiting factor to their large use. Since the cost of the substrates (e.g. glucose, sucrose) used in the fermentation process plays a crucial role in determining the PHA production costs, the use of cheap feedstocks such as agro-industrial residues is a useful strategy to overcome this limitation. In the present work, PHAs produced from pure cultures using vegetable fried oils (also named used cooking oil, UCO) as carbon sources were characterized in order to evaluate the influence of such substrate on polymer properties. With the same aim, PHAs produced from mixed microbial cultures (MMCs) which are another promising alternative to lower PHA production costs [202], were also studied. At first, a synthetic mixture of acetic and propionic acid was used as substrate for PHA production from MMCs. This carbon substrate was selected taking into account that the acidogenic fermentation of agro-industrial byproducts typically generates organic acids with both even and odd number of carbon atom. Once the process performance was assessed, including the quality of the polymer produced, a real waste i.e. olive oil mill wastewater (OMW) was used as carbon source instead of the synthetic substrate. Both PHAs produced from synthetic substrate and OMW were characterized.

The research work on PHAs produced from MMCs was performed within the EU-Project EcoBioCap 'Ecoefficient Biodegradable Composite Advanced Packaging' (FP7/2011-2015).

3.1.1.1. PHAs from mixed culture: solid state characterization

PHAs produced by MMCs and using as substrate a synthetic <u>mixture of acetic and propionic acid</u> were investigated. The results of this work have been published in [133]. PHAs were produced in three successive stages: a) selection of PHA-storing microorganisms in a sequencing batch reactor; b) PHA accumulation in the cells; c) polymer recovery. In order to investigate whether composition and properties of the polymers produced changed during fermentation, the process was performed under

continuous operation for at least 180 days. During this period of time, samples were collected as described below. After 6h of PHA accumulation stage, the entire liquid volume of the reactor was automatically sent to an extraction reactor where it was mixed with a digestion solution (either NaOH 1 M or NaClO with 5% active Cl_2) in order to recover the polymer from the cells. Two digestion solutions were tested. On average, once a day all the content of the extraction reactor was centrifuged and the residual solids (mainly cell debris and PHA granules) were stored at -18°C. Finally, several frozen samples produced over one week of operation were collected and the mixture was lyophilized.

High productivity of around 1.43 g/L day was obtained at the end of the accumulation stage. As concerns yield and purity of the recovered polymer, in the case of NaClO extraction the values obtained were 100% w/w and 90% w/w; whereas when using NaOH both values decreased to 87 %w/w and 75% w/w. This points out the higher efficiency of NaClO as PHA extracting agent.

Gas chromatographic (GC) analysis of lyophilized samples revealed that the obtained PHAs were PHBV copolymers with HV fraction in the range from 8 to 13 %mol were obtained. The observed composition fluctuations can be attributed to the intrinsic dynamics of MMC biological processes, since the carbon mixed substrate as well as the operating conditions were not changed during the whole production process.

PHBV lyophilized samples were characterized by Thermogravimetric (TGA) and Differential Scanning Calorimetry (DSC) analyses.

Figure 6 compares two TGA curves of PHBV samples recovered by NaClO and NaOH treatments respectively, taken as an example. The results indicate that PHBV samples recovered using NaClO are thermally stable up to 200°C (weight loss <1% at this temperature) and that they degrade in a single step showing temperature of maximum degradation rate (Tmax) in the range 281–291°C. It is known PHBV thermal degradation is associated with random scission of the polymer chain leading to evolution of crotonic acid [163,203]. A different thermal behavior was observed for PHBV samples recovered by NaOH digestion, as illustrated in Figure 5. Such samples show lower thermal stability, with an initial weight loss of about 3% between room temperature and 100°C and then a main degradation step with Tmax in the range 212–216°C which is associated with PHBV

thermal degradation. The curve also show multiple degradation steps in the T-range of 300-600°C that are attributed to thermal degradation of cellular debris still present in the recovered samples as indicated by the lower PHA purity obtained by NaOH recovery (75% w/w vs 87% w/w).

Comparison of the results on all available samples examined shows that they exhibit curves similar to those shown in Figure 5. Thus, it can be concluded that PHA thermal stability is not significantly influenced by the operation time of the PHA-producing reactor (over the 180 days investigates), while it is strongly affected by the extraction agent used (NaClO or NaOH).
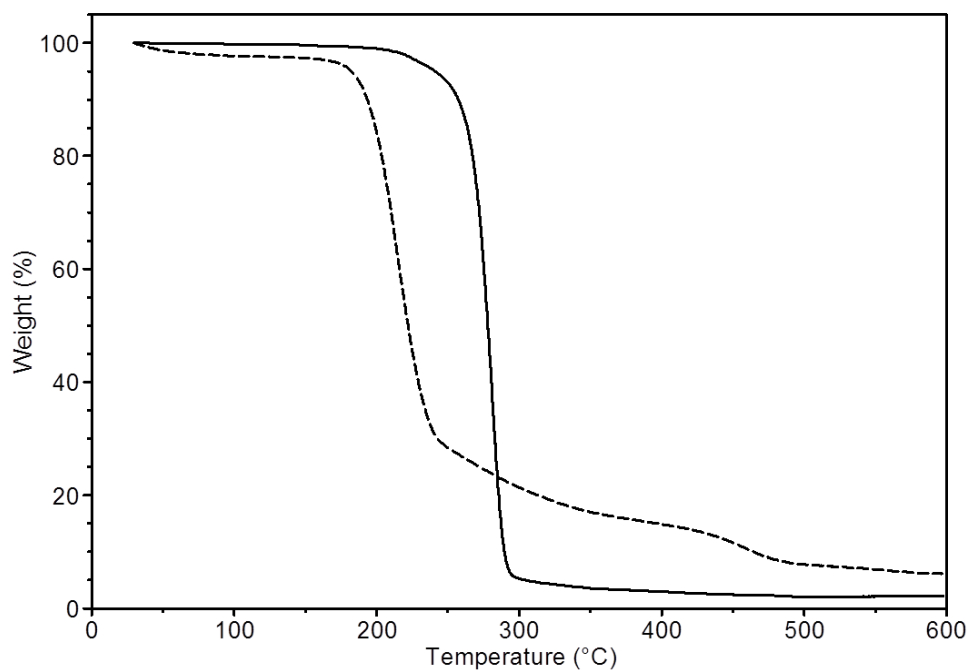

Figure 5. Typical TGA curve of PHA produced using the synthetic substrate. The polymer was recovered by using either NaClO (continuous curve) or NaOH (dash curve).

Differential scanning calorimetry (DSC) was performed on lyophilized PHA samples at 20°C/min from -80 up to 210°C after quench cooling. The DSC curve of a PHBV sample recovered using NaClO is shown as an example in Figure 6.
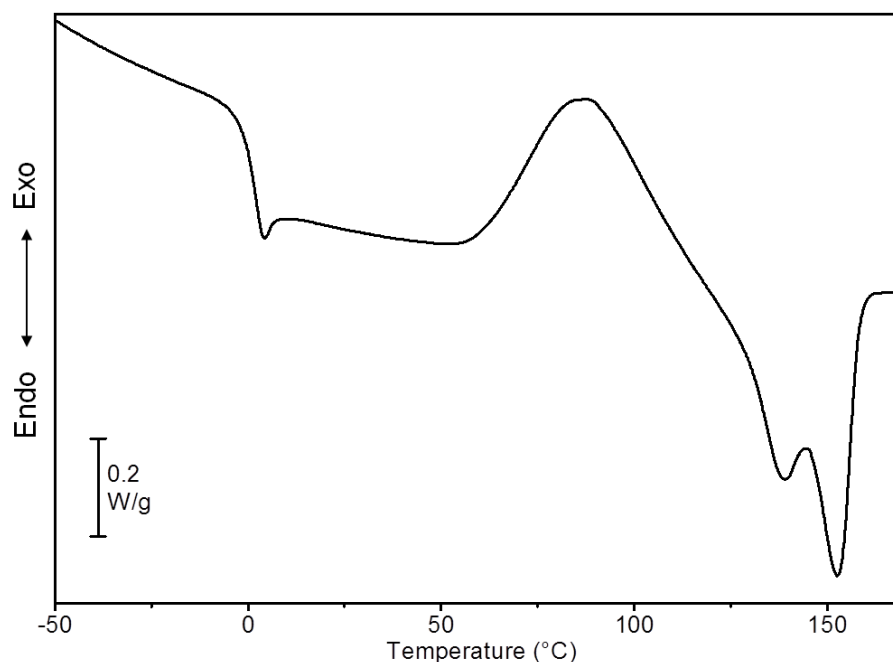
Figure 6. Typical DSC heating curve of PHA produced using the synthetic substrate. The polymer was recovered by NaClO digestion.

This sample has Tg = 0°C, Tc and Tm at 88°C and 153°C, respectively, with associated crystallization and melting enthalpies of 32 J/g (ΔHc) and 35 J/g (ΔHm), respectively. The thermal behavior of the analyzed PHA agrees with earlier literature data on bacterial polyesters with similar composition [110,165,204].

No DSC results are therefore reported for PHAs recovered using NaOH. In agreement with the above TGA results showing that PHAs recovered by NaOH digestion are thermally unstable (Figure 5), DSC measurements on such samples were not reproducible and after two subsequent scans up to 185°C they showed a 10% of weight loss.

All the samples produced at different time exhibit curves similar thermal behavior to those shown in Figure 6.

From TGA and DSC measurements on PHBV samples corresponding to different operation time, it can be concluded that the thermal polymer behavior, although it was strongly affected by the extraction agent used (NaClO or NaOH), it did not substantially change showing that the overall PHA production process is robust and stable over time.

The same 3-step process described above to produce PHAs from a synthetic substrate was also performed using <u>olive oil mill wastewaters</u> (OMW) under continuous operation for at least 90 days. Such waste substrate contained polyphenol components that were removed prior to OMW use in order both to decrease the antimicrobial activity of the waste feedstock and to recover such natural antioxidants that can be used for other purposes. The organic matter purified from polyphenols was then subjected to acidogenic fermentation to produce a waste rich in volatile fatty acids to be used as substrate for PHA production. After the accumulation stage, the samples were centrifuged to separate the cells from the residual substrate not consumed by bacteria and then the biomass was transferred to the extractor reactor to recover the polymer from the cells. Based on the results obtained using synthetic substrate described above, NaClO (5% active Cl) digestion solution was used to perform the polymer recovery from the cells. After centrifugation, the sediment was stored at -18°C. Several frozen samples produced over one week of operation were collected and the mixture was lyophilized.

Opposed to 100% w/w yield and high purity (around 90% w/w) obtained for the recovered PHAs produced with synthetic substrate, for those produced with OMW a loss of PHA during recovery and a polymer purity around 80% w/w were obtained. The result indicates that NaClO was less efficient towards the biomass samples produced using the waste substrate than towards cells grown on the synthetic substrate.

In order to check the dependence of both PHA composition and thermal degradation properties on operation time, lyophilized samples selected among those produced at the beginning, at the middle and at the end of the production process were analyzed by GC and TGA analyses respectively.

GC results reveal that PHBV copolymers with HV fraction from 12 to 15 %mol were obtained which is a similar composition range to that obtained for the copolymers produced with synthetic substrate (from 8 to 13 %mol).

Figure 7 displays the typical TGA curve of PHA produced using OMW (dashed curve) together with that of the polymer produced using synthetic substrate (continuous curve) for comparison purposes. As shown in the Figure, the main degradation step occurs in the same T-range (around 284°C) in both samples. However, TGA curve of PHAs produced by using

OMW show lower thermal stability up to 200°C (weight loss around 2.5 %) and a higher residue content at 600°C (around 5%). This is likely due to the impurities present in such samples that affect the thermal degradation behavior during TGA measurements.
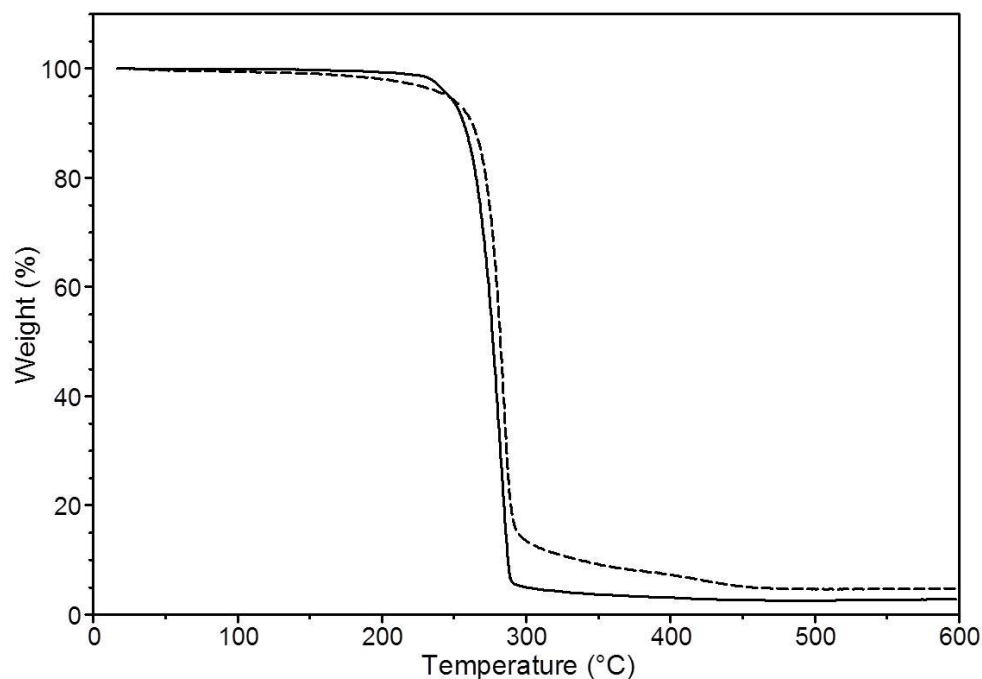

Figure 7. Typical TGA curve of PHA produced using OMW and recovered by NaClO digestion (dashed curve). For comparison, TGA curve of PHA produced using synthetic substrate and recovered by NaClO is displayed (continuous curve).

The overall conclusion of this work on PHA production is that PHAs can be efficiently produced from MMCs and waste substrates. Polymer composition and thermal stability of the PHA samples analyzed recovered by NaClO are not influenced by the operation time. However, impurities present in samples grown on OMW substrate affect the PHA thermal stability. Thus, optimization of the recovery procedure conditions is required (e.g. addition of several washing steps between accumulation and extraction stage and/or after recovery process), in order to obtain higher purity, yield and optimal thermal stability of the recovered PHA.

3.1.1.2. PHAs from pure culture (*Cupriavidus necator*)

PHAs produced by *Cupriavidus necator* DSM 428 have been characterized in this work. Different fried oils were used as carbon source: a) soybean; b) peanut and sunflower; c) rapeseed, sunflower and grapeseed; d) unknown oils provided by university canteen. Table 3 reports the composition of the oils used in terms of their fatty acids content determined by gas chromatography (GC). The Table also reports the PHA content in the cells (PHA yield, % w/w) grown on such frying oils. GC analysis reveals that the polymers produced were composed of HB monomers whatever oil was used.

Table 3. Used cooking oil (UCO) composition in terms of fatty acids content and PHA production yield by using such oils as carbon substrate in the fermentation process.

Used cooking oil (UCO)	UCO fatty acids content (wt%)					PHA yield (% w/w)[a]
	Palmitic ($C_{16:0}$)	Stearic ($C_{18:0}$)	Oleic ($C_{18:1}$)	Linoleic ($C_{18:2}$)	Linolenic ($C_{18:3}$)	
Soybean oil	14	4	24	54	4	65
Mixture of Peanut and Sunflower oil	10	2	40	48	-	45
Mixture of rapeseed, oleisol, sunflower, grape	7	2	62	24	5	43
Oils provided by university canteen	10	3	39	48	-	79

[a] percentage of PHAs with respect to cell dry weight (CDW)

The data in Table 3 show that the UCO composition affects the amount of PHA accumulated by the cells. Indeed, a different yield ranging from 43% to 79% is obtained.

In order to evaluate the impact of the waste substrate composition on thermal properties of the produced PHB, such polyesters, after recovery from the cells by chloroform extraction as described in [205], were characterized by Thermogravimetric (TGA) and Differential

Scanning Calorimetry (DSC) analyses. Prior to solvent extraction, the biomasses were washed with hexane to remove the residual oil.

TGA results (not shown) reveal that the polymers produced using the different tested oils are thermally stable up to 200°C (weight loss <1%). Then, they degrade in a single step showing maximum degradation rate (Tmax) in the range 282-284 °C.

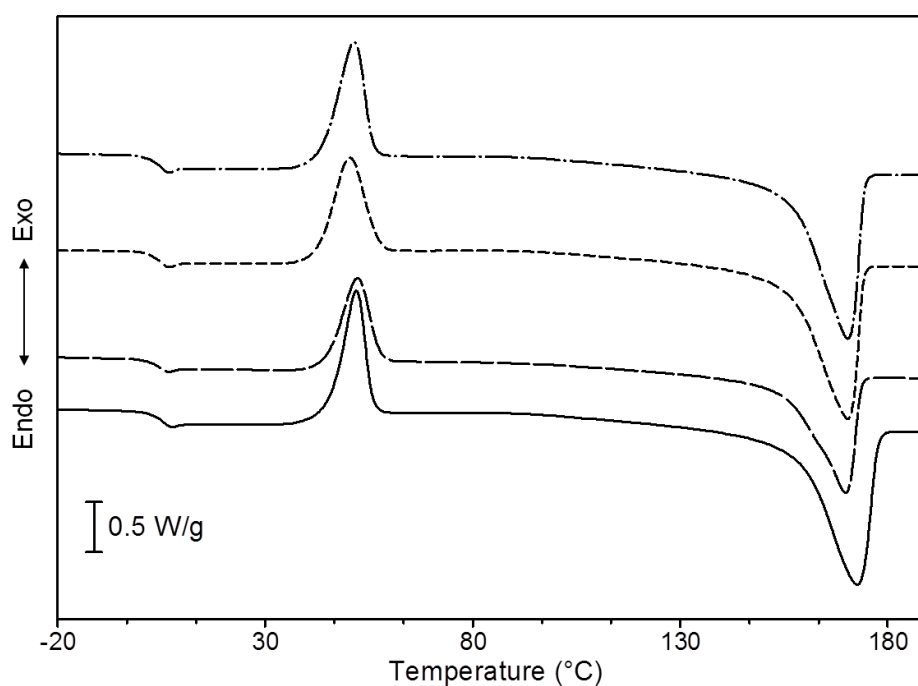DSC curves of PHB samples produced by using the different UCOs are shown in Figure 8.

Figure 8. DSC curves (heating scan: from -80 to 210 °C, after quench) of PHA samples produced by using UCOs: soybean (dash-dot); peanut and sunflower (short-dash); rapeseed, sunflower and grapeseed (long-dash); university canteen (solid).

DSC curves show that all PHA produced have similar thermal behavior with glass transition temperature (Tg) at 3-4°C, crystallization at Tc= 51-52°C and melting at Tm= 170-173°C) with associated enthalpies ΔHc= 40-55 J/g and ΔHm= 40-60 J/g respectively. These results agree with those reported in the literature for PHB [110].

It is therefore demonstrated that PHB with good thermal stability and thermal properties respectively, can be produced by using *C. necator* cells and used cooking oil (UCO). As previously mentioned, PHB yield depends on oil composition.

3.1.2. Solvent-free recovery of PHAs from the bacterial cells

Biomasses with PHB content of 81% and of 37% (determined by GC) produced by using *C. necator* grown on UCO from university canteen and different fermentation conditions, were analyzed by TGA. Those biomasses were dried at 50°C for 2.5 h under vacuum prior to the analysis. The TGA curves are shown in Figure 9.
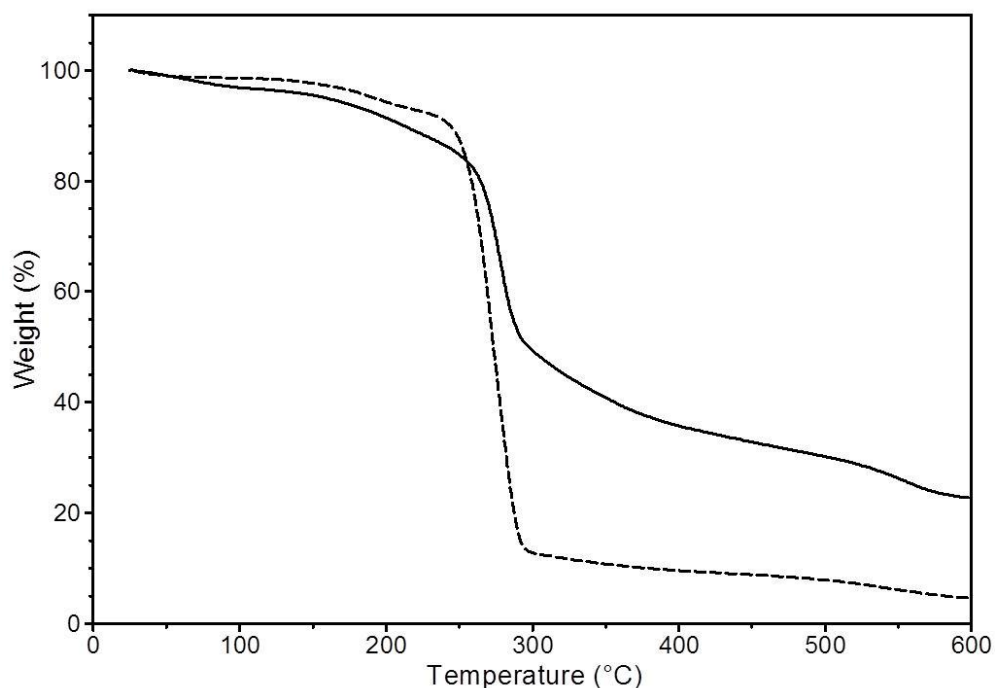

Figure 9. TGA curves of dried *C. necator* DSM 428 cells with a PHB content of 80% (dashed curve) and 37% (w/w) (continuous curve), as assessed by gas chromatography.

Both biomasses show a rather complex thermogravimetric behavior with a marked weight loss step centered around 270-280°C, the temperature range where thermal degradation of plain PHB occurs [163]. It is interesting to note that the main weight loss step of the analyzed biomasses in the TGA curves of Figure 9 has different intensity and that it can be

quantified as $\Delta m = 80\%$ (dashed curve) and $\Delta m = 39\%$ (continuous curve). Remarkably, these values very closely match the PHB content in each biomass obtained from GC. It is therefore suggested, in agreement with earlier results [206], that the PHB content within the cells can be assessed with a good level of accuracy from the weight loss step associated with thermal degradation of the polymer, that lays in the T-range 270-280°C.

The biomass with 37% w/w of PHB content having a large fraction non-PHA cell mass (NPCM) to be disrupted, solubilized and eliminated, was selected to perform extraction experiments in order to test the effectiveness of the method proposed with a sort of worse-case example.

After biomass collection by centrifugation of the cultivation broth (9 000 g, 20 min), the *C. necator* cells were re-suspended in deionized water and finally separated from the aqueous portion by centrifugation. No washing with hexane was performed to eliminate UCO residues from the biomass, as it was required in the case of solvent extraction (see section 3.1.1.2), because the residual oil was removed during the recovery step as described below.

Based on previous research studies [143,148,149,207], PHA recovery was carried out using a protease (Alcalase), an anionic surfactant (SDS), and a chelating agent (EDTA).

Such extracting agents were used in the following concentrations with respect to dry biomass: Alcalase (0.3 AU g^{-1}, where AU= Anson Units), sodium dodecyl sulfate (SDS, 0.3 g g^{-1}). They were incubated with *C. necator* cells in Na_2HPO_4 buffer solution (pH 8.3) at 55 °C for 1 h under continuous stirring (150 rpm).

In the applied protocol, the surfactant SDS was used to disrupt the cells, since it penetrates between cell's lipid bilayer membranes. With increasing SDS concentration, cell lysis occurs, leading to the incorporation of membrane phospholipids into micelles [208]. The added chelating EDTA molecule assists SDS by complexing divalent cations (mainly Mg^{2+} and Ca^{2+}), thus destabilizing the outer cell membrane. After cells lysis, the cellular material is solubilized through Alcalase digestion and the remaining insoluble matter is incorporated in SDS micelles [148], including UCO residues of the fermentation process possibly present. Solubilized cellular material and insoluble PHB granules were finally separated by centrifugation (20 000 g, 30 min) followed by 3 further water-washing/centrifugation steps.

In enzymatic digestion performed in previous works [148,149], cells were subjected to a heat pretreatment to promote cell lysis and protein denaturation. In the present work this step was eliminated, and cell disruption was successfully achieved by means of SDS and EDTA, according to a chelate-surfactant recovery strategy earlier suggested [143,145], and proteins were efficiently removed by Alcalase enzyme digestion [148,149].

PHB purity (%, w/w) after the recovery procedure was assessed by TGA analysis. The recovered samples were dried at 50°C for 2.5 h under vacuum, prior to the analysis. TGA curve of dried recovered PHB granules is shown in Figure 10, together with the TGA curve of the starting biomass shown in Figure 9 (section 3.1.1.2).
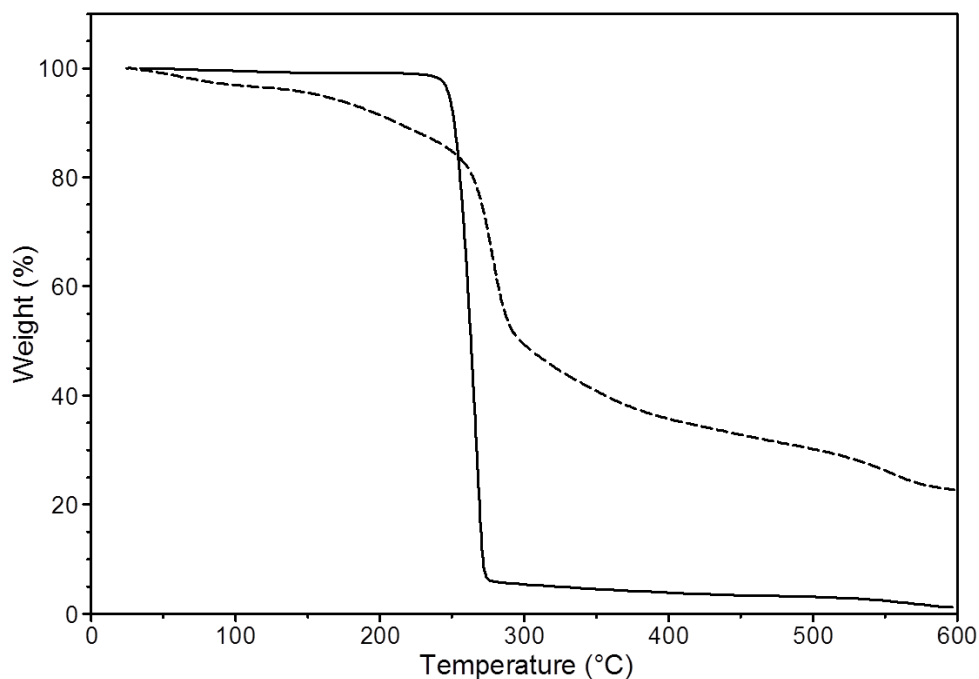

Figure 10. TGA curves of dried *C. necator* DSM 428 cells (dashed) and of PHB granules recovered from the cells by enzymatic digestion (continuous).

TGA results show that the recovered PHB granules is stable up to 220 °C ($\Delta m = 1\%$ at this temperature) and that they exhibit a single weight loss with maximum degradation rate (T_{max}) at 266 °C (Figure 10, continuous curve). Such a weight loss accounts for 94% of the initial sample weight, demonstrating that high purity PHB granules can be obtained starting

from a biomass with a mere 37% PHB content. This results testifies that the adopted procedure provides an efficient disruption, separation and elimination of non-PHB cell components.

Dried recovered PHB granules were investigated by differential scanning calorimetry (DSC). Heating scans were run at 20 °C min^{-1}, from -80 °C to 210 °C, after quenching from the melt (Figure 11).
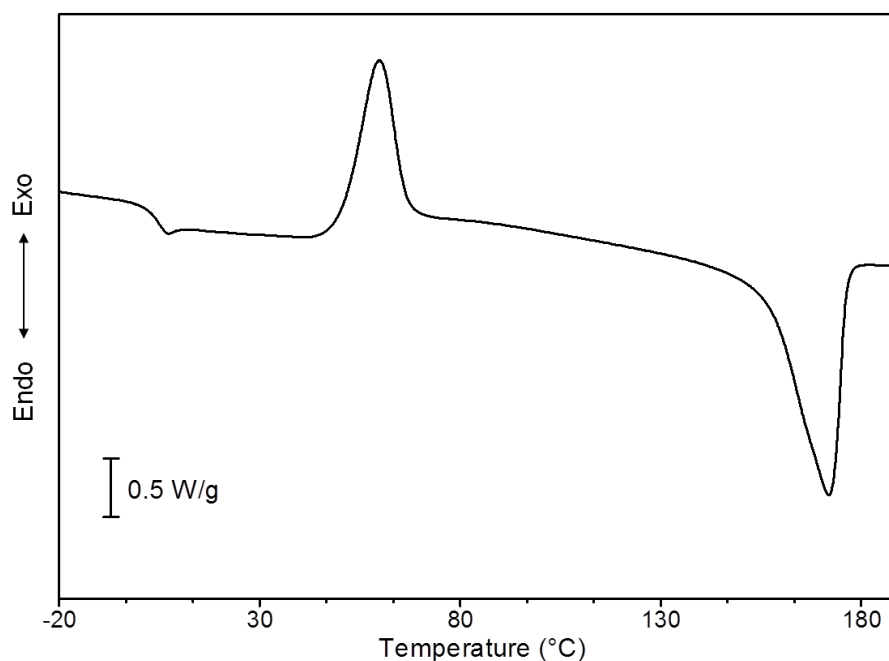

Figure 11. DSC curve (2nd heating scan) of dried and melt-quenched PHB granules recovered by enzymatic digestion from *C. necator* DSM 428 cells.

The DSC curve shows an endothermal baseline shift associated with the glass transition (T_g= 3°C) followed by a cold-crystallization exotherm (T_c= 60°C) and, finally, by a melting endotherm (T_m= 172°C), in excellent agreement with earlier results [204].

Images of PHB granules recovered were captured by scanning electron microscopy (SEM). Prior to examination, pellet PHB samples were re-suspended in distilled water and the resulting PHB suspension was deposited on stub, dried and then sputter-coated with gold. A representative SEM image is shown in Figure 12.
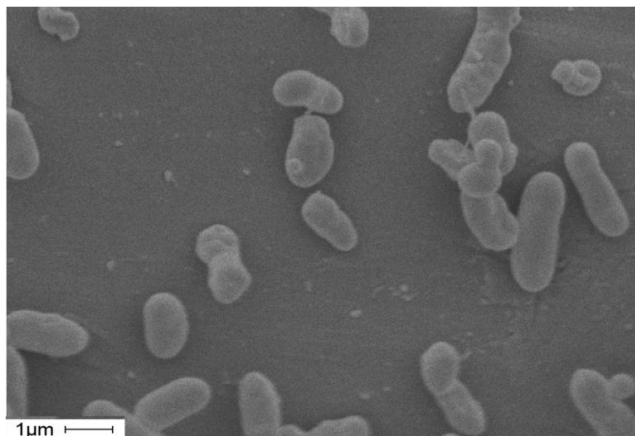
Figure 12. SEM micrograph of PHB recovered granules from *Cupriavidus necator* DSM 428 cells.

PHB granules in the size range 400-1000 nm have been observed in agreement with earlier results on PHB granules produced by *C. necator* cells [161]. The presence of some granule aggregates was also observed.

Both a wet pellet sample and a room temperature dried (24 h) pellet were analyzed by WAXS (Figure 13) in order to ascertain where the polymer is in a semicrystalline form or if it has maintained the amorphous character of the native granules.

Figure 13. X-ray diffraction patterns of dried (24 h at RT, continuous curve) and wet (dashed curve) PHB granules recovered from *C. necator* DSM 428 cells.

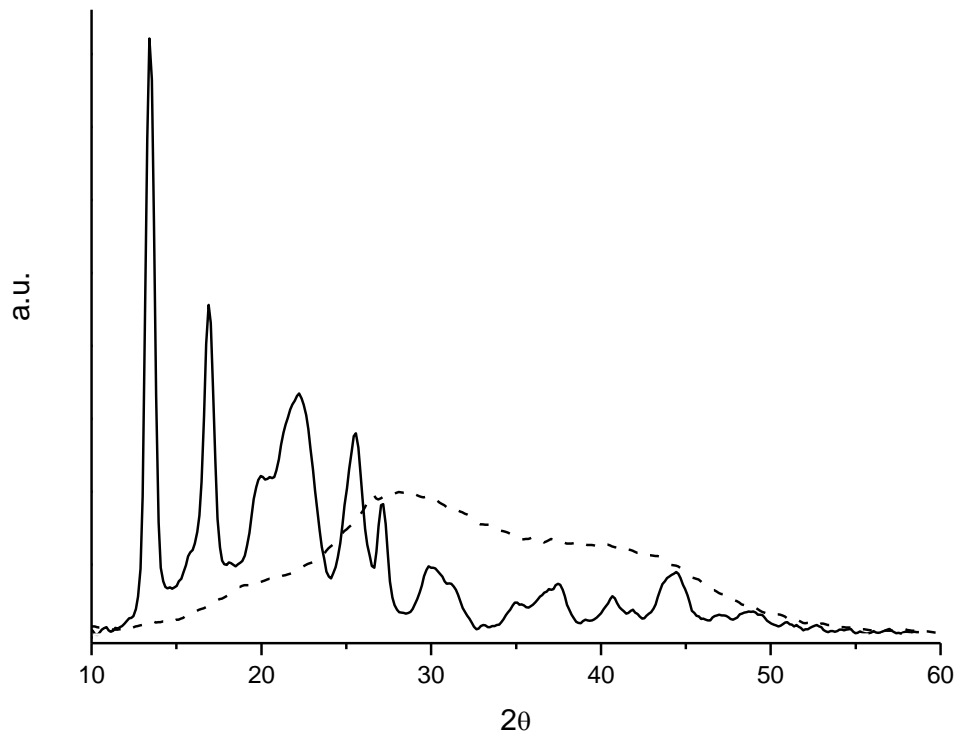The X-ray diffractogram of PHB wet granules (dashed curve, Figure 13) exhibits only an amorphous diffraction halo centered at $2\theta = 20°$ that partially overlapps the water WAXS signal. Conversely, after drying the polymer granules at room temperature (continuous curve, Figure 13), all main reflections of the X-ray diffraction pattern of crystalline PHB appear [209,210]. It is known that PHB granules within bacterial cells are amorphous, that they are characterized by very low crystal nucleation density and that they crystallize only upon removal (or damage) of the granule coating layer as a consequence of heterogeneous nucleation [158]. WAXS results clearly shows that wet PHB granules recovered as described in this work remained amorphous like in intact cells, whereas they crystallize upon drying as a consequence of water loss, granule volume contraction and, likely, surface layer damage.

It can be concluded that the enzymatic method employed is mild and selective in removing non-PHB cell material and that it keeps the granule surface layer intact, preserving the amorphous state of PHB.

It is worth pointing out that when strong and aggressive recovery procedures are applied, in addition to granule coating damage and consequent inability to recover PHB in the amorphous state [159], thermal properties and stability are often affected and a decrease of molecular weight may be observed [155]. In contrast, the previously recovered PHB shows excellent thermal properties.

3.2. Modifications of PHAs

3.2.1. Plasticization and reinforcement of PHAs for food packaging applications

The aim of this work was to develop biodegradable and bio-based composites based on a PHBV matrix and agro-industrial by-products (wheat straw fibers) for food packaging applications. Lignocellulosic fibers such as wheat straw fibers (WSF) as low cost and widely available fillers were used in order to decrease the final PHBV cost through replacement of a part of the polymer with fibers. PHBV is a rather brittle material. Incorporation of high modulus fibers is unreasonable unless softening of the matrix is performed prior to fiber incorporation. Thus, plasticization of the matrix which, as known, allows to improve polymer flexibility, was firstly performed. According with the aim to develop biodegradable materials for food packaging application, the substances to be tested as suitable plasticizers for PHBV were selected among those biodegradable and non-toxic for food contact according with legislative requirements concerning food packaging application [211]. Since blends were prepared by melt extrusion at high temperature, such substances were selected based on their thermal resistance at the working temperatures in order to minimize loss of plasticizer by evaporation and degradation during material processing. Hence, the following additives were used as PHBV plasticizers: ATBC, GTA and PEG at different molecular weight (see Table 2, section 2.1). Effective plasticization of the polymer was evaluated by thermal and mechanical characterization of the blends obtained. Wheat straw fibers (WSF) were incorporated in plasticized PHBV matrix and the impact of the fillers on PHBV properties was investigated.

This work was performed within the EcoBioCap (Ecoefficient Biodegradable Composite Advanced Packaging) European Project during a visiting research activity in research group of Prof. Nathalie Gontard at INRA-IATE - Joint Research Unit in Agro-Polymer, Engineering and Emerging Technology – of University of Montpellier (France).

3.2.1.1. Samples processing

PHBV/plasticizer blends (5, 10 and 20% w/w of plasticizer content) and composites (with 20% w/w of WSF) were prepared by melt extrusion after specific pre-treatments described

in section 2.2.1. Unlike alternative methods to prepare blends at laboratory scale like solvent casting, melt processing is the conventional method for producing plastics in industry due to the its large-scale applicability. Different extruder settings (temperature and screw profiles, speed, feed position) were tested to obtain the optimal processing conditions. Figure 14 represents feed positions and one of the two screw profile used, while Table 4 reports the temperature applied to extrude each sample. Only in the case of PEG-400 and PEG-1000 plasticizers a different screw profile was used.
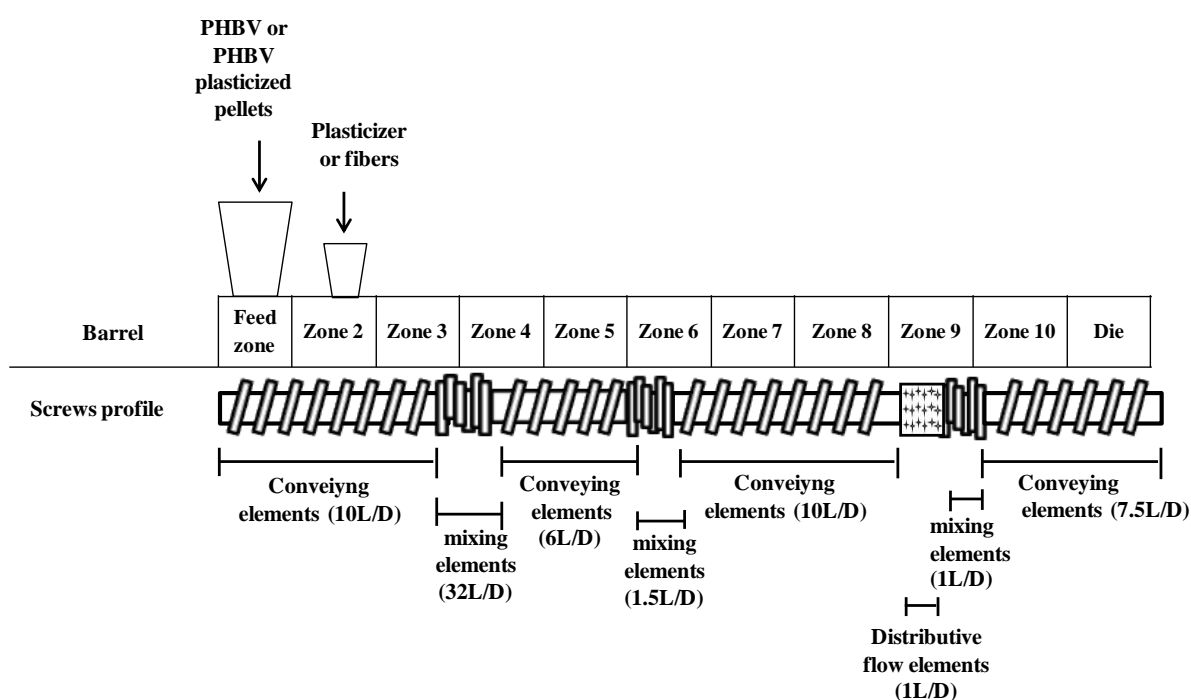

Figure 14. Representation of the extruder settings used for PHBV samples preparation.

Table 4. Temperature profiles used for PHBV samples extrusion.

Sample	Temperature (°C)									
	Zone 2	Zone 3	Zone 4	Zone 5	Zone 6	Zone 7	Zone 8	Zone 9	Zone 10	Die
PHBV										
PHBV/ATBC	180	180	180	170	170	160	160	160	150	140
PHBV/GTA										
PHBV/PEG-400	180	180	180	180	180	180	170	170	160	160
PHBV/PEG-1000	190	190	180	180	180	180	170	170	170	160
PHBV/PEG-4000										
PHBV or plasticized PHBV/WSF	180	180	180	170	170	160	160	160	160	150

All PHBV samples were processed by assembling the screws as represented in Figure 14 and by setting the speed at 500 rpm, except PHBV extruded with solid plasticizers like PEG-1000 and PEG-4000 for which different extruder settings were used. Indeed, by applying the same temperature profile used for extrusion of PHBV with lowest molecular weight (400) PEG to solid plasticizers (either PEG-1000 or PEG-4000), a high speed (900 rpm) was required to avoid accumulation of the plasticizer at the surface of the extruded polymer. Thus, in order not to expose the polymer to excessive shearing which can cause macromolecular chain scission, for such samples the ten-zone heating profile was increased as reported in Table 4 and the speed was lowered at 300 rpm. Furthermore, the screws were assembled with reverse screw elements just after the mixing elements (1.5L/D) in order to improve polymer and plasticizer mixing. All the extruded samples obtained were water-cooled, then cut in pellets and finally they were hot-pressed to obtain sample sheets (as described in section 2.2.1). Upon samples storage, only in the case of PHBV formulated with either 20% of PEG-400 or PEG-1000 exudation of the plasticizer from the sheet surface was observed, indicating that at this content the polymer is not fully compatible with those additives.

In order to check if PHBV and plasticizers mixing could be improved, selected blends of PHBV containing 10% of plasticizer were re-processed in the same correspondent conditions. Comparison of thermal and mechanical behavior of samples subjected to one or two extrusion cycles, did not show significant differences. This was taken as proof that the conditions described above provided optimal mixing.

3.2.1.2. PHBV plasticization: thermal and mechanical properties

Plasticization is known to cause a decrease of polymer glass transition temperature (Tg) as consequence of the enhancement of the free volume (the volume fraction not occupied by the macromolecules) conferring further molecular mobility to the amorphous phase. This effect generally leads to melting point depression in plasticized samples [176,212-214]. To investigate if the additives used effectively act as plasticizers for PHBV, DSC analysis was performed on plasticized samples. The DSC results (second heating scan at 20°C/min from -100 to 200°C, after sample quenching) on PHBV samples containing 10 wt.% of the plasticizer content are reported in Table 5, which also contains the degree of crystallinity (Xc, %) measured by WAXS. The DSC curves of the same plasticized samples are also shown in Figure 15.

Table 5. Thermal properties (2nd heating scan after quench) and crystallinity of plasticized PHBV samples containing 10% (w/w) of the additive content.

Sample	Tg (°C)	ΔCp (J/g°C)	Tm (°C)	ΔH_m[a] (J/g)	Xc[b] (%)
PHBV	3	0.30	170	82	66
PHBV/ATBC	-14	0.41	164	86	68
PHBV/GTA	-8	0.38	166	89	67
PHBV/PEG-400	-12	0.45	164	91	67
PHBV/PEG-1000	-	-	166	87	64
PHBV/PEG-4000	-	-	168	85	65

[a] melting enthalpy normalized to PHBV weight fraction in the blend.

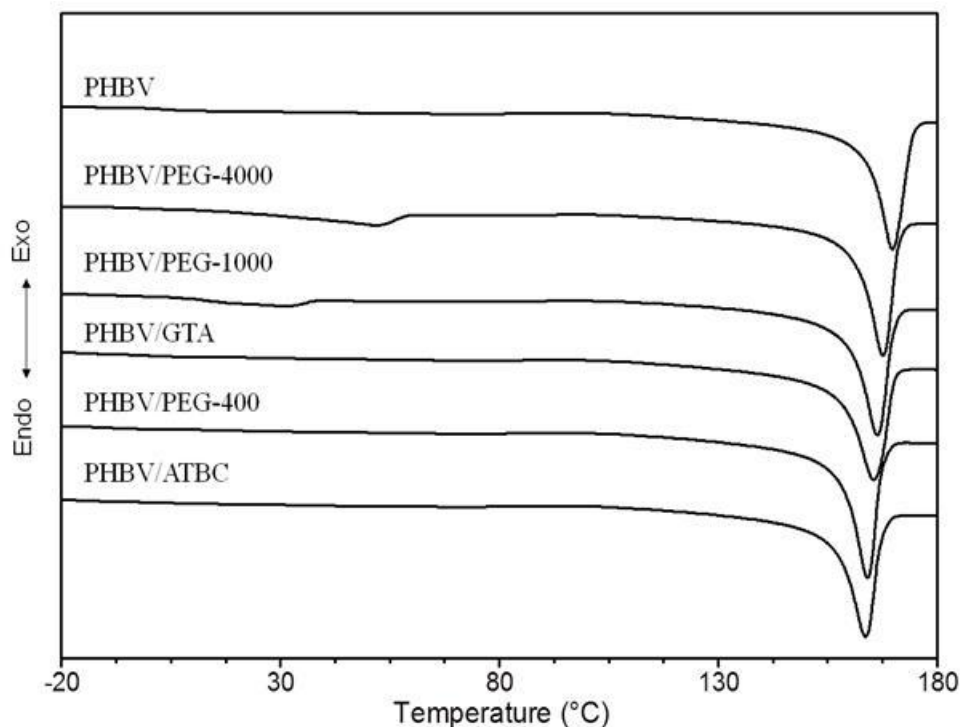[b] percentage of crystallinity (±10) determined by WAXS.

Figure 15. DSC curves (2nd heating scan after quench) of plasticized PHBV samples containing 10% (w/w) of the additive content.

A depression of PHBV glass transition temperature, not identifiable in Figure 15, but rather clear in magnified curves, as well as of its melting point is observed for the polymer blended with ATCB, GTA and PEG-400 (see Table 5). The strongest Tg reduction is observed for PHBV plasticized using ATBC (Tg= -14°C). This behavior indicates that all mentioned additives act as plasticizer for the polyester. Furthermore, detection of only one Tg in the blends suggests a complete miscibility of the samples at 10wt% of plasticizer content.

A different behavior is observed in Figure 15 for both PHBV/PEG-1000 and PHBV/PEG-4000 blends. DSC curves of such samples show an endothermal baseline shift around -60°C and a small endhotherm located in a wide temperature range (from -20 to 40°C for PHBV/PEG-1000 and to 60°C for PHBV/PEG-4000,) that are respectively associated with

the glass transition and melting of PEG plasticizer. Such wide endhotherms hide the glass transition of PHBV amorphous phase and thus it was not measured.

The presence of those thermal events suggest that PEG-1000 and PEG-4000 blends are not completely miscible with the polyester. A degree of miscibility is however attested by the slight melting point depression observed for those blends in Table 5. Considering that PEG-400 form a completely miscible blend (only one Tg detected), it is clear that miscibility decreases, as expected, with increasing molecular weight.

As concerns the normalized melting enthalpy values of PHBV in all plasticized blends (Table 5), they do not significantly change with respect to that of pure PHBV. This means that the polymer crystallizes to the same extent in the blends as in the pure state. This behavior is confirmed by WAXS analysis. Indeed, the degree of crystallinity (Xc) values calculated from X-Ray diffractograms of all plasticized samples are similar to that of pure PHBV (Table 5).

The mentioned phenomena of exudation concerning PEG-400 and PEG-1000 during storage clearly reflects the poor compatibility of these plasticizers with PHBV. The other substances (ATCB and GTA) that show an efficient plasticization effect, i.e. good miscibility with the polymer although their higher tendency to migrate, they do not give any evidence of exudation.

The aim of plasticizer addition to PHBV was to reduce polymer brittleness. Mechanical properties of PHBV samples were assessed by tensile stress-strain measurements. Prior to tensile testing, the samples were conditioned at RT for 48h over P_2O_5 under vacuum, in order to let PHBV develop a constant crystallinity degree and to release any adsorbed water. The tensile tests were performed on dog-bone shaped specimens (5 mm wide) die-cut from hot-pressed sheets (0.25 mm thick). The cross head speed was 10 mm $\cdot$ min^{-1} and the initial gage length was 40 mm. Young's modulus (E), tensile strength (σ_b) and elongation to break (ε_b) of the melt processed PHBV with 5, 10 and 20% of plasticizer content are show in Figure 16.
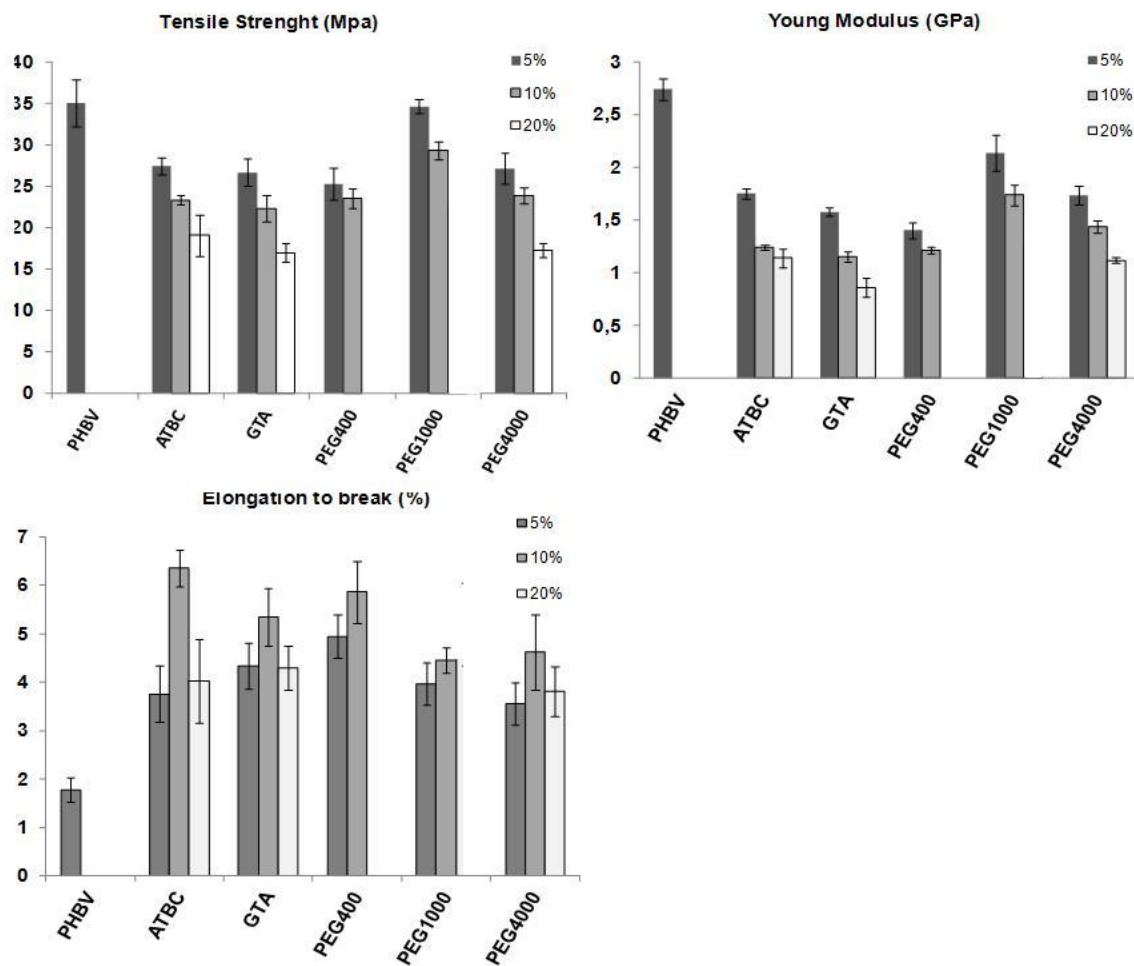
Figure 16. Mechanical properties of plasticized PHBV samples with 5, 10 or 20% of additive content. The error bars represent the standard deviations.

The Figure shows that with increasing plasticizer content both the sample tensile modulus and the tensile strength decrease. As concerns the elongation at break, it increases as the plasticizer content increases up to 10% reaching the highest value for PHBV/ATCB sample (6.4±0.4%), and then it decreases when the 20% of the plasticizer is present. Analyzing the tensile properties exhibited by blends with different plasticizer content, the amount of 10% allows to obtain a good balance between decreasing of E and tensile strength and increasing of elongation to break value.

Changes in mechanical properties of PHBV with the addition of PEG-1000 and PEG-4000 that resulted not miscible by DSC results, suggests that although they are thermodynamically immiscible blends, they are compatible at the mechanical level.

Comparing the thermal and mechanical behavior of all samples, the best results were obtained by using ATCB plasticizer. PHBV/ATCB blend (80/10 w/w%) shows the best plasticization effect exhibiting the strongest Tg depression (-14°C) and the best mechanical properties among the plasticized samples analyzed with E= 1.2±0.0 GPa, σ_b= 23.3±0.6 MPa and ε_b= 6.4±0.4 %. For this reason, PHBV/ATCB blend was selected as plasticized matrix for the development of composite material of PHBV and WSF.

3.2.1.3. PHBV composites: thermal and mechanical properties

Composite material of plasticized PHBV (PHBV/ATBC, 90/10 %w/w) was prepared by melt extrusion with 20% (w/w) of WSF. Such sample was analyzed by DSC and the results are shown in Table 6 which also reports crystallinity degree (Xc,%) measured by WAXS analysis. The thermal properties of the reference PHBV/ATBC blend is also shown for comparison purposes.

Table 6. Thermal properties (2nd heating scan after quench) and crystallinity of composite of plasticized PHBV (ATBC, 10% w/w) and WSF (20%, w/w). For comparison purposes, the reference plasticized polymer is also reported.

Sample	Tg (°C)	ΔCp (J/g°C)	Tm (°C)	ΔH_m[a) (J/g)	Xc[b) (%)
PHBV/ATBC	-14	0.41	164	86	66
PHBV/ATBC/WSF	-14	0.42	163	94	57

[a) melting enthalpy normalized to PHBV weight fraction in the blend.

[b) percentage of crystallinity (±10) determined by WAXS.

The only appreciable difference in results of Table 6 is a slight increase of normalized melting enthalpy in the presence of fibers (ca. 9%). The literature reports earlier results

where cellulose fibers from flax acted as nucleants for trancrystallinity in a PHA composite [215].

PHBV composites were subjected to stress-strain measurements performed as previously described for plasticized samples (see section 3.2.1.2) and the results are shown in Figure 17.
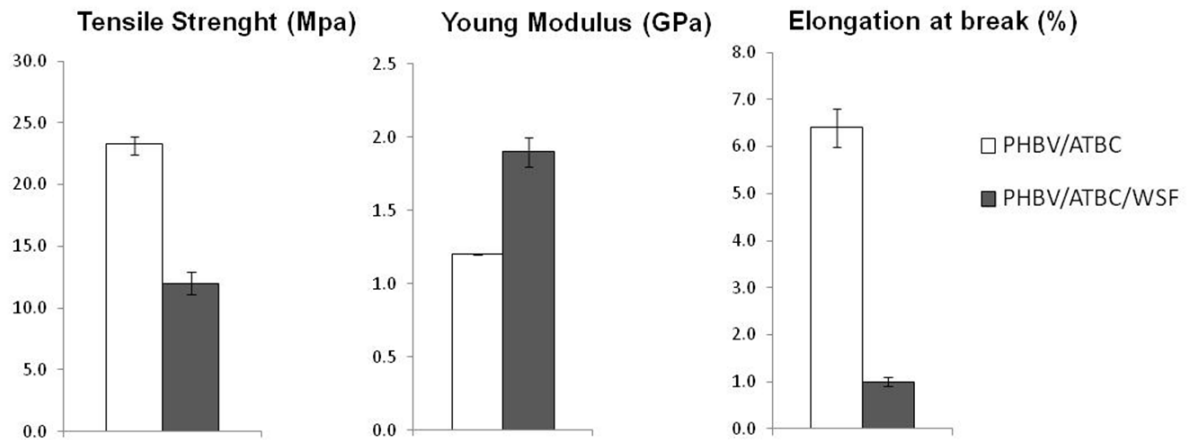

Figure 17. Mechanical properties of plasticized PHBV sample with 20% of WSF. For comparison purposes, the reference plasticized PHBV is also reported. The error bars represent the standard deviations.

As shown in the Figure, addition of high modulus fibers causes an increasing of PHBV Young modulus (E) in plasticized PHBV. As expected, elongation at break (ε_b) decreases in the composite nullifying the increasing of this parameter by the addition of the plasticizer. Also, the tensile strength of the composite decreases with respect to the reference blends without WSF. These results suggests a poor interfacial adhesion between the hydrophilic fibers and the hydrophobic matrix. Indeed, when a good adhesion is established between the composite components, the load applied is transferred from the polymeric phase to the fibers causing a reinforcement of the material. This effect leads to an increasing of the tensile strength that it is not observed for the composites analyzed in this work. However, different methodologies of fiber treatments that have not been investigated in this work can be explored (e.g. surface chemical modifications [216]) to overcome this problem.

In conclusion, in this work PHBV was mixed with plasticizers that are biodegradable and non-toxic for food contact. All the materials were prepared by melt extrusion of the components exploring the processing conditions for the achievement of their optimal mixing. The plasticizers, depending on their content, allow to decrease polymer rigidity and to slightly improve PHBV flexibility. Fibers embedded in plasticized PHBV show poor mechanical properties. Further investigations aimed to overcome the lack of adhesion at the fiber-matrix interface could led to the development of PHBV composites in which the fibers not only serve to lower polymer cost but also to improve PHBV mechanical properties.

3.2.2. PHAs via microwave-assisted transesterification copolymerization

Novel biodegradable poly(3-hydroxybutyrate-co-butyleneadipate), P(HB-co-BA), copolymers, synthesized from poly-3-hydroxybutyrate, PHB, and polybutyleneadipate, PBA, via microwave-assisted transesterification were investigated. The results of this work have been published in [199].

Table 7 reports reaction times, composition, molecular weight, sequence length and randomness of the P(HB-co-BA) copolymers investigated (labeled as B1, B2, B3 and B4).

Table 7. Composition, molecular weight, sequence length and randomness of P(HB-*co*-BA) copolyesters.

Sample	Reaction time (hours)	(HB)/(BA) [a]	Mw x 10^{-3} [b]	Mw/Mn [c]	L_{HB} [d]	L_{BA} [e]	DR [f]
B1	2.5	66/34	11.4	1.4	23	37	0.07
B2	3	64/36	11.4	1.3	13	17	0.13
B3	4	66/34	13.1	1.3	13	13	0.15
B4	5	61/39	15.7	1.2	5.1	5.4	0.38

[a] Molar composition of the copolyesters measured by ^{1}H-NMR.

[b] Weight average molecular weights determined by gel permeation chromatography (GPC).

[c] Polydispersity index.

[d] Average block length of HB measured by ^{13}C-NMR.

[e] Average block length of BA measured by ^{13}C-NMR.

[f] Degree of randomness measured by ^{13}C-NMR.

The Table shows that by varying reaction times, copolymers with different average block length of BA and HB units (L_{BA}, L_{HB}) and degree of randomness (DR) are obtained.

Copolymers posses molecular weights ranging from 11400 to 15700 Da with polydipersity between 1.2 and 1.4.

P(HB-*co*-BA) copolymers and the reference homopolymers, PHB and PBA, were subjected to differential scanning calorimetry (DSC). Each sample was preliminarily heated to 210°C to erase previous thermal history, then it was analyzed after both controlled cooling at 10°C/min and after quench cooling, performing DSC heating scans from -80 to 210°C (20°C/min).

Figure 18. DSC cooling curves (10°C/min) of the P(HB-*co*-BA) copolyesters and of the reference PHB and PBA homopolymers.

During the controlled cooling (Figure 18) both homopolymers showed a crystallization exotherm located at different temperature, higher in PHB (Tc = 97°C) than in PBA (Tc = 32°C). The associated crystallization enthalpy is similar (ca. 70 J/g). Copolymer B1 exhibits a clear exotherm in a T-range close to that of PBA crystallization, whereas copolymer B2 shows a less intense two-peak exotherm in the same temperature interval.

Copolymers B3 and B4 do not show evident crystallization phenomena during controlled cooling at 10°C/min.

Upon subsequent heating (Figure 19) PBA and PHB show melting endotherms at 53°C and 162°C respectively, and exhibit a remarkably different undercooling (ΔT = Tm-Tc is 21 °C in PBA and 65 °C in PHB).
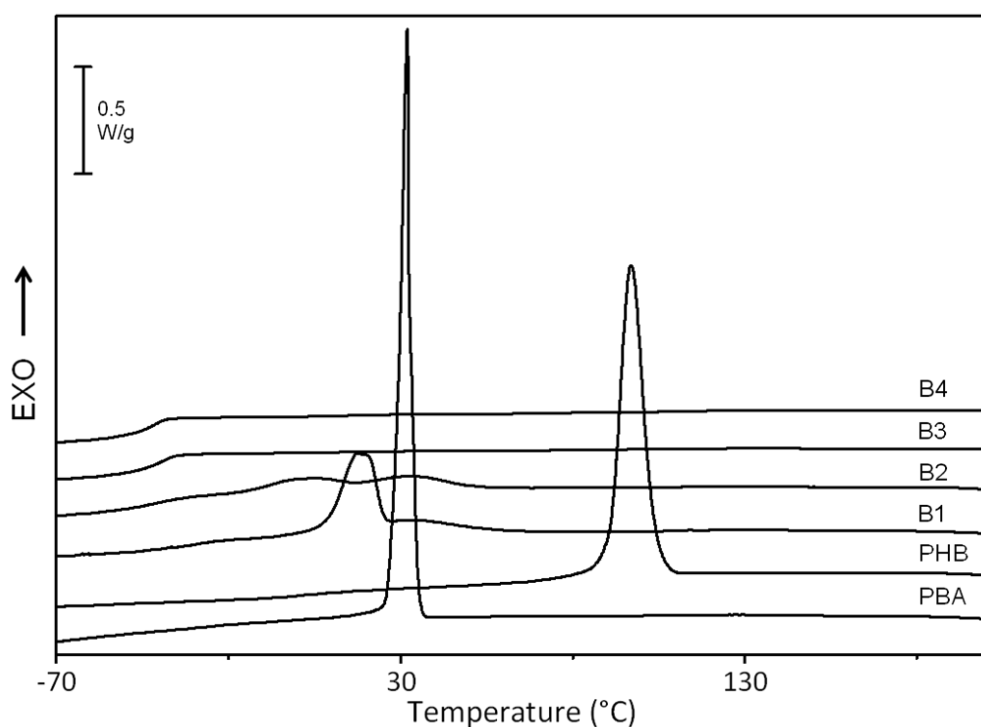

Figure 19. DSC heating curves (20°C/min) of the P(HB-*co*-BA) copolyesters and of the reference PHB and PBA homopolymers, after controlled cooling at 10 °C/min.

All copolymers but B4 show melting endotherms in Figure 19. Copolymer B4 has the highest degree of randomness (see Table 7) and it is reasonable that in this sample the development of crystallinity is inhibited. In the curves of B2 and B3 cold crystallization exotherms are also observed during the heating run. All melting events tend to be present as multiple endotherms, also evident in the reference homopolymers (see shoulder preceding or following main peak in PBA and PHB respectively). Copolymers B1, B2 and B3 show a melting endotherm at temperatures higher than PBA Tm. This implies that the crystal phase

59

concerned is stable in a range where PBA crystals cannot exist, hence it is likely due to melting of PHB-type crystals. The melting temperature of such PHB-type crystals is lower than Tm of the corresponding homopolymer, showing that these microblock copolymers behave, in this respect, similarly to random copolymers [217].

In the heating run after quenching (Figure 20) copolymers show cold crystallization and melting phenomena, except B4 that is unable to crystallize as already observed after controlled cooling in Figure 19.
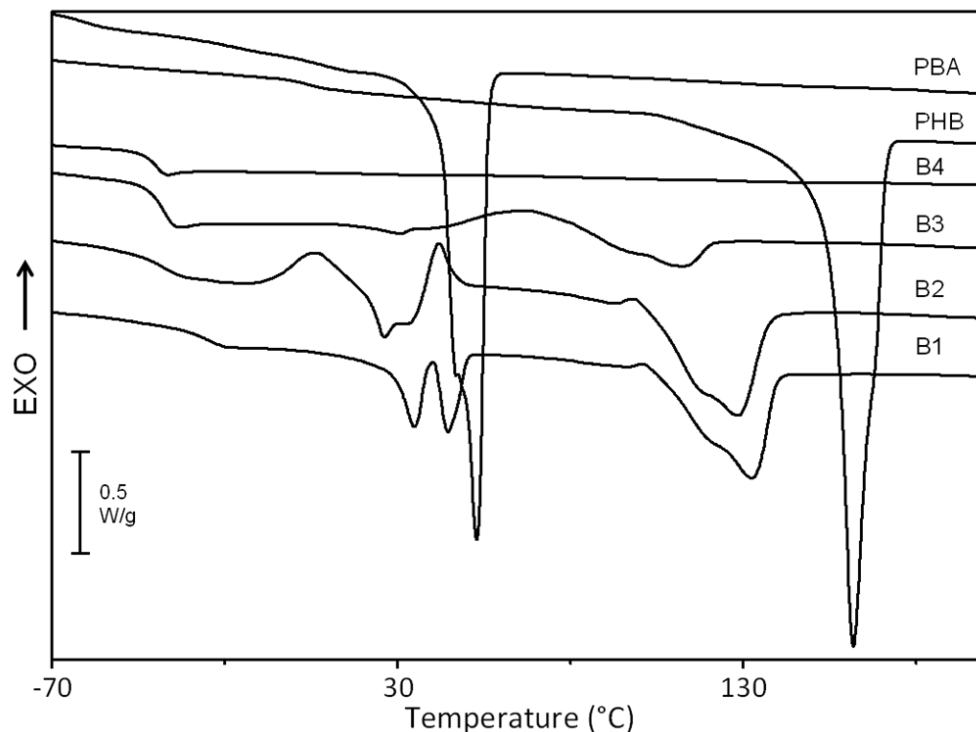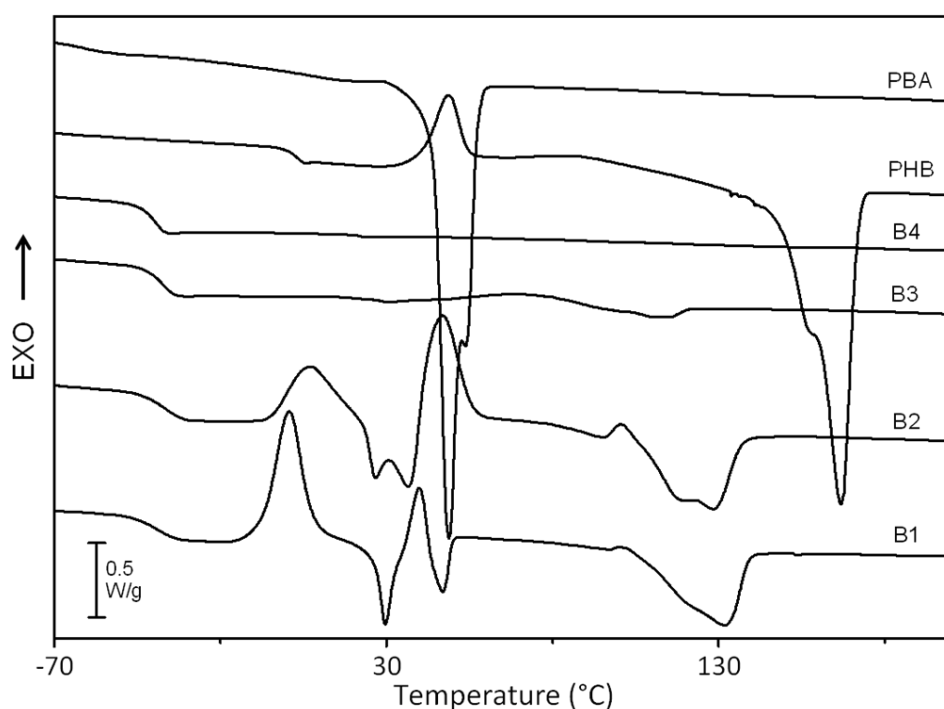

Figure 20. DSC heating curves (20°C/min) of the P(HB-*co*-BA) copolyesters and of the reference PHB and PBA homopolymers, after quench cooling.

After quenching all copolymers show an endothermal baseline shift associated with the glass transition whose value lays in the range between the Tg of PBA (-62°C) and PHB (2°C).

WAXS analysis was performed at room temperature on the pristine samples obtained *via* solution precipitation (purification procedure, see Section 2.1) and the results are shown in Figure 21.
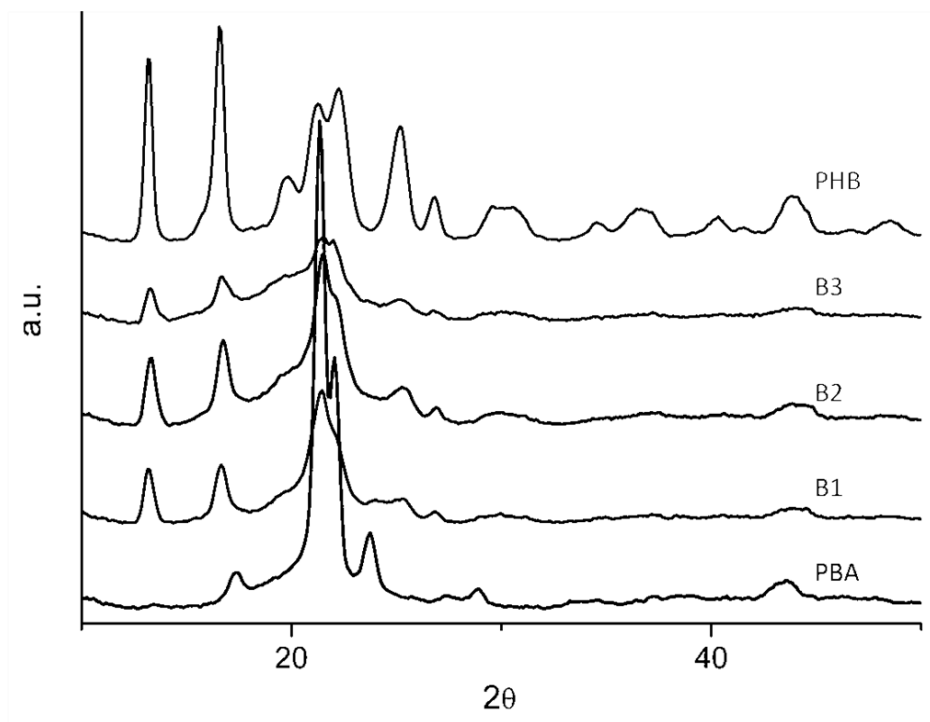
Figure 21. WAXS diffractograms of the P(HB-*co*-BA) copolyesters and of the reference PHB and PBA homopolymers.

The WAXS diffractograms clearly show for B1, B2, and B3 the reflections typical of the PHB lattice [218].

In Figure 19 and Figure 20 the melting phenomena that lay below the PBA melting temperature are tentatively attributed to fusion of PBA-type crystal phase, though it cannot be excluded that they might also involve highly depressed melting of PHB-type crystals. It is worth pointing out that the mentioned PBA-type crystal phase melts very close to room temperature and that its detection may be difficult by means of room temperature WAXS measurements (Figure 21).

In conclusion, the P(HB-*co*-BA) copolymers investigated in this work represent a new family of biodegradable copolyesters with structure varying from semicrystalline to totally amorphous.

3.3. Polymers with complex molecular architecture obtained from bio-based monomers: polyamide 11

3.3.1. Synthesis and rheological properties

In this work, linear and star-shaped Polyamide 11 structures have been investigated. Star-PA11 polymers were obtained by co-polycondensation of a given amount of 11-aminoundecanoic acid monomer with different amounts of a comonomer having either three amine functionalities (T3) or four acidic functionalities (T4).

The general scheme of a polycondensation of this kind is shown below (Scheme 1) in which AB type monomers react in the presence of a multifunctional compound RA_f, where f is the number of A-type functional groups (in order to get star-shaped polymers, $f \geq 3$) and R is the core of the compound. The product of such reacting system is a mixture of linear chains and star polymers in which f chains, at most, are attached to the central branch point [219].

Scheme 1. Macromolecular species that may be obtained by co-polycondensation of AB type monomer with a multifunctional comonomer, RA_f.

In order to predict the macromolecular complexity of star shaped polycondensates resulting from the reaction, the statistical model developed by Yuan [219] is applied to PA11 samples. This model quantifies the content, average molecular weight (M_n) and dispersity index (D) of linear chains and of macromolecules with different arm number (at most equivalent to comonomer functionality) in the final product. Table 8 collects the M_n and D values calculated considering a high conversion of the polymerization reaction according to the equations proposed in the model [219], from the initial feed of AB monomer and of multifunctional agent and from the experimental concentration of end groups, obtained by titration.

Table 8. Number average molecular weight (M_n) of linear and of star species in PA11 samples, evaluated by model calculations [219].

Sample	Multifunctional agent		Overall M_n	$D^{a)}$	M_n (1-arm)	M_n (2-arm)	M_n (3-arm)	M_n (4-arm)
	Content (mol%)	$f^{b)}$						
Linear	0	_	$14126^{c)}$	1.8				
1	0.125	3	22794	2.1	17446	34893	52339	_
2	0.45	3	22246	1.7	10767	21533	32300	_
3	1.45	3	10368	1.5	4093	8187	12280	_
4	0.125	4	21532	2.2	15015	30030	45044	60057
5	1.45	4	8966	1.5	3029	6059	9088	12118

[a] Polydispersity

[b] Functionality

[c] Experimental value from SEC

The data in Table 8 show that, with increasing content of a given multifunctional comonomer (either T3 or T4), the overall average molar mass (M_n) of the PA11 samples decreases and the molecular weight distribution narrows. The values reached at the highest amount of multifunctional agent tested (1.45mol%) are lower than those of the linear polymer. Moreover, at a given comonomer feed, molecular weight decreases with increasing functionality (compare sample 1 with sample 4 and sample 3 with sample 5, see Table 8).

The melt viscosity behavior as function of the shear rate of the PA11 samples analyzed in this work is shown in Figure 22. The Figure compares the melt viscosity curves of all star PA11 samples (Table 8) with that of the reference linear polyamide.
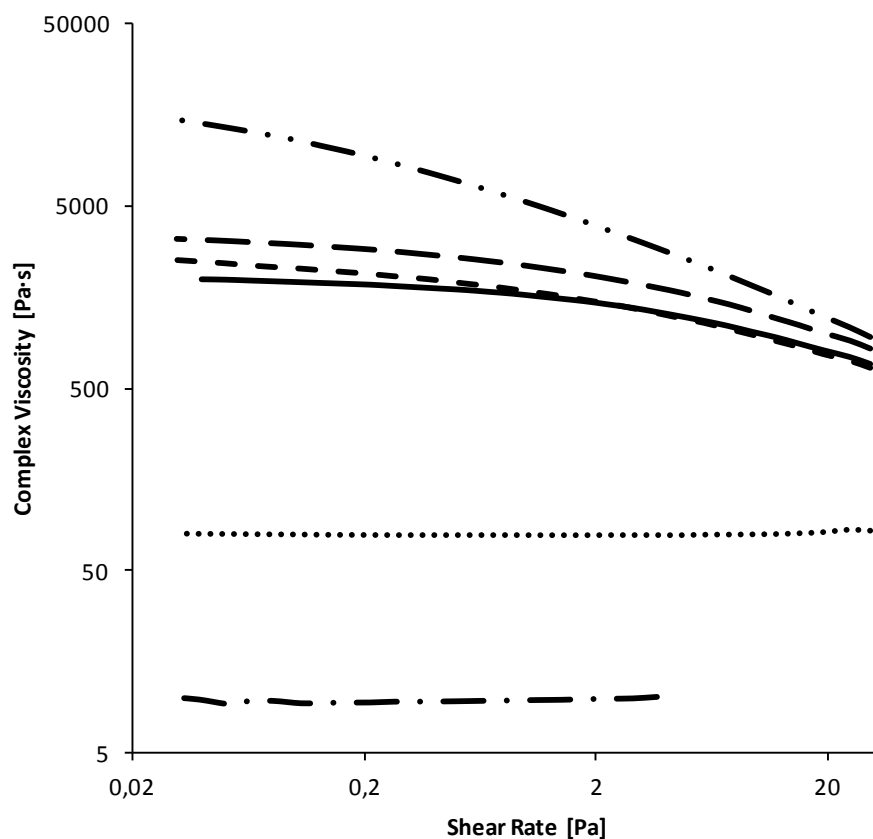

Figure 22. Rheological curves of: Linear PA11 (solid), sample 1 (long-dash), sample 2 (short-dash), sample 3 (dot), sample 4 (dash-double dot) and sample 5 (dash-dot).

In the field of low shear rates, melt viscosity of samples synthesized in the presence of the trifunctional agent (T3) increases at first when 0.125mol% of comonomer is used (sample 1), then it decreases approaching that of linear PA11 at 0.45mol% T3 (sample 2). Further addition of the trifunctional agent (1.45mol%, sample 3) causes a significant viscosity drop associated with an apparent loss of shear rate dependence. In the case of star PA11 samples polymerized using T4 as comonomer, the described behavior is emphasized, with a strong increase of melt viscosity at 0.125mol% (sample 4) and a drastic drop at 1.45mol% (sample 5).

It is known that the shear behavior in the melt of star–shaped macromolecules differs from that of their linear analogues and that it essentially depends on the number and length of the arms [220-222]. In the case of monodispered star polyisoprene it was shown [222] that above functionality 4 no effect of arm number was detected, while arm length caused a relevant viscosity increase, associated with entanglement formation. The behavior of the present samples can therefore be analyzed in terms of the "span molecular weight" (M_s) defined in the case of stars [222,223] as twice the arm molar mass, i.e. the longest linear span in the macromolecule. The M_s values of the PA11 stars with T3 are 34kDa, 20kDa, 8kDa for samples 1,2 and 3 respectively. For the T4 series, M_s values are 30kDa (sample 4) and 6kDa (sample 5). Such M_s data may be compared with the critical molar mass for entanglement formation in linear PA11 that is around M_e = 13000Da. This value was obtained by Prof. Di Silvestro's research group performing frequency sweep experiments on a series of linear PA11 samples. In Figure 22 samples 1 and 4, that show higher viscosity than linear Ny11, have M_s well above M_e and can consequentially form entanglements. The difference in rheological behavior of the two star samples, i.e. notably higher viscosity in sample 4, is attributed to different functionality (f = 3 in sample 1, f = 4 in sample 4) that alters the entanglement density [221,223,224]. Samples 3 and 5 with very low M_s are unable to form entanglements and display in Figure 22 the reduced viscosity behavior expected for short-branch stars with compact structure.

The above results show that PA11 samples obtained in this work posses a broad spectrum of branched species, of molecular weights and of viscoelastic behaviors that can be

rationalized by the Yuan model [219]. A strong dependence of the melt viscosity on amount and type of multifunctional agent used is found for the PA11 samples analyzed. It is therefore possible to modulate melt properties and hence processability of the bio-based PA11 polymer through copolymerization with a suitable multifunctional agent, by simply controlling monomer feed ratio and reaction conversion.

3.3.2. Solid-state properties

All PA11 samples were subjected to thermogravimetric analysis. The obtained TGA curves (not shown) were very similar and were composed of three degradation steps: (i) a minor one around 420°C, followed by (ii) the main degradation event centered at 470°C (weight loss ca. 80%) and finally (iii) a minor weight loss at 490°C. The solid residue at 700°C was in all cases lower than 1%. From such results it can be concluded that the molecular architecture seems not to influence thermal degradation of PA11. The effect of increasing temperature on PA11 was deeply investigated in the literature. The three steps observed in the present samples were earlier attributed respectively (i) to loss of low molecular weight oligomers [225], (ii) to complex decomposition processes leading to volatiles and to crosslinked structures that (iii) eventually degrade in the last weight loss step [226].
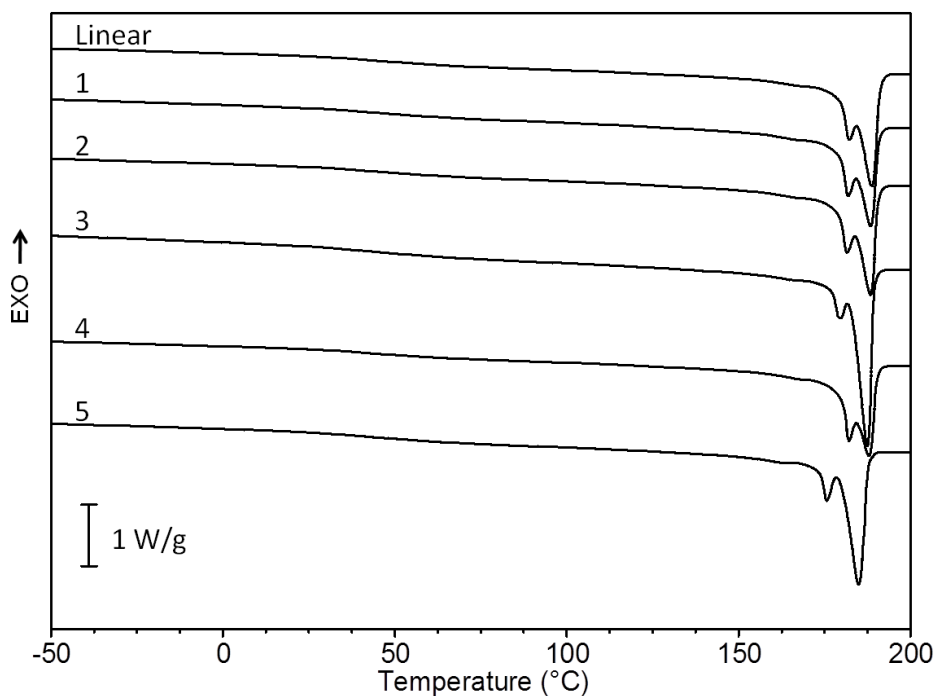
Figure 23. DSC heating curves (after controlled cooling from the melt) of star PA11 samples and of the reference linear polymer.

The calorimetric behavior of the star PA11 samples (DSC heating curves after controlled cooling from the melt) is shown in Figure 23. No appreciable differences are observed in samples with different arm length subjected to the same thermal history, except for a slight downshift of the complex melting endotherm in sample 5. A baseline shift associated with the glass transition (Tg around 45°C) can be detected in all curves, that is followed by a multiple melting endotherm (main peak at 190°C in all samples except sample 5 where Tm = 185°C). The enthalpy associated with melting is the same in all cases (56 ± 2 J g^{-1}). A multiple melting process has been previously reported for linear Ny11 [227,228] and the present results show that this complex melting behavior is also common to star shaped PA11 samples. In order to investigate the phenomena that underlay melting in star as well as in linear PA11, temperature-modulated (TMDSC) measurements were performed. Figure 24 shows, as an example of star-PA11, the total heat flow (T) and its components, reversible (R) and nonreversible (NR), for sample 5 that has the highest branching density

67

and the strongest difference in melt viscosity behavior compared with linear Ny11 (Figure 22).
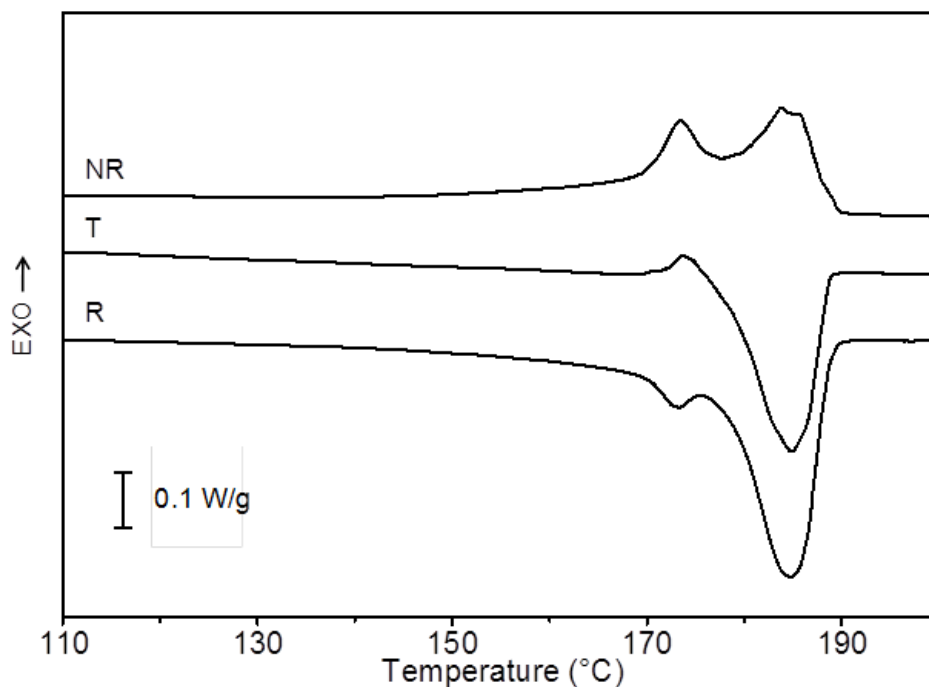

Figure 24. Temperature modulated DSC (TMDSC) heating curvesof sample 5 after controlled cooling from the melt at 10°C/min to T = 10°C. The three curves are: total heat flow (T), reversible heat flow (R), not reversible heat flow (NR).

Decomposition of the T curve into its components clearly illustrates that melting (appearing in the R curve) and crystallization (in the NR curve) occur concomitantly in the range 130°C-195°C. This result clarifies that the two-peak endotherm observed in the DSC curve of sample 5 in Figure 23 is due to melting and re-crystallization phenomena. Analogous TM-DSC results (not shown) were obtained for all other star PA11 investigated in this work as well as for the linear sample. It can be concluded that melting and re-crystallization processes occurring during the thermal scan generate the typical multiple endotherm in the total heat flow curve of PA11. This result highlights the great tendency of PA11 to crystallize and to rearrange its crystal phase to better quality crystals during the thermal scan irrespective of its linear or star structure.

The TGA and DSC results discussed above demonstrate that incorporation of arms in the PA11 backbone to yield a star-shaped structure doesn't significantly affect the overall thermal behavior of the polymer.

All PA11 samples were subjected to dynamic mechanical analysis and the obtained tan δ curves for the PA11 samples synthesized using T3 comonomer and for the linear polymer as a reference are displayed in Figure 25.
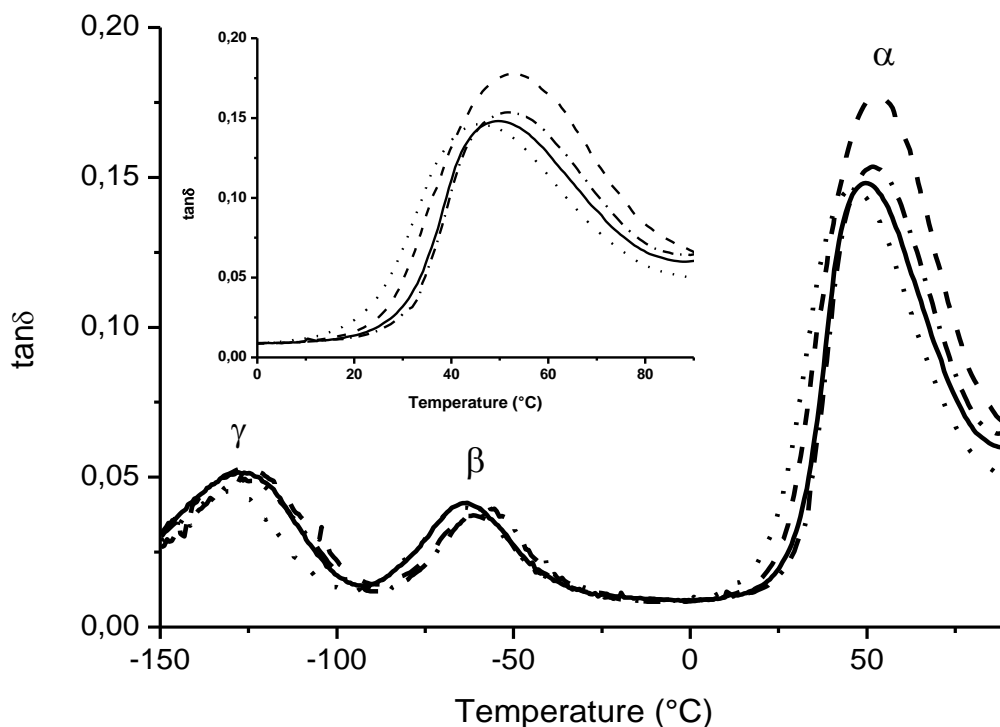

Figure 25. DMTA curves at 3 Hz and 3 °C/min of PA11 samples: Linear (solid), sample 1 (dash), sample 2 (dash-dot) and sample 3 (dot). Insert: magnification of α-relaxation.

Linear and star-shaped PA11 display three solid-state viscoelastic relaxations in the range of temperatures investigated. Like most aliphatic polyamides [229], PA11 shows the main α-peak centered around 50°C associated with the glass transition, the β relaxation that is water sensitive and is attributed to local motions involving the amide bonds and finally a low-temperature γ peak associated with local motions of the methylene sequences.

No substantial differences are observed in the curves of Figure 12 with changing PA11 structure. Indeed local motions in the glassy state are not expected to be affected significantly by the presence of branching points, unless in the event of a substantial inhibition of the polyamide crystallization ability that would increase the amorphous fraction and enhance relaxation intensity. However this is not the case of the present PA11 samples, that display the same melting enthalpy by DSC and therefore possess analogous crystal phase content.

The insert in Figure 25 highlights small shifts on the temperature scale of the main glass transition relaxation. The peak temperature (50°C for linear Ny11) slightly up-shifts to 53°C and 52°C for samples 1 and 2 respectively, while it slightly down-shifts to 46°C for sample 3. The observed behavior, revealed by the sensitive DMTA technique, may be tentatively associated with the different ability of the analyzed PA11 samples to form entanglements, that was already evidenced by the melt viscosity curves of Figure 22. In addition, in the case of sample 3 the decrease of $T\alpha$ might be also attributed to enhanced mobility related to the high number of chain ends in such a sample.

It is known that PA11 exhibits polymorphism with crystal structure that changes on heating: the triclinic alpha-phase, stable at RT, gradually transforms into a pseudohexagonal gamma-phase at higher temperatures, and the transition is reversible [230].

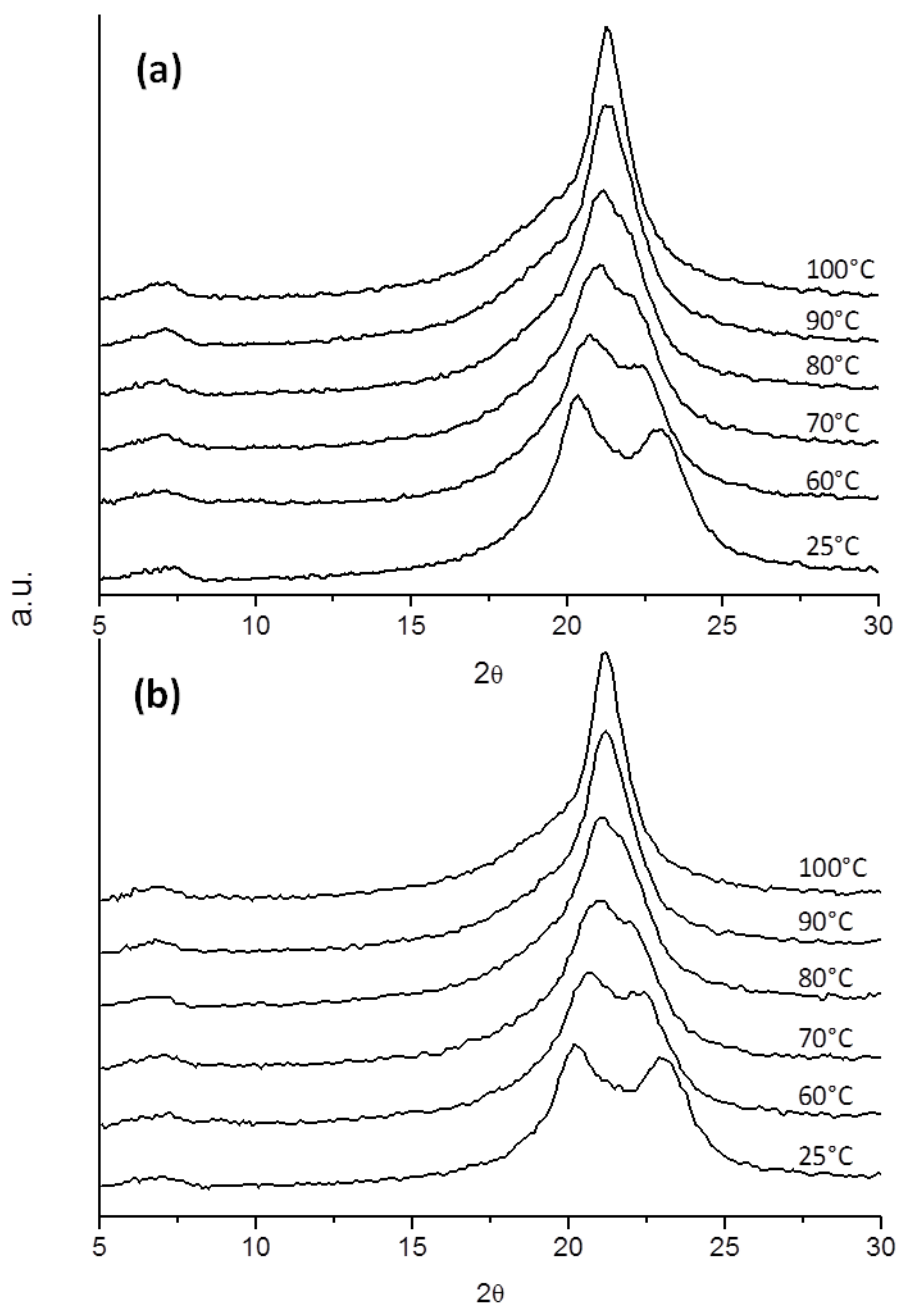Figure 26. WAXS diffractograms of Linear PA11 (a) and of sample 3 (b), collected at various temperatures (indicated on curves) during heating.

In order to investigate whether the presence of star structures alters the polymorphic behavior of PA11, X-ray diffraction analysis under a temperature ramp (from RT to 160°C at 3°C/min) was performed. The results on sample 3 are compared in Figure 26 with those

of linear PA11 analyzed in the same experimental conditions (see Section 2.3.5 for procedure). Selected diffractograms, collected upon heating from RT to 100°C (see Experimental Section for procedure), are shown. Curves recorded at higher temperature in the range 100°C <T< 160°C did not change appreciably, being similar to that shown in Figure 26 for T= 100°C.

At room temperature, linear and star samples show very similar diffraction patterns. They display a weak reflection and two more intense peaks, that are respectively located in the linear sample at $2\theta = 7.1°$, $2\theta = 20.4°$ and $2\theta = 22.9°$, in agreement with the α-phase diffraction pattern of PA11 reported in the literature [230]. During the heating scan, the latter two peaks gradually converge to a single peak at $2\theta = 21.3°$(see diffractograms collected at T=100°C in Figure 26a and Figure 26b), whereas the weakest reflection at $2\theta = 7.1°$ is maintained. The behavior as a function of temperature is the same in both linear and star-shaped samples. Indeed, with increasing temperature the reflections progressively move from those typical of the α-phase to those of the PA11 γ–phase. The α-γ transition is practically completed at 100°C. Reversibility of the transition was assessed in WAXS cooling scans (not shown). Also sample 5, containing T4 in place of T3 comonomer, was subjected to WAXS analysis under the same temperature ramp and identical results were obtained (curves not shown). It can be concluded that, in the range of comonomer type and compositions explored, the introduction of star structures does not alter the alpha-gamma transition of PA11.

The influence of branching on PA11 mechanical properties was assessed by tensile stress-strain measurements and the results are collected in Table 9. The film obtained by compression molding from sample 5 was too fragile to be subjected to mechanical testing.

Table 9. Tensile mechanical properties of PA-11 samples.

Sample	E (Gpa)[a]	ε_y (%)[a]	σ_y (Mpa) [a]	ε_b (%)[a]	σ_b (Mpa) [a]
Linear	1.09 ±0,51	28 ±2	41.2 ±1,3	>100	–
1	0.97 ±0,43	26 ±2	35.7 ±1,5	>100	–

2	1,08 ±0,66	28 ±3	36.9 ±1,9	>100	–
3	0.93 ±0,43	–	–	22 ±4	35.9 ±3.0
4	1.02±0.56	26±5	37.5±1.6	>100	–

[a] E = Young's modulus, ε_y = yield strain, σ_y= yield stress, ε_b= strain at break, σ_b= stress at break

Samples 1, 2 and 4 display a behavior very similar to that of linear PA11, with large elongation at break (>100%), whereas sample 3 with the highest content of T3 multifunctional comonomer shows a lower but still interesting deformability range (ε_b =20%), associated with a tensile strength similar to that of the other samples (σ_b ca. 35MPa). No clear yield point is reached by sample 3 before rupture. This behavior can be associated with the short length of the arms of sample 3 that also leads to low melt viscosity (Figure 9). The great fragility shown by sample 5 is attributed to the even shorter arm length of this star-shaped PA11 and to its inability to form efficient entanglements, also reflected by its rheological behavior.

In conclusion, the results of this work show that, in the range of comonomer functionality and content explored, thermal properties (TGA, DSC and DMTA) do not significantly vary with changing macromolecular architecture. All star-shaped polyamide samples easily crystallize and they undergo the alpha-gamma crystal phase transition upon heating that is typical of linear PA11. As concerns the mechanical behavior, the present results show that careful selection of chain controller type and amount may allow to improve the rheological properties of the PA11 melt for easier processing, while preserving the material mechanical performance.

It is therefore concluded that copolycondensation of 11-aminoundecanoic acid with selected multifunctional comonomers provides a very convenient - and industrially scalable - method for the production of PA11 polymers containing a concentration of star-type chains that can be tuned to yield the desired rheological and solid-state properties.

3.4. Solide-state properties of polyaminoesters synthesized by enzymatic catalysis

Synthesis of polymers using enzymes as catalysts is an environmentally friendly process suitable as alternative approach to the use of toxic heavy metal catalysts currently used in polymer chemistry [231]. Enzymes posses the advantages to be bio-sourced, to operate at mild temperatures reducing process energy consumption and to be recyclable when immobilized, allowing to reduce catalyst cost [231].

In this work, novel poly(β-amino esters) synthesized via lipase-catalyzed polymerization were investigated: Poly[3-(4-(methylene)piperidin-1-yl)propanoate], PMPP, homopolymer and Poly[pentadecalactone-co-3-(4-(methylene)piperidin-1-yl)propanoate], Poly(PDL-co-MPP), copolymers. Immobilized CALB was used as enzymatic catalyst. Chemical structures of the polymers obtained are reported in Figure 27. The results of this work have been published in [200].
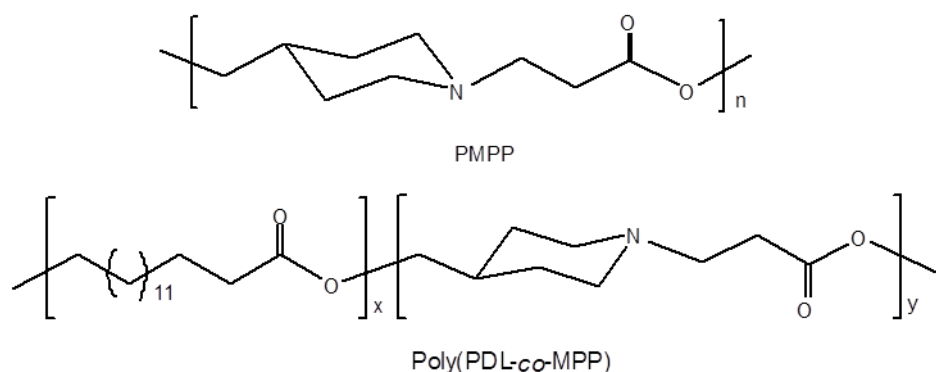

Figure 27. Chemical structures of Poly[3-(4-(methylene)piperidin-1-yl)propanoate], PMPP, homopolymer and Poly[pentadecalactone-co-3-(4-(methylene)piperidin-1-yl)propanoate], Poly(PDL-co-MPP), copolymers.

Both ^{1}H and ^{13}C NMR analyses indicate that the copolymers synthesized are totally random polymers.

Table 10 collects molecular weight (Mw), polydispersity (Mw/Mn) and composition of (PDL-co-MPP) copolymers synthesized starting from different feed molar ratio. The copolymers are labeled as P-x, in which x is the percentage molar ratio of PDL units.

Table 10. Feed molar ratio, molecular weight and composition of (PDL-co-MPP) copolymers.

Sample	PDL/EHMPP (Feed molar ratio)	$M_w{}^a$	$M_w/M_n{}^a$	PDL Content (Mol%)^b
P-21	20:80	15900	1.6	21%
P-36	35:65	16300	1.6	36%
P-51	50:50	24800	1.5	51%
P-67	65:35	24100	1.7	67%
P-82	80:20	27200	1.6	82%

a) molecular weight (Mw) and polydispersity (Mw/Mn) measured by gel permeation chromatography (GPC).

b) composition calculated from the ^{1}H NMR spectra.

As shown in Table 10, the poly(PDL-co-MPP) compositions were readily controlled by varying the monomer feed ratio employed during the copolymerization. The purified copolymers had a Mw ranging from 15900 to 27200 Da with polydipersity between 1.5 and 1.7.

Poly(PDL-co-MPP) copolymers and the reference homopolymers PMPP and PPDL were subjected to thermogravimetric analysis (TGA). The resulting TGA curves and data are collected in Figure 28 and Table 11 respectively.
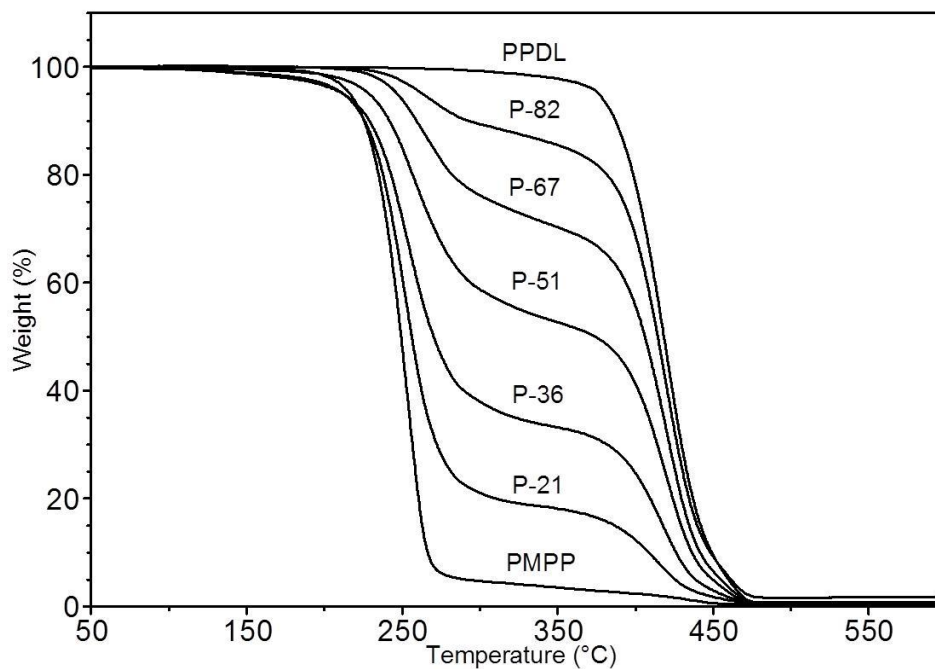
Figure 28. TGA curves of poly(PDL-co-MPP) copolymers and of homopolymers PPDL and PMPP.

Table 11. TGA results of poly(PDL-co-MPP) copolymers and of homopolymers PPDL and PMPP.

Sample	PDL (wt%)	MPP (wt%)	$T_{max}{}^a$ (°C)		Δm 1st step^b (wt%)	Normalized Δm^c (wt%)
PMPP	0	100	253	-	94	100
P- 21	27	73	252	415	76	81
P- 36	44	56	254	417	59	62
P- 51	60	40	256	420	40	42
P- 67	74	26	262	419	24	25
P- 82	87	13	266	419	11	11
PPDL	100	0	-	417	1	1

a) temperature of maximum degradation rate.

b) weight loss in the T range 200°C-300°C (1st step).

<superscript>c)</superscript> weight loss in the T range 200°C-300°C (from previous column) normalized towards Δm of PMPP.

The curves in Figure 28 highlight the different thermal stability of the homopolymers, with the degradation temperature of PPDL being 160°C higher than that of PMPP. All poly(PDL-co-MPP) copolymers degrade in two well defined weight loss steps. The TGA data, collected in Table 11, show that the temperature of maximum degradation rate (Tmax) of the two degradation events in poly(PDL-co-MPP)s very well correlates with the Tmax's of the reference homopolymers. Quantification of the weight loss in the first degradation step and its normalization towards the weight loss of homopolymer PMPP yields a value (Table 11) that reasonably compares with the MPP content of each copolymer. This observation suggests that the first step is associated with thermal degradation of the MPP fraction in the copolymer and the second step is related to that of the more stable PDL units/sequences.

In order to support such a hypothesis, FT-IR measurements were carried out on copolymer P-51 after a TGA scan interrupted at 330°C, i.e. at an intermediate temperature between the two weight losses (Figure 28). FT-IR spectra of sample P-51 before (P-51-A) and after (P-51-B) the TGA measurements and of the reference homopolymers PPDL and PMPP, for the sake of comparison, are reported in Figure 29.
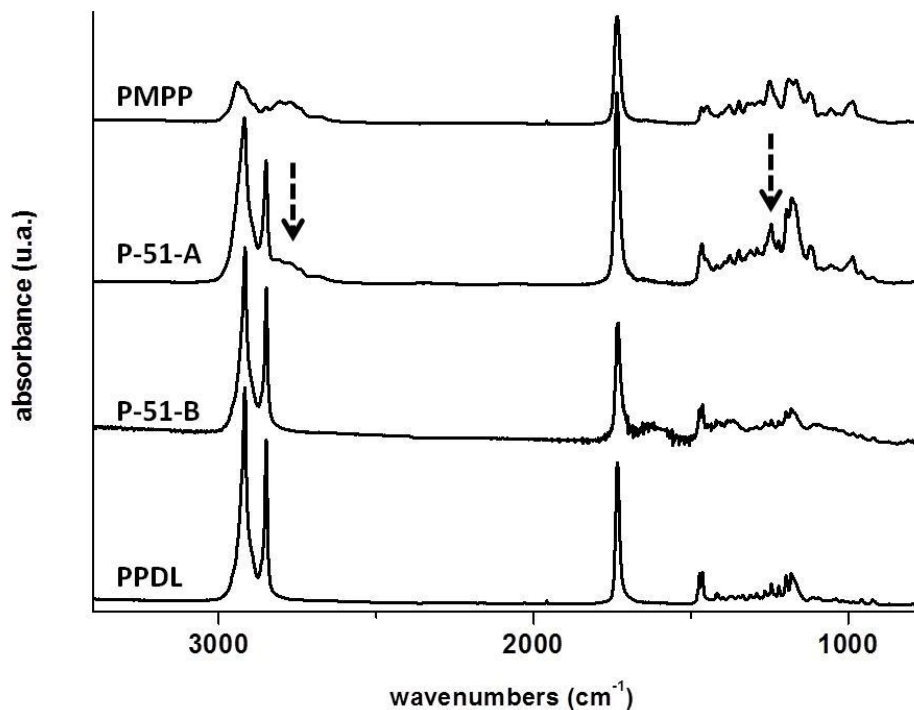
Figure 29. FT-IR spectra of sample P-51 before (P-51-A) and after (P-51-B) a TGA measurement interrupted at 330°C (after the first degradation step). FT-IR spectra of reference homopolymers PPDL and PMPP are also reported for the sake of comparison.

In Figure 29 the FT-IR spectrum of P-51 before the TGA scan (P-51-A) shows typical bands of both homopolymers. The bands marked with arrows, in the regions 2940-2800 cm$^-$1 and 1250-1020 cm$^-$1 are attributed to CH stretching and CN stretching vibrations of the piperidine moiety in the MPP unit (see Figure 27) respectively. Such bands disappear from the spectrum of P-51 after the first TGA degradation event (P-51-B). The spectrum of this sample becomes similar to that of PPDL. This result is taken as evidence of the involvement of the MPP units in the first (low-T) degradation process.

DSC scans were run at 20°C/min from -80 up to 150°C applying controlled cooling (10°C/min) between the scans. Figure 30 shows the DSC curves (1st heating scan) of poly(PDL-*co*-MPP) copolymers together with those of the reference homopolymers.
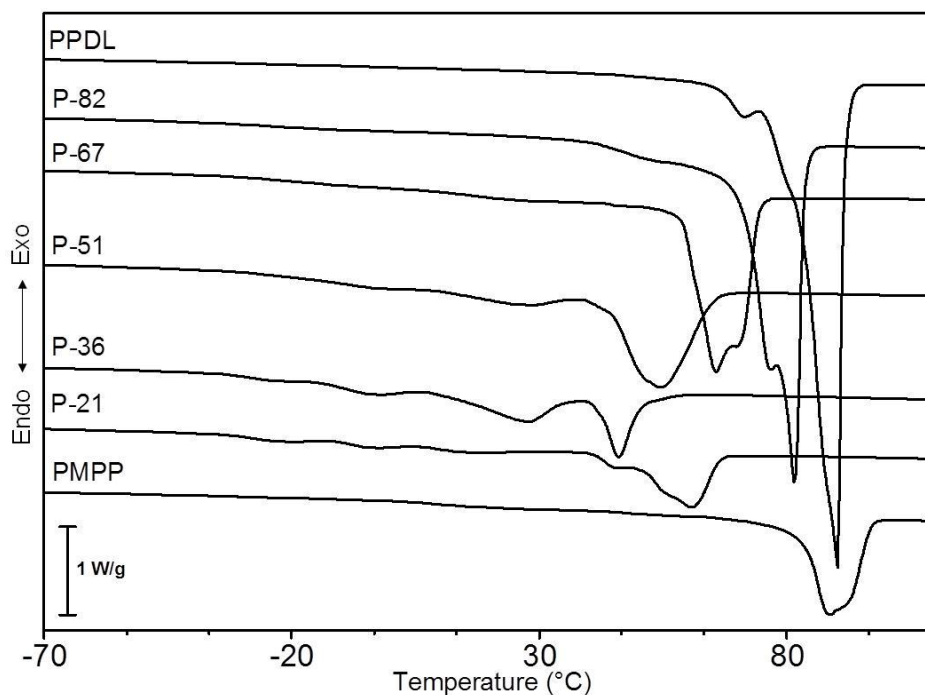
Figure 30. DSC heating curves (20°C/min) of poly(PDL-co-MPP) copolymers and of the reference PPDL and PMPP homopolymers.

All samples analyzed show a melting endotherm located at different temperatures depending on copolymer composition. Comparing the copolymer curves with those of PMPP and PPDL, it is evident that the endotherms shift to lower temperatures with respect to that of each homopolymer with increasing comonomer content. Worth noting is that PPDL and PMPP melt in the same T-range.

Figure 31 shows a plot of the final melting temperature (Tm) vs. composition for the polymers. Since most analyzed samples showed complex melting endotherms with multiple peaks and shoulders, the final melting temperature at the intercept between the tangent to the peak on the high-T side and the baseline after the endothermal event was taken as Tm. In the presence of melting and recrystallization phenomena, this is the melting temperature of the most perfect crystals that develop during the heating scan at the applied heating rate.
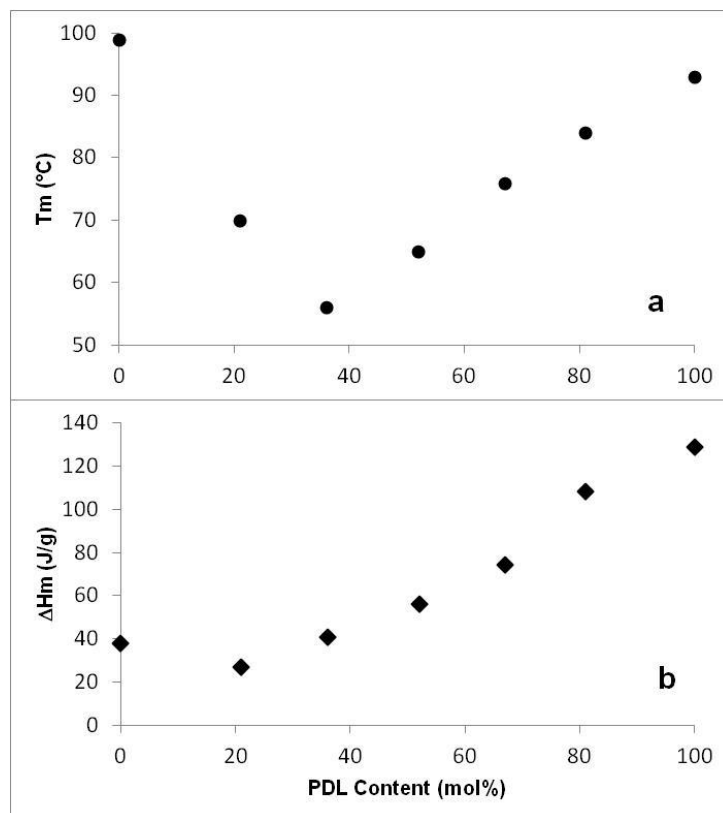
Figure 31. Composition dependence of T_m ($\bullet$) and ΔH_m ($\blacklozenge$) of poly(PDL-*co*-MPP) copolymers and of the reference homopolymers (PPDL and PMPP).

Figure 31 illustrates that Tm decreases with increasing comonomer content reaching a minimum in P-36 copolymer. The melting enthalpy, also plotted in Figure 31, highlights the different ΔH_m values of the two homopolymers and the decrease of this parameter in copolymers with decreasing PDL content.

In random copolymers, it is expected that ΔH_m decreases with increasing comonomer content whereas it is much less common to observe crystallinity over the whole composition range, especially at intermediate compositions, as displayed by the present copolymers in Figure 30. The presence of the PDL units, well known to favor crystallinity in copolymers [232-234], might be the key to the observed behavior of poly(PDL-*co*-MPP). Upon controlled cooling of the copolymers (Figure 32), P-21 - like PMPP - does not crystallize while all other copolymers show a clear crystallization exotherm whose temperature increases with increasing PDL content. In the subsequent heating scan (not

shown), curves similar to those obtained in the 1st scan (Figure 30) were obtained for PPDL and for all copolymers except P-21, which showed a very modest cold crystallization and melting ($\Delta H_c = \Delta H_m = 3$ J/g). PMPP remained totally amorphous in the applied experimental conditions.
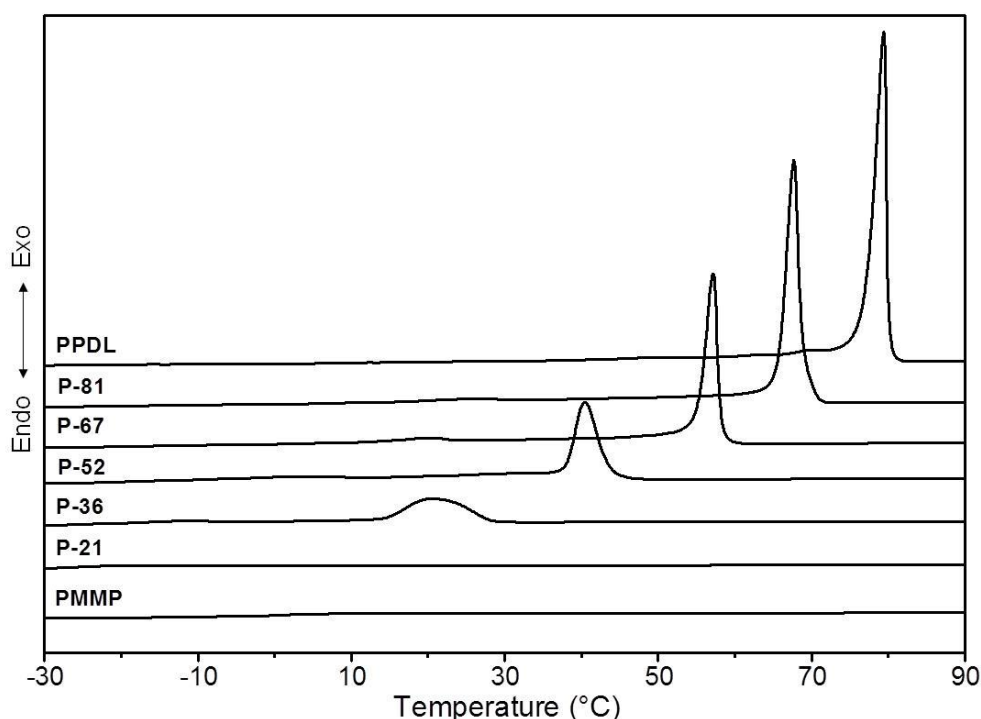

Figure 32. DSC cooling curves (10°C/min) of poly(PDL-co-MPP) copolymers and of the reference homopolymers (PPDL and PMPP).

From DSC results, it can be concluded that although PMPP and the copolymers rich in MPP units do not easily crystallize upon cooling from melt, the homopolymer and all copolymers obtained via precipitation from solution are semi-crystalline materials.

WAXS analysis was applied to the semi-crystalline polymers obtained by precipitation from solution (purification procedure). Figure 33 shows the X-ray diffractogram of the newly synthesized PMPP, never studied by WAXS before, while Table 12 lists the d-spacing values calculated from the 2θ positions of the main reflections (marked on the curve).

Figure 33. WAXS diffractogram of PMPP homopolymer.
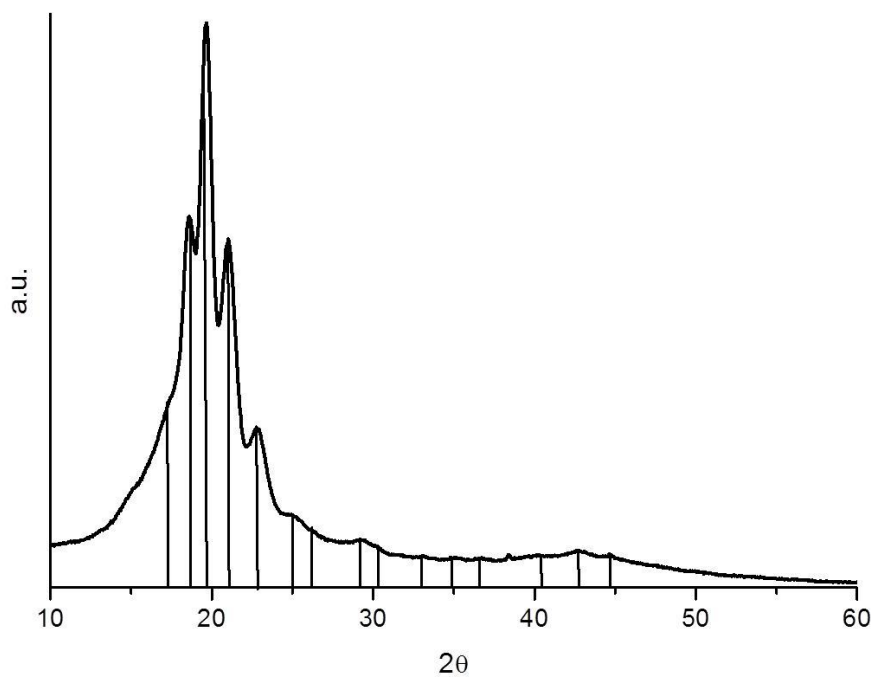
Table 12. Structural Parameters: d-Spacing and position (2θ) of main reflections of PMPP.

No. peaks	d-spacing [Å]	2θ [°]
1	5.11	17.36
2	4.77	18.60
3	4.52	19.65
4	4.23	21.01
5	3.89	22.85
6	3.56	25.00
7	3.38	26.34
8	3.05	29.25
9	2.96	30.17
10	2.71	33.11
11	2.57	34.89

12	2.45	36.66
13	2.24	40.25
14	2.12	42.69
15	2.04	44.46

The crystallinity degree of PMPP, calculated as the ratio of the crystalline peak areas to the total area under the scattering curve, is 31%.

Figure 34 compares the diffractogram of PMPP with that of the other homopolymer (PPDL) and with those of all poly(PDL-co-MPP) copolymers.
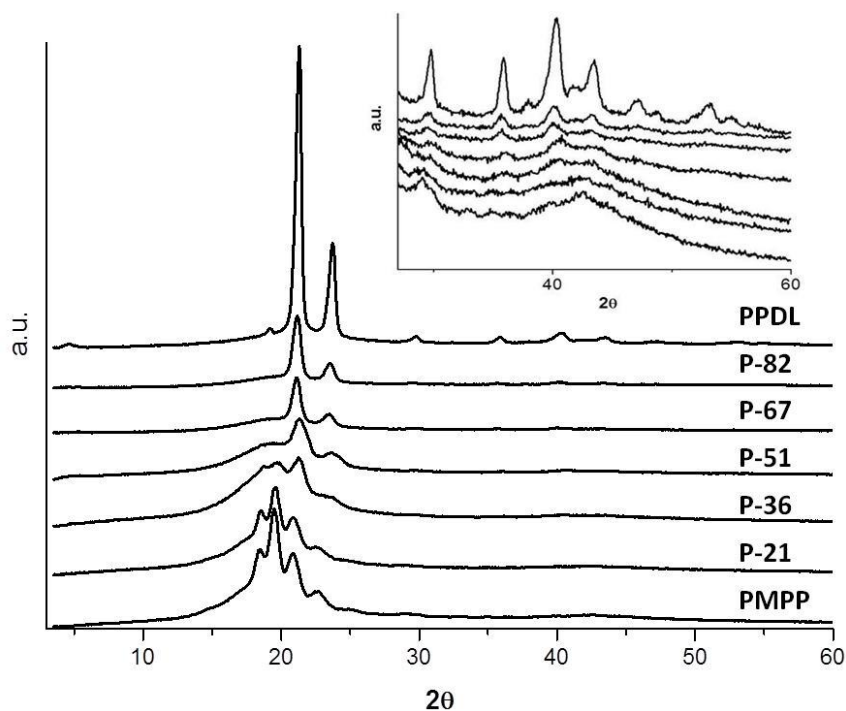
Figure 34. WAXS diffractograms of poly(PDL-*co*-MPP) copolymers and of the reference homopolymers (PPDL and PMPP). Insert: magnification of the 2θ range = 30-60 deg.

The X-ray curve of PPDL displays, as expected from earlier literature results [235], main reflections at $2\theta = 4.17°$, $21.31°$, $23.79°$ and its degree of crystallinity is higher than that of the other homopolymer, i.e. 47% , in agreement with the higher melting enthalpy of PPDL in Figure 31. The diffractograms of the copolymers in Figure 34 show different patterns. In

particular, while the reflections in the WAXS curve of copolymer P-21 are at the same positions as those of PMPP, copolymers with PDL content above 51 mol% display the same crystal pattern as that of PPDL. Hence P-21 develops PMPP-type crystals whereas copolymers P-51, P-67 and P-82 crystallize in the PPDL lattice. The X-ray curve of copolymer P-36 is peculiar because it shows reflections pertaining to the diffraction patterns of both homopolymers. This result demonstrates that in P-36, whose melting temperature is located at the minimum in Figure 31, PMPP-type and PPDL-type crystals co-exist. The multiple endotherm of sample P-36 in Figure 30 is therefore most probably due to melting of the two types of crystals rather than due to melting and re-crystallization of a single crystal phase.

In conclusion, WAXS analysis showed that the copolymers rich in PDL ($\geq$51 mol%) crystallize in PPDL lattice and those with $\leq$21 mol% PDL content develop PMPP-type crystals while in the copolymer with 36 mol% PDL, PMPP-type and PPDL-type crystals co-exist.

PMPP hopolymer and poly(PDL-co-MPP) copolymers investigated in this work, represent a new type of poly(β-amino esters) that are potentially useful biomaterials for specific biomedical applications (e.g., gene delivery).

4. CONCLUSIONS

In the present research project structure-property relations in polymers from renewable sources (bio-based polymers) such as microbially produced polymers i.e., polyhydrohyalkanoates (PHAs), or polymers chemically synthesized using bio-based monomers, i.e. polyammide 11 (PA11) were investigated.

Polyhydrohyalkanoates produced by (i) pure cultures (*Cupriavidus necator* bacteria) grown on used cooking oil and (ii) from mixed microbial cultures using as carbon source either a synthetic or a waste substrate, i.e. olive oil mill wastewater, were investigated. The results of this work demonstrate that PHAs from both pure and mixed cultures with good properties can be obtained by using waste substrates as carbon source, contributing to improve sustainability of the process.

A strong influence on polymer properties of the extraction procedure used to recover the polymer from the cells was observed indicating that the recovery method adopted in PHA production is a crucial step in the determining quality of the final material. Thus, a chemically assisted enzymatic recovery method that is mild and selective in removing non-PHA cell material, was developed. Such a method allows to obtain PHA granules with excellent thermal properties and in its native form, i.e. granules in the amorphous state that can be useful for specific applications (e.g. paper coating).

In addition, biodegradable and bio-based composites using a commercial PHA, poly(hydroxybutyrate-co-valerate), PHBV, as polymeric matrix were developed for food packaging applications. Biodegradable, non-toxic (for food contact) plasticizers and low cost, widely available lignocellulosic fibers (wheat straw fibers) were incorporated in such polymeric matrix, in order to decrease PHA brittleness and the polymer cost, respectively. By exploring the useful melt processing conditions to prepare the materials, the optimal mixing of the components was achieved. The plasticizers, depending on their content, allow to decrease polymer rigidity and to slightly improve PHBV flexibility and thus providing a good matrix material for the composite with lignocellulosic fibers.

PHAs produced via synthetic routes such as microwave assisted transesterification were also studied in this work. The dependence of solid-state properties of a series of novel poly(3-hydroxybutyrate-co-butyleneadipate), P(HB-co-BA), copolymers on their chemical

structure was assessed. Such copolymers represent a new family of biodegradable copolyesters with structure varying from semicrystalline to totally amorphous. They are potential suitable for different applications like compatibilization of immiscibile PHB/PBA blends and development of matrices for drug delivery systems in the biomedical field.

As concerns the study of polymers chemically synthesized using monomers from renewable sources, polyamide 11 (PA11) that is, in addition to be totally bio-based, an important engineering polymer applied in several industrial fields, was studied in this Thesis. Novel star-shaped PA11 polymers with different arm number and length have been characterized in order to investigate the impact of such architectural modifications on PA11 properties. It is shown that introduction of arms in polymer structure allows to modulate melt viscosity behavior which is advantageous for industrial applications. Also, it is found that several important solid-state properties, in particular mechanical properties, may be affected by the presence of branching, to slight or great extent depending on the functionality and concentration of the comonomer used in polyamides synthesis.

Lastly, novel poly(β-amino esters) synthesized via enzymatic-catalyzed polymerization have been investigated in this work. Solid-state characterization of a series of copolymers showed that materials with a wide range of properties can be obtained depending on their composition. Such copolymers are potentially useful biomaterials for specific biomedical applications (e.g., gene delivery).

5. REFERENCES

1. Corma A, Iborra S, Velty A. Chemical Routes for the Transformation of Biomass into Chemicals. Chem Rev 2007;107:2411-2502.

2. Cherubini F. The biorefinery concept: Using biomass instead of oil for producing energy and chemicals. Energy Convers Manag 2010;51:1412-1421.

3. http://www.iea-bioenergy.task42-biorefineries.com

4. World Commission on Environment and Development. "Our Common Future, Chapter 2: Towards Sustainable Development". http://www.un-documents.net/ocf-02.htm

5. Shen L, Haufe J, Patel MK. Product overview and market projection of emerging bio-based plastics. PRO-BIP final report 2009. http://en.european-bioplastics.org/.

6. Avérous L and Pollet E. Biodegradable Polymers. In:Avérous L and Pollet E editors. Environmental Silicate Nano-Biocomposites. Springer London; 2012.pp. 13-39.

7. Babu RP, O'Connor K, Seeram R. Current progress on bio-based polymers and their future trends. Prog Biomater 2013;2:1-16.

8. Brydson JA. The Historical Development of Plastics Materials. In:Brydson JA editors. Plastics Materials (Seventh Edition). Oxford:Butterworth-Heinemann; 1999.pp. 1-18.

9. Shen L, Worrell E, Patel M. Present and future development in plastics from biomass. Biofuels Bioprod Bioref 2010;4:25-40.

10. www.european-bioplastics.org

11. Pawelzik P, Carus M, Hotchkiss J, Narayan R, Selke S, Wellisch M, Weiss M, Wicke B, Patel MK. Critical aspects in the life cycle assessment (LCA) of bio-based materials – Reviewing methodologies and deriving recommendations. Resources, Conservation and Recycling 2013;73:211-228.

12. Narayan R. Carbon footprint of bioplastics using biocarbon content analysis and life-cycle assessment. MRS Bulletin 2011;36:716-721.

13. Narayan R. Rationale, Drivers, Standards, and Technology for Biobased Materials. In:Renewable Resources and Renewable Energy. CRC Press; 2006.pp. 3-18.

14. ISO 14067. International Organization for Standardization; Greenhouse gases - Carbon footprint of products - Requirements and guidelines for quantification and communication, 2013

15. ISO 14044. International Organization for Standardization. Environmental management Life cycle assessment Requirements and guidelines, 2006

16. ISO 14040. International Organization for Standardization. Environmental management Life cycle assessment Principles and Framework; 2006

17. ASTM D6866, Standard Test Methods for Determining the Biobased Content of Solid, Liquid, and Gaseous Samples Using Radiocarbon Analysis, ASTM International, 2012

18. http://www.okcompost.be/en/recognising-ok-environment-logos/ok-biobased/

19. http://www.okcompost.be/

20. http://www.dincertco.de/

21. ASTM D6400, Labeling of Plastics Designed to be Aerobically Composted in Municipal or Industrial Facilities, ASTM International, 2012

22. Vroman I, Tighzert L. Biodegradable Polymers. Materials 2009;2:307-344.

23. Lucas N, Bienaime C, Belloy C, Queneudec Ml, Silvestre F, Nava-Saucedo JE. Polymer biodegradation: Mechanisms and estimation techniques A review. Chemosphere 2008;73:429-442.

24. Lenz RW, Marchessault RH. Bacterial Polyesters: Biosynthesis, Biodegradable Plastics and Biotechnology. Biomacromolecules 2004;6:1-8.

25. EN 13432, Requirements for packaging recoverable through composting and biodegradation - Test scheme and evaluation criteria for the final acceptance of packaging, European Committee for Standardization, 2000

26. EN 14995, Plastics – Evaluation of compostability – Test scheme and specifications", European Committee for Standardization, 2006

27. ISO 17088, Specifications for compostable plastics, International Organization for Standardization, 2012

28. ISO 18606, Packaging and the environment - Organic recycling, International Organization for Standardization, 2013

29. AS 4736, Biodegradable plastics - Biodegradable plastics suitable for composting and other microbial treatment, Australian standard, 2006

30. EN 14046, Packaging Evaluation of the ultimate aerobic biodegradability and disintegration of packaging materials under controlled composting conditions, Method by analysis of released carbon dioxide, European Committee for Standardization, 2003

31. ISO 1485, Determination of the ultimate aerobic biodegradability of plastic materials under controlled composting conditions - Method by analysis of evolved carbon dioxide, International Organization for Standardization, 2012

32. EN 14045, Packaging - Evaluation of the disintegration of packaging materials in practical oriented tests under defined composting conditions, European Committee for Standardization, 2003

33. http://www.compost.it/

34. http://www.bpiworld.org/

35. Inkinen S, Hakkarainen M, Albertsson AC, Södergård Anders. From Lactic Acid to Poly(lactic acid) (PLA): Characterization and Analysis of PLA and Its Precursors. Biomacromolecules 2011;12:523-532.

36. Ahmed J, Varshney SK. Polylactides−Chemistry, Properties and Green Packaging Technology: A Review. International Journal of Food Properties 2011;14:37-58.

37. Highly Functional Bioplastics (PLA compounds) Used for Electronic Products

38. Lasprilla AJR, Martinez GAR, Lunelli BH, Jardini AL, Filho RM. Poly-lactic acid synthesis for application in biomedical devices − A review. Biotechnol Adv 2012;30:321-328.

39. Ogunniyi DS. Castor oil: A vital industrial raw material. Bioresource Technology 2006;97:1086-1091.

40. Harmsen PFH, Hackmann MM, Bos HL. Green building blocks for bio-based plastics. Biofuels, Bioprod Bioref 2014;n/a.

41. http://www.arkema.com/

42. Fuessl A, Yamamoto M, Schneller A. 5.03 - Opportunities in Bio-Based Building Blocks for Polycondensates and Vinyl Polymers. In:Matyjaszewski K and Möller Martin editors. Polymer Science: A Comprehensive Reference. Amsterdam:Elsevier; 2012.pp. 49-70.

43. Bechthold I, Bretz K, Kabasci S, Kopitzky R, Springer A. Succinic Acid: A New Platform Chemical for Biobased Polymers from Renewable Resources. Chem Eng Technol 2008;31:647-654.

44. Xu J and Guo BH. Microbial Succinic Acid, Its Polymer Poly(butylene succinate), and Applications. In:Chen GG-Q editors. Plastics from Bacteria. Springer Berlin Heidelberg; 2010.pp. 347-388.

45. Cukalovic A, Stevens CV. Feasibility of production methods for succinic acid derivatives: a marriage of renewable resources and chemical technology. Biofuels, Bioprod Bioref 2008;2:505-529.

46. Chen GQ, Patel MK. Plastics Derived from Biological Sources: Present and Future: A Technical and Environmental Review. Chem Rev 2011;112:2082-2099.

47. Plastics - The Fact 2013. An analysis of European latest plastics production, demand and waste data. http://www.plasticseurope.org

48. Gökhan Çaylý, Selim Küsefoðlu. Biobased polyisocyanates from plant oil triglycerides: Synthesis, polymerization, and characterization. J Appl Polym Sci 2008;109:2948-2955.

49. http://www.duponttateandlyle.com/

50. Kurian JV. A New Polymer Platform for the Future - Sorona® from Corn Derived 1,3-Propanediol. J Polym Environ 2005;13:159-167.

51. Rebsdat S and Mayer D. Ethylene Glycol. In:Ullmann's Encyclopedia of Industrial Chemistry. Wiley-VCH Verlag GmbH & Co. KGaA; 2000.pp. 531-546.

52. Kröger M, Prüße U, Klaus-Dieter V. A new approach for the production of 2,5-furandicarboxylic acid by in situ oxidation of 5-hydroxymethylfurfural starting from fructose. Top Catal 2000;13:237-242.

53. Gopalakrishnan P, Narayan-Sarathy S, Ghosh T, Mahajan K, Belgacem M. Synthesis and characterization of bio-based furanic polyesters. J Polym Res 2013;21:1-9.

54. Gandini A. The irruption of polymers from renewable resources on the scene of macromolecular science and technology. Green Chem 2011;13:1061-1083.

55. Bozell JJ, Petersen GR. Technology development for the production of biobased products from biorefinery carbohydrates-the US Department of Energy's "Top 10" revisited. Green Chem 2010;12:539-554.

56. Krässig H, churz J, Steadman RG, Schliefer K, Albrecht W, Mohring M, Schlosser H. Cellulose. In:Ullmann's Encyclopedia of Industrial Chemistry. Wiley-VCH Verlag GmbH & Co. KGaA; 2004.pp. 279-332.

57. Czaja W, Krystynowicz A, Bielecki S, Brown J. Microbial cellulose - the natural power to heal wounds. Biomaterials 2006;27:145-151.

58. Kim J, Cai Z, Chen Y. Biocompatible Bacterial Cellulose Composites for Biomedical Application. Journal of Nanotechnology in Engineering and Medicine 2009;1:011006.

59. Fu L, Zhang J, Yang G. Present status and applications of bacterial cellulose-based materials for skin tissue repair. Carbohydrate Polymers 2013;92:1432-1442.

60. Shi Z, Zhang Y, Phillips GO, Yang G. Utilization of bacterial cellulose in food. Food Hydrocolloids 2014;35:539-545.

61. Miao C, Hamad W. Cellulose reinforced polymer composites and nanocomposites: a critical review. Cellulose 2013;20:2221-2262.

62. Pérez S and Mazeau K. Conformations, Structures, and Morphologies of Celluloses. In:Polysaccharides. CRC Press; 2004.pp.

63. Klemm D, Heublein B, Fink HP, Bohn A. Cellulose: Fascinating Biopolymer and Sustainable Raw Material. Angew Chem Int Ed 2005;44:3358-3393.

64. Satyanarayana KG, Arizaga GGC, Wypych F. Biodegradable composites based on lignocellulosic fibers - An overview. Progr Polym Sci 2009;34:982-1021.

65. Abe K, Iwamoto S, Yano H. Obtaining Cellulose Nanofibers with a Uniform Width of 15 nm from Wood. Biomacromolecules 2007;8:3276-3278.

66. Eichhorn SJ. Cellulose nanowhiskers: promising materials for advanced applications. Soft Matter 2011;7:303-315.

67. Azizi Samir MAS, Alloin F, Dufresne A. Review of Recent Research into Cellulosic Whiskers, Their Properties and Their Application in Nanocomposite Field. Biomacromolecules 2005;6:612-626.

68. Edgar KJ, Buchanan CM, Debenham JS, Rundquist PA, Seiler BD, Shelton MC, Tindall D. Advances in cellulose ester performance and application. Progr Polym Sci 2001;26:1605-1688.

69. Fink HP, Weigel P, Purz HJ, Ganster J. Structure formation of regenerated cellulose materials from NMMO-solutions. Prog Polym Sci 2001;26:1473-1524.

70. Kamel S, Ali N, Jahangir K, Shah SM, El-Gendy AA. Pharmaceutical significance of cellulose: A review. Express Polym Lett 2008;2:758-778.

71. Pérez S, Bertoft E. The molecular structures of starch components and their contribution to the architecture of starch granules: A comprehensive review. Starch - Stärke 2010;62:389-420.

72. Ratto JA, Stenhouse PJ, Auerbach M, Mitchell J, Farrell R. Processing, performance and biodegradability of a thermoplastic aliphatic polyester/starch system. Polymer 1999;40:6777-6788.

73. Ramsay BA, Langlade V, Carreau PJ, Ramsay JA. Biodegradability and mechanical properties of poly-(beta-hydroxybutyrate-co-beta-hydroxyvalerate)-starch blends. Appl Environ Microbiol 1993;59:1242-1246.

74. Shogren RL, Doane WM, Garlotta D, Lawton JW, Willett JL. Biodegradation of starch/polylactic acid/poly(hydroxyester-ether) composite bars in soil. Polym Degrad Stab 2003;79:405-411.

75. Tomasik P and Schilling CH. Chemical modification of starch. In:Adv Carbohydr Chem Biochem. Academic Press; 2004.pp. 175-403.

76. Carvalho AJF, Job AE, Alves N, Curvelo AAS, Gandini A. Thermoplastic starch/natural rubber blends. Carbohydr Polym 2003;53:95-99.

77. Willett JL, Shogren RL. Processing and properties of extruded starch/polymer foams. Polymer 2002;43:5935-5947.

78. Schwach E, Avérous L. Starch-based biodegradable blends: morphology and interface properties. Polym Int 2004;53:2115-2124.

79. Avella M, De Vlieger JJ, Errico ME, Fischer S, Vacca P, Volpe MG. Biodegradable starch/clay nanocomposite films for food packaging applications. Food Che 2005;93:467-474.

80. De Carvalho AJF, Curvelo AAS, Agnelli JAM. Wood pulp reinforced thermoplastic starch composites. Int J Polym Mater 2002;51:647-660.

81. Anglès M.Neus, Dufresne A. Plasticized Starch/Tunicin Whiskers Nanocomposites. 1. Structural Analysis. Macromolecules 2000;33:8344-8353.

82. http://www.novamont.com/

83. http://dev.biop.eu/

84. Aranaz I, Mengibar M, Harris R, Paños I, Miralles B, Acosta N, Galed G, Heras À. Functional characterization of chitin and chitosan. Curr Chem Biol 2009;3:203-230.

85. Bhattarai N, Gunn J, Zhang M. Chitosan-based hydrogels for controlled, localized drug delivery. Adv Drug Deliv Rev 2010;62:83-99.

86. Balamurugan M. Chitosan: A perfect polymer used in fabricating gene delivery and novel drug delivery systems. J Pharm Pharm Sci 2012;4:54-56.

87. Fei Liu X, Lin Guan Y, Zhi Yang D, Li Z, De Yao K. Antibacterial action of chitosan and carboxymethylated chitosan. J Appl Polym Sci 2001;79:1324-1335.

88. Di Martino A, Sittinger M, Risbud MV. Chitosan: A versatile biopolymer for orthopaedic tissue-engineering. Biomaterials 2005;26:5983-5990.

89. Shukla SK, Mishra AK, Arotiba OA, Mamba BB. Chitosan-based nanomaterials: A state-of-the-art review. Int J Biol Macromol 2013;59:46-58.

90. Ravi Kumar M. A review of chitin and chitosan applications. React Funct Polym 2000;46:1-27.

91. Sabra W, Zeng AP, Deckwer WD. Bacterial alginate: physiology, product quality and process aspects. Appl Microbiol Biotechnol 2001;56:315-325.

92. Donati I and Paoletti S. Material Properties of Alginates. In:Rehm BHA editors. Alginates: Biology and Applications. Springer Berlin Heidelberg; 2009.pp. 1-53.

93. Draget KI, Taylor C. Chemical, physical and biological properties of alginates and their biomedical implications. Food Hydrocolloids 2011;25:251-256.

94. Dettmar PW, Strugala V, Craig Richardson J. The key role alginates play in health. Food Hydrocolloids 2011;25:263-266.

95. Aliste AJ, Vieira FF, Del Mastro NL. Radiation effects on agar, alginates and carrageenan to be used as food additives. Radiat Phys Chem 2000;57:305-308.

96. Oussalah M, Caillet S, Salmieri S, Saucier L, Lacroix M. Antimicrobial effects of alginate-based film containing essential oils for the preservation of whole beef muscle. J of Food Protect 2006;69:2364-2369.

97. Thomas A, Harding KG, Moore K. Alginates from wound dressings activate human macrophages to secrete tumour necrosis factor-alpha. Biomaterials 2000;21:1797-1802.

98. Hampson FC, Farndale A, Strugala V, Sykes J, Jolliffe IG, Dettmar PW. Alginate rafts and their characterisation. Int J Pharm 2005;294:137-147.

99. Lee CH, Singla A, Lee Y. Biomedical applications of collagen. Int J Pharm 2001;221:1-22.

100. Parenteau-Bareil R, Gauvin R, Berthod F. Collagen-Based Biomaterials for Tissue Engineering Applications. Materials 2010;3:1863-1887.

101. Chiou BS, Robertson GH, Rooff LE, Cao T, Jafri H, Gregorski KS, Imam SH, Glenn GM, Orts WJ. Water absorbance and thermal properties of sulfated wheat gluten films. J Appl Polym Sci 2010;116:2638-2644.

102. Chiou BS, Jafri H, Cao T, Robertson GH, Gregorski KS, Imam SH, Glenn GM, Orts WJ. Modification of wheat gluten with citric acid to produce superabsorbent materials. J Appl Polym Sci 2013;129:3192-3197.

103. Ture H, Gallstedt M, Johansson E, Hedenqvist MS. Wheat-gluten/montmorillonite clay multilayer-coated paperboards with high barrier properties. Ind Crop Prod 2013;51:1-6.

104. Guillaume C, Pinte J, Gontard N, Gastaldi E. Wheat gluten-coated papers for bio-based food packaging: Structure, surface and transfer properties. Food Res Int 2010;43:1395-1401.

105. Heralp TJ, Gnanasambandam R, McGuire BH, Hachmeister KA.. Degradable Wheat Gluten Films: Preparation, Properties and Applications. J Food Sci 1995;60:1147-1150.

106. Sudesh K, Abe H, Doi Y. Synthesis, structure and properties of polyhydroxyalkanoates: biological polyesters. Progr Polym Sci 2000;25:1503-1555.

107. Jendrossek D. Polyhydroxyalkanoate Granules Are Complex Subcellular Organelles (Carbonosomes). J Bacteriol 2009;191:3195-3202.

108. Lemoigne M. Produit de déshydratation et de polymérisation de l'acide ß-oxybutyrique. Bull Soc Chim Biol 1926;8:770-782.

109. Lemoigne M. Etudes sur l'autolyse microbiènne origine de l'acide ß-oxybutyrique formé par autolyse. Ann Inst Pasteur 1927;41:148-165.

110. Doi Y. Microbial polyesters, VCH, New York, 1990. John Wiley & Sons, Inc.; 1991.

111. Laycock B, Halley P, Pratt S, Werker A, Lant P. The chemomechanical properties of microbial polyhydroxyalkanoates. Prog Polym Sci 2012;

112. Holmes PA. Applications of PHB - a microbially produced biodegradable thermoplastic. Physics in Technology 1985;16:32.

113. Witholt B, Kessler B. Perspectives of medium chain length poly(hydroxyalkanoates), a versatile set of bacterial bioplastics. Curr Opin Biotech 1999;10:279-285.

114. Valentin H, Schönebaum A, Steinbüchel A. Identification of 4-hydroxyvaleric acid as a constituent of biosynthetic polyhydroxyalkanoic acids from bacteria. Appl Microbiol Biotechnol 1992;36:507-514.

115. Doi Y, Kunioka M, Nakamura Y, Soga K. Nuclear magnetic resonance studies on unusual bacterial copolyesters of 3-hydroxybutyrate and 4-hydroxybutyrate. Macromolecules 1988;21:2722-2727.

116. Du GC, Chen J, Yu J, Lun S. Feeding strategy of propionic acid for production of poly(3-hydroxybutyrate-co-3-hydroxyvalerate) with Ralstonia eutropha. Biochem Eng J 2001;8:103-110.

117. Page WJ, Manchak J, Rudy B. Formation of poly(hydroxybutyrate-co-hydroxyvalerate) by Azotobacter vinelandii UWD. Appl Environ Microb 1992;58:2866-2873.

118. Pederson EN, McChalicher CWJ, Srienc F. Bacterial Synthesis of PHA Block Copolymers. Biomacromolecules 2006;7:1904-1911.

119. Tripathi L, Wu LP, Meng D, Chen J, Chen GQ. Biosynthesis and Characterization of Diblock Copolymer of P(3-Hydroxypropionate)-block-P(4-hydroxybutyrate) from Recombinant Escherichia coli. Biomacromolecules 2013;14:862-870.

120. Kahar P, Tsuge T, Taguchi K, Doi Y. High yield production of polyhydroxyalkanoates from soybean oil by Ralstonia eutropha and its recombinant strain. Polym Degrad Stab 2004;83:79-86.

121. Fidler S, Dennis D. Polyhydroxyalkanoate production in recombinant Escherichia coli. FEMS Microbiol Lett 1992;103:231-235.

122. Doi Y, Segawa A, Kawaguchi Y, Kunioka M. Cyclic nature of poly(3-hydroxyalkanoate) metabolism in Alcaligenes eutrophus. FEMS Microbiol Lett 1990;67:165-170.

123. Fukui T, Doi Y. Efficient production of polyhydroxyalkanoates from plant oils by Alcaligenes eutrophus and its recombinant strain. Appl Microbiol Biotechnol 1998;49:333-336.

124. Kahar P, Tsuge T, Taguchi K, Doi Y. High yield production of polyhydroxyalkanoates from soybean oil by Ralstonia eutropha and its recombinant strain. Polym Degrad Stab 2004;83:79-86.

125. Lee WH, Loo CY, Nomura CT, Sudesh K. Biosynthesis of polyhydroxyalkanoate copolymers from mixtures of plant oils and 3-hydroxyvalerate precursors. Bioresource Technol 2008;99:6844-6851.

126. Verlinden RA, Hill DJ, Kenward MA, Williams CD, Piotrowska-Seget Z, Radecka IK. Production of polyhydroxyalkanoates from waste frying oil by Cupriavidus necator. AMB Express 2011;1:11.

127. Solaiman D, Ashby R, Hotchkiss A, Foglia T. Biosynthesis of Medium-chain-length Poly(hydroxyalkanoates) from Soy Molasses. Biotechnol Lett 2006;28:157-162.

128. Beccari M, Bertin L, Dionisi D, Fava F, Lampis S, Majone M, Valentino F, Vallini G, Villano M. Exploiting olive oil mill effluents as a renewable resource for production of biodegradable polymers through a combined anaerobic–aerobic process. J Chem Technol Biotechnol 2009;84:901-908.

129. Majone M, Massanisso P, Carucci A, Lindrea K, Tandoi V. Influence of storage on kinetic selection to control aerobic filamentous bulking. Water Sci Technol 1996;34:223-232.

130. Serafim LS, Lemos P, Albuquerque M, Reis M. Strategies for PHA production by mixed cultures and renewable waste materials. Appl Microbiol Biotechnol 2008;81:615-628.

131. Johnson K, Jiang Y, Kleerebezem R, Muyzer G, van Loosdrecht MCM. Enrichment of a Mixed Bacterial Culture with a High Polyhydroxyalkanoate Storage Capacity. Biomacromolecules 2009;10:670-676.

132. Albuquerque MGE, Torres CAV, Reis MAM. Polyhydroxyalkanoate (PHA) production by a mixed microbial culture using sugar molasses: Effect of the influent substrate concentration on culture selection. Water Res 2010;44:3419-3433.

133. Villano M, Valentino F, Barbetta A, Martino L, Scandola M, Majone M. Polyhydroxyalkanoates production with mixed microbial cultures: from culture selection to polymer recovery in a high-rate continuous process. New Biotechnol 2013;http://dx.doi.org/10.1016/j.nbt.2013.08.001

134. Beun JJ, Dircks K, Van Loosdrecht MCM, Heijnen JJ. Poly-β-hydroxybutyrate metabolism in dynamically fed mixed microbial cultures. Water Res 2002;36:1167-1180.

135. Dionisi D, Majone M, Tandoi V, Beccari M. Sequencing Batch Reactor: Influence of Periodic Operation on Performance of Activated Sludges in Biological Wastewater Treatment. Ind Eng Chem Res 2001;40:5110-5119.

136. Salehizadeh H, Van Loosrecht MCM. Production of polyhydroxyalkanoates by mixed culture: recent trends and biotechnological importance. Biotechnol Adv 2004;22:261-279.

137. Snell KD, Peoples OP. Polyhydroxyalkanoate Polymers and Their Production in Transgenic Plants. Metab Eng 2002;4:29-40.

138. Ramsay JA, Berger E, Voyer R, Chavarie C, Ramsay BA. Extraction of poly-3-hydroxybutyrate using chlorinated solvents. Biotechnol Tech 1994;8:589-594.

139. Madkour MH, Heinrich D, Alghamdi MA, Shabbaj II, Steinbuchel A. PHA Recovery from Biomass. Biomacromolecules 2013;

140. Anis S, Nurhezreen MI, Sudesh K, Amirul AA. Enhanced Recovery and Purification of P(3HB-co-3HHx) from Recombinant Cupriavidus necator Using Alkaline Digestion Method. Appl Biochem Biotechnol 2012;167:524-535.

141. Choi Ji, Lee SY. Efficient and economical recovery of poly(3-hydroxybutyrate) from recombinant Escherichia coli by simple digestion with chemicals. Biotechnol Bioeng 1999;62:546-553.

142. Yu J, Chen LXL. Cost-Effective Recovery and Purification of Polyhydroxyalkanoates by Selective Dissolution of Cell Mass. Biotechnol Progr 2006;22:547-553.

143. Kim M, Cho KS, Ryu H, Lee E, Chang Y. Recovery of poly(3-hydroxybutyrate) from high cell density culture of Ralstonia eutropha by direct addition of sodium dodecyl sulfate. Biotechnol Lett 2003;25:55-59.

144. Yang YH, Brigham C, Willis L, Rha C, Sinskey A. Improved detergent-based recovery of polyhydroxyalkanoates (PHAs). Biotechnol Lett 2011;33:937-942.

145. Chen Y, Chen J, Yu C, Du G, Lun S. Recovery of poly-3-hydroxybutyrate from Alcaligenes eutrophus by surfactant−chelate aqueous system. Process Biochem 1999;34:153-157.

146. Chen Y, Yang H, Zhou Q, Chen J, Gu G. Cleaner recovery of poly(3-hydroxybutyric acid) synthesized in Alcaligenes eutrophus. Process Biochem 2001;36:501-506.

147. Lo CW, Wu HS, Wei YH. High throughput study of separation of poly(3-hydroxybutyrate) from recombinant Escherichia coli XL1 blue. Journal of the Taiwan Institute of Chemical Engineers 2011;42:240-246.

148. de Koning GJM, Witholt B. A process for the recovery of poly(hydroxyalkanoates) from Pseudomonads Part 1: Solubilization. Bioprocess and Biosyst Eng 1997;17:7-13.

149. Kathiraser Y, Aroua MK, Ramachandran KB, Tan IKP. Chemical characterization of medium-chain-length polyhydroxyalkanoates (PHAs) recovered by enzymatic treatment and ultrafiltration. J Chem Technol Biotechnol 2007;82:847-855.

150. Kapritchkoff FM, Viotti AP, Alli RCP, Zuccolo M, Pradella JGC, Maiorano AE, Miranda EA, Bonomi A. Enzymatic recovery and purification of polyhydroxybutyrate produced by Ralstonia eutropha. J Biotechnol 2006;122:453-462.

151. Neves A, Muller J. Use of enzymes in extraction of polyhydroxyalkanoates produced by Cupriavidus necator. Biotechnol Progr 2012;28:1575-1580.

152. Geciova J, Bury D, Jelen P. Methods for disruption of microbial cells for potential use in the dairy industry—a review. Int Dairy J 2002;12:541-553.

153. Harrison STL. Bacterial cell disruption: A key unit operation in the recovery of intracellular products. Biotechnol Adv 1991;9:217-240.

154. Jung IL, Phyo KH, Kim KC, Park HK, Kim IG. Spontaneous liberation of intracellular polyhydroxybutyrate granules in Escherichia coli. Res Microbiol 2005;156:865-873.

155. Berger E, Ramsay BA, Ramsay JA, Chavarie C, Braunegg G. PHB recovery by hypochlorite digestion of non-PHB biomass. Biotechnol Tech 1989;3:227-232.

156. Barnard GN, Sanders JKM. Observation of mobile poly(β-hydroxybutyrate) in the storage granules of Methylobacterium AM1 by in vivo 13C-NMR spectroscopy. FEBS Letters 1988;231:16-18.

157. Reddy MM, Vivekanandhan S, Misra M, Bhatia SK, Mohanty AK. Biobased plastics and bionanocomposites: Current status and future opportunities. Progress in Polymer Science 2013;38:1653-1689.

158. de Koning GJM, Lemstra PJ. The amorphous state of bacterial poly[(R)-3-hydroxyalkanoate] in vivo. Polymer 1992;33:3292-3294.

159. Kawaguchi Y, Doi Y. Structure of native poly(3-hydroxybutyrate) granules characterized by X-ray diffraction. FEMS Microbiol Lett 1990;70:151-155.

160. Wong S, Shanks R, Hodzic A. Properties of Poly(3-hydroxybutyric acid) Composites with Flax Fibres Modified by Plasticiser Absorption. Macromol Mater Eng 2002;287:647-655.

161. Marchessault RH. Application of Polyhydroxyalkanoate Granules for Sizing of Paper. Biomacromolecules 2010;11:989-993.

162. Kusaka S, Abe H, Lee SY, Doi Y. Molecular mass of poly[(R)-3-hydroxybutyric acid] produced in a recombinant Escherichia coli. Appl Microbiol Biotechnol 1997;47:140-143.

163. Grassie N, Murray EJ, Holmes PA. The thermal degradation of poly(-(d)-ß-hydroxybutyric acid): Part 1-Identification and quantitative analysis of products. Polym Degrad Stab 1984;6:47-61.

164. Bluhm TL, Hamer GK, Marchessault RH, Fyfe CA, Veregin RP. Isodimorphism in bacterial poly(β–hydroxybutyrate-co-β-hydroxyvalerate). Macromolecules 1986;19:2871-2876.

165. Scandola M, Ceccorulli G, Pizzoli M, Gazzano M. Study of the crystal phase and crystallization rate of bacterial poly(3-hydroxybutyrate-co-3-hydroxyvalerate). Macromolecules 1992;25:1405-1410.

166. Kunioka M, Tamaki A, Doi Y. Crystalline and thermal properties of bacterial copolyesters: poly(3-hydroxybutyrate-co-3-hydroxyvalerate) and poly(3-hydroxybutyrate-co-4-hydroxybutyrate). Macromolecules 1989;22:694-697.

167. Cao A, Asakawa N, Yoshie N, Inoue Y. High-resolution solid-state 13C n.m.r. study on phase structure of the compositionally fractionated bacterial copolyester poly(3-hydroxybutyric acid-co-3-hydroxypropionic acid)s. Polymer 1999;40:3309-3322.

168. Holmes PA. Biologically Produced (R)-3-Hydroxy- Alkanoate Polymers and Copolymers. In:Bassett DC editors. Developments in Crystalline Polymers. Springer Netherlands; 1988.pp. 1-65.

169. Liu WJ, Yang HL, Wang Z, Dong LS, Liu JJ. Effect of nucleating agents on the crystallization of poly(3-hydroxybutyrate-co-3-hydroxyvalerate). J Appl Polym Sci 2002;86:2145-2152.

170. Reinecke H, Navarro R, Pérez M. Plasticizers. In:Encyclopedia of Polymer Science and Technology. John Wiley & Sons, Inc.; 2002.pp.

171. Choi JS, Park WH. Effect of biodegradable plasticizers on thermal and mechanical properties of poly(3-hydroxybutyrate). Polym Test 2004;23:455-460.

172. Correa MCS, Branciforti MC, Pollet E, Agnelli JAM, Nascente PAP, Av+®rous L. Elaboration and Characterization of Nano-Biocomposites Based on Plasticized Poly(Hydroxybutyrate-Co-Hydroxyvalerate) with Organo-Modified Montmorillonite. J Polym Environ 2012;20:283-290.

173. Bibers I, Tupureina V, Dzene A, Kalnins M. Improvement of the deformative characteristics of poly-β-hydroxybutyrate by plasticization. Mech Compos Mater 1999;35:357-364.

174. Parra DF, Fusaro J, Gaboardi F, Rosa DS. Influence of poly (ethylene glycol) on the thermal, mechanical, morphological, physical chemical and biodegradation properties of poly (3-hydroxybutyrate). Polym Degrad Stab 2006;91:1954-1959.

175. Savenkova L, Gercberga Z, Nikolaeva V, Dzene A, Bibers I, Kalnin M. Mechanical properties and biodegradation characteristics of PHB-based films. Process Biochem 2000;35:573-579.

176. Baltieri RC, Innocentini Mei LH, Bartoli J. Study of the influence of plasticizers on the thermal and mechanical properties of poly(3-hydroxybutyrate) compounds. Macromol Symp 2003;197:33-44.

177. Ishikawa K, Kawaguchi Y, Doi Y. Plasticization of bacterial polyester by the addition of acylglycerols and its enzymatic degradability. Kobunshi Ronbunshu 1991;48:221-226.

178. Zhao L, Kai W, He Y, Zhu B, Inoue Y. Effect of aging on fractional crystallization of poly(ethylene oxide) component in poly(ethylene oxide)/poly(3-hydroxybutyrate) blends. J Polym Sci Phys 2005;43:2665-2676.

179. You JW, Chiu HJ, Don TM. Spherulitic morphology and crystallization kinetics of melt-miscible blends of poly(3-hydroxybutyrate) with low molecular weight poly(ethylene oxide). Polymer 2003;44:4355-4362.

180. Park SH, Lim ST, Shin TK, Choi HJ, Jhon MS. Viscoelasticity of biodegradable polymer blends of poly(3-hydroxybutyrate) and poly(ethylene oxide). Polymer 2001;42:5737-5742.

181. Zhang L, Deng X, Huang Z. Miscibility, thermal behaviour and morphological structure of poly(3-hydroxybutyrate) and ethyl cellulose binary blends. Polymer 1997;38:5379-5387.

182. Iriondo P, Iruin JJ, Fernandez-Berridi MJ. Thermal and infra-red spectroscopic investigations of a miscible blend composed of poly(vinyl phenol) and poly(hydroxybutyrate). Polymer 1995;36:3235-3237.

183. Kumagai Y, Doi Y. Enzymatic degradation and morphologies of binary blends of microbial poly(3-hydroxy butyrate) with poly(ε-caprolactone), poly(1,4-butylene adipate and poly(vinyl acetate). Polym Degrad Stab 1992;36:241-248.

184. Blümm E, Owen AJ. Miscibility, crystallization and melting of poly(3-hydroxybutyrate)/ poly(l-lactide) blends. Polymer 1995;36:4077-4081.

185. Lovera D, M+írquez L, Balsamo V, Taddei A, Castelli C, M++ller AJ. Crystallization, Morphology, and Enzymatic Degradation of Polyhydroxybutyrate/Polycaprolactone (PHB/PCL) Blends. Macromol Chem Phys 2007;208:924-937.

186. Shanks RA, Hodzic A, Wong S. Thermoplastic biopolyester natural fiber composites. J Appl Polym Sci 2004;91:2114-2121.

187. Avella M, Martuscelli E, Pascucci B, Raimo M, Focher B, Marzetti A. A new class of biodegradable materials: Poly-3-hydroxy-butyrate/steam exploded straw fiber composites. I. Thermal and impact behavior. J Appl Polym Sci 1993;49:2091-2103.

188. Avella M, Rota GL, Martuscelli E, Raimo M, Sadocco P, Elegir G, Riva R. Poly(3-hydroxybutyrate-co-3-hydroxyvalerate) and wheat straw fibre composites: thermal, mechanical properties and biodegradation behaviour. J Mater Sci 2000;35:829-836.

189. Singh S, Mohanty AK. Wood fiber reinforced bacterial bioplastic composites: Fabrication and performance evaluation. Compos Sci Technol 2007;67:1753-1763.

190. Buzarovska A, Bogoeva-Gaceva G, Grozdanov A, Avella M. Crystallization behavior of polyhydroxybutyrate in model composites with kenaf fibers. J Appl Polym Sci 2006;102:804-809.

191. http://www.tianan-enmat.com

192. http://www.mirelplastics.com

193. Chen GQ, Wu Q. The application of polyhydroxyalkanoates as tissue engineering materials. Biomaterials 2005;26:6565-6578.

194. Chen GQ. A microbial polyhydroxyalkanoates (PHA) based bio- and materials industry. Chem Soc Rev 2009;38:2434-2446.

195. Martin DP, Williams SF. Medical applications of poly-4-hydroxybutyrate: a strong flexible absorbable biomaterial. Biochem Eng J 2003;16:97-105.

196. Pouton CW, Akhtar S. Biosynthetic polyhydroxyalkanoates and their potential in drug delivery. Adv Drug Deliver Rev 1996;18:133-162.

197. Rai R, Keshavarz T, Roether JA, Boccaccini AR, Roy I. Medium chain length polyhydroxyalkanoates, promising new biomedical materials for the future. Mat Sci Eng R 2011;72:29-47.

198. Grage K, Jahns AC, Parlane N, Palanisamy R, Rasiah IA, Atwood JA, Rehm BHA. Bacterial Polyhydroxyalkanoate Granules: Biogenesis, Structure, and Potential Use as Nano-/Micro-Beads in Biotechnological and Biomedical Applications. Biomacromolecules 2009;10:660-669.

199. Impallomeni G, Carnemolla GM, Puzzo G, Ballistreri A, Martino L, Scandola M. Characterization of biodegradable poly(3-hydroxybutyrate-co-butyleneadipate) copolymers obtained from their homopolymers by microwave-assisted transesterification. Polymer 2013;54:65-74.

200. Martino L, Scandola M, Jiang Z. Enzymatic synthesis, thermal and crystalline properties of a poly(β-amino ester) and poly(lactone-co-β–amino ester) copolymers. Polymer 2012;53:1839-1848.

201. Montaño-Leyva B, Ghizzi DdS, Gastaldi E, Torres-Chàvez P, Gontard N, Angellier-Coussy H. Biocomposites from wheat proteins and fibers: Structure/mechanical properties relationships. Ind Crop Prod 2013;43:545-555.

202. Reis MAM, Serafim LS, Lemos PC, Ramos AM, Aguiar FR, Van Loosdrecht MCM. Production of polyhydroxyalkanoates by mixed microbial cultures. Bioprocess and Biosystems Engineering 2003;25:377-385.

203. Kunioka M, Doi Y. Thermal degradation of microbial copolyesters: poly(3-hydroxybutyrate-co-3-hydroxyvalerate) and poly(3-hydroxybutyrate-co-4-hydroxybutyrate). Macromolecules 1990;23:1933-1936.

204. Scandola M, Pizzoli M, Ceccorulli G, Cesàro A, Paolletti S, Navarini L. Viscoelastic and thermal properties of bacterial poly(d-(ˉ)-β-hydroxybutyrate). Int J Biol Macromol 1988;10:373-377.

205. Fiorese ML, Freitas F, Pais J, Ramos AM, de Aragão GMF, Reis MAM. Recovery of polyhydroxybutyrate (PHB) from Cupriavidus necator biomass by solvent extraction with 1,2-propylene carbonate. Eng Life Sci 2009;9:454-461.

206. Hahn SK, Chang YK. A themogravimetric analysis for poly(3-hydroxybutyrate) quantification. Biotechnol Tech 1995;9:873-878.

207. Holmes PA, Lim GB, US4910145 A (1990).

208. King AT, Davey MR, Mellor IR, Mulligan BJ, Lowe KC. Surfactant effects on yeast cells. Enzyme and Microbial Technology 1991;13:148-153.

209. Cornibert J., Marchessault RH. Physical properties of poly-β-hydroxybutyrate: IV. Conformational analysis and crystalline structure. J Mol Biol 1972;71:735-756.

210. Barham PJ. Nucleation behaviour of poly-3-hydroxy-butyrate. J Mater Sci 1984;19:3826-3834.

211. European Commission. Commission Regulation (EU) No. 10/2011 on plastic materials and articles intended to come into contact with food. Off J Eur Union 2011; L12-1-L12/89.

212. Wang L, Zhu W, Wang X, Chen X, Chen GQ, Xu K. Processability modifications of poly(3-hydroxybutyrate) by plasticizing, blending, and stabilizing. J Appl Polym Sci 2008;107:166-173.

213. Labrecque LV, Kumar RA, Davé V, Gross RA, McCarthy SP. Citrate esters as plasticizers for poly(lactic acid). J Appl Polym Sci 1997;66:1507-1513.

214. Chen GQ. A microbial polyhydroxyalkanoates (PHA) based bio- and materials industry. Chem Soc Rev 2009;38:2434-2446.

215. Zini E, Focarete ML, Noda I, Scandola M. Bio-composite of bacterial poly(3-hydroxybutyrate-co-3-hydroxyhexanoate) reinforced with vegetable fibers. Compos Sci Technol 2007;67:2085-2094.

216. Baiardo M, Frisoni G, Scandola M, Licciardello A. Surface chemical modification of natural cellulose fibers. J Appl Polym Sci 2002;83:38-45.

217. Wunderlich B. Chapter X - Copolymer and Isomer Melting. In:Wunderlich B editors. Macromolecular Physics. San Diego:Academic Press; 1980.pp. 254-339.

218. Gazzano M, Tomasi G, Scandola M. X-ray investigation on melt-crystallized bacterial poly(3-hydroxybutyrate). Macromol Chem Physic 1997;198:71-80.

219. Yuan CM, Di Silvestro G, Speroni F, Guaita C, Zhang H. Control of Macromolecular Architecture of Polyamides by Poly-Functional Agents, 1. Theoretic and Experimental Approaches to Star-Branched Polyamides. Macromol Chem Phys 2001;202:2086-2092.

220. McKee MG, Unal S, Wilkes GL, Long TE. Branched polyesters: recent advances in synthesis and performance. Progress in Polymer Science 2005;30:507-539.

221. Kraus G, Gruver JT. Rheological Properties of Multichain Polybutadienes. Rubber Chemistry and Technology 1965;38:893-906.

222. Fetters LJ, Kiss AD, Pearson DS, Quack GF, Vitus FJ. Rheological behavior of star-shaped polymers. Macromolecules 1993;26:647-654.

223. Dorgan JR. Melt rheology of poly(lactic acid): Entanglement and chain architecture effects. Journal of Rheology 1999;

224. Hadjichristidis N, Roovers J. Linear viscoelastic properties of mixtures of 3- and 4-arm polybutadiene stars. Polymer 1985;26:1087-1090.

225. Levchik SV, Costa L, Camino G. Effect of the fire-retardant, ammonium polyphosphate, on the thermal decomposition of aliphatic polyamides. I. Polyamides 11 and 12. Polym Degrad Stab 1992;36:31-41.

226. Levchik SV, Weil ED, Lewin M. Thermal decomposition of aliphatic nylons. Polym Int 1999;48:532-557.

227. Mandelkern L, Fatou JG, Denison R, Justin J. A calorimetric study of the fusion of molecular weight fractions of linear polythylene (1). J Polym Sci B Polym Lett 1965;3:803-807.

228. Gogolewski S. Effect of annealing on thermal properties and crystalline structure of polyamides. Nylon 11 (polyundecaneamide). Colloid & Polymer Sci 1979;257:811-819.

229. Hoffman JD. Anelastic and dielectric effects in polymeric solids, N. G. McCrum, B. E. Read, and G. Williams, Wiley, New York, 1967. pp. 617. J Appl Polym Sci 1969;13:397.

230. Nair SS, Ramesh C, Tashiro K. Crystalline Phases in Nylon-11: Studies Using HTWAXS and HTFTIR. Macromolecules 2006;39:2841-2848.

231. Gross RA, Ganesh M, Lu W. Enzyme-catalysis breathes new life into polyester condensation polymerizations. Trends Biotechnol 2010;28:435-443.

232. Jiang Z, Azim H, Gross RA, Focarete ML, Scandola M. Lipase-Catalyzed Copolymerization of ω-Pentadecalactone with p-Dioxanone and Characterization of Copolymer Thermal and Crystalline Properties. Biomacromolecules 2007;8:2262-2269.

233. Ceccorulli G, Scandola M, Kumar A, Kalra B, Gross RA. Cocrystallization of Random Copolymers of ω-Pentadecalactone and ε-Caprolactone Synthesized by Lipase Catalysis. Biomacromolecules 2005;6:902-907.

234. Kalra B, Kumar A, Gross RA, Baiardo M, Scandola M. Chemoenzymatic Synthesis of New Brush Copolymers Comprising Poly(ω-pentadecalactone) with Unusual Thermal and Crystalline Properties. Macromolecules 2004;37:1243-1250.

235. Gazzano M, Malta V, Focarete ML, Scandola M, Gross RA. Crystal structure of poly(ω-pentadecalactone). J Polym Sci Part B Polym Phys 2003;41:1009-1013.

6. LIST OF PUBLICATIONS

Publications in scientific journals

Martino L, Scandola M, Jiang Z. Enzymatic synthesis, thermal and crystalline properties of a poly(b-amino ester) and poly(lactone-co-b-amino ester) copolymers. Polymer 2012;53:1839-1848.

Impallomeni G, Carnemolla GM, Puzzo G, Ballistreri A, Martino L, Scandola M. Characterization of biodegradable poly(3-hydroxybutyrate-co-butyleneadipate) copolymers obtained from their homopolymers by microwave-assisted transesterification. Polymer 2013;54:65-74.

Villano M, Valentino F, Barbetta A, Martino L, Scandola M, Majone M. Polyhydroxyalkanoates production with mixed microbial cultures: from culture selection to polymer recovery in a high-rate continuous process. New Biotechnol 2013;http://dx.doi.org/10.1016/j.nbt.2013.08.001.

Martino L., Cruz M.V., Scoma A., Freitas F.,Bertin L., Scandola M., Reis M. A. M. Recovery of amorphous polyhydroxybutyrate granules from Cupriavidus necator cells grown on used cooking oil. International Journal of Biological Macromolecules, In press.

Martino L., Basilissi L., Farina H., Aldo Ortenzi M., Zini E., Silvestro G., Scandola M.. Biobased polyamide 11: synthesis, rheology and solid-state properties of star structures. European Polymer Journal, Submitted.

Scientific contribution to international congresses

Guillard V., Angellier-Coussy H., Berthet M., Martino L., Guillaume C., Gontard N., 'How bioplastics can improve sustainability of food chain?', European Symposium on Biopolymers- ESBP2013, Lisbon (Portugal), 7-9 October 2013.

Angellier-Coussy H., Berthet M., Martino L., Gastaldi E., Gontard N., 'Eco-efficient, biodegradable and tailormade biocomposites from PHBV and wheat straw fiber', European Symposium on Biopolymers- ESBP2013, Lisbon (Portugal), 7-9 October 2013.

Martino L., Berthet M., Angellier-Coussy H., Jost V., 'Plasticization of Poly(3-hydroxybutyrate-co-3-hydroxyvalerate)', Annual meeting - Ecobiocap, Budapest (Hungary), 17-19 April 2013.

Martinez G.A., Bertin L., Rebecchi S., Scoma A., Martino, L., Scandola M., Fava F., 'Production of polyhydroxyalkanoates from fermented olive mill wastewaters by employing a pure culture of Cupriavidus necator', ESBP2013, Lisbon (Portugal), 7-9 October 2013.

Martino L., Scandola M., Scoma A., Bertin L., Cruz M., Reis M.A.M., 'Polyhydroxyalkanoates (PHAs) solvent-free recovery from Cupriavidus Necator biomass grown on fried oils', ESBP2013, Lisbon (Portugal), 7-9 October 2013.

Martino L., Scandola M., 'PHA Solvent-free Recovery', 4th Workshop on Polyhydroxyalkanoate Production by Microbial Mixed Cultures, Roma (IT), September 2012.

M. Scandola, L. Martino, A. Scoma, M. Cruz, F. Freitas, A.R. Gouveia, M.A.M. Reis, Production of polyhydroxyalkanoates (PHAs) from used frying oils and polymer recovery using different strategies, Environmental Engineering and Management Journal, March 2012, Vol.11, No. 3, Supplement, S58.

Di Silvestro G., Ortenzi M., Farina H., Yuan C.M., Basilissi L., Zini E., Martino L., Scandola M., 'Polylactic acid and Polyamide11 with controlled macromolecular architecture'. XII GEP Congress . European Polymer Congress - EPF2011- Granada (Spain). 26th June - 1st July 2011. (pp. 179). ISBN: 978-84-694-3124-5.

Cruz M., Freitas F., Scandola M., Martino L., Reis M.A.M. 'Polyhydroxyalkanoates (PHA) production by Cupriavidus Necator DSM 428 using frying oils as a sole carbon sources'. 3rd International Conference on Biodegradable and Biobased Polymers-BIOPOL 2011-Strasburgo (France). 29-31 August 2011.

Scientific contribution to national congresses

Martino, L, 'Studio delle correlazioni proprieta'-struttura in polimeri da fonti rinnovabili', AIM Macrogiovani 2012, Milano.

Farina H., Di Silvestro G., Basilissi L., Scandola M., Martino L., 'PA11-PLA block copolymers for PLA-PA11 blend compatibilization', XVIII Congresso Nazionale della Divisione di Chimica Industriale della Società Chimica Italiana - Le sfide della Chimica Industriale per una Innovazione Sostenibile, Firenze, Giugno 2012.

Di Silvestro G., Ortenzi M., Farina H., Yuan C.M., Basilissi L., Zini E., Martino L., Scandola M., 'Polylactic acid and Polyamide 11 with controlled macromolecular architecture; synthesis and characterization' AIM XX Convegno Italiano di Scienza e Tecnologia delle Macromolecole, Terni, 4-8 settembre, 2011, Atti pag 59-62.